# Harnessing Endogenous Systems for Cancer Therapy

**Klauber, Thomas Christopher Bogh; Andresen, Thomas Lars**

*Publication date:*
2015

*Document Version*
Publisher's PDF, also known as Version of record

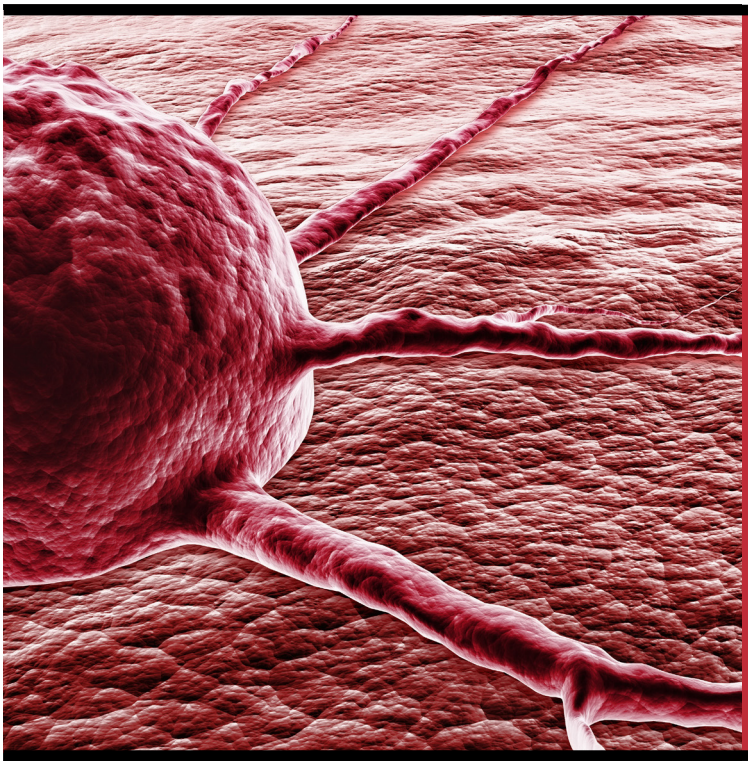

# Harnessing Endogenous Systems for Cancer Therapy

Thomas Klauber
PhD Thesis June 2015

DTU Nanotech
Department of Micro- and Nanotechnology

DTU Nanotech
Department of Micro- and Nanotechnology

# Harnessing Endogenous Systems for Cancer Therapy

PhD Thesis
January 2015

Thomas Klauber

Supervisor: Thomas L. Andresen

# Preface and acknowledgements

This thesis is submitted as part of the requirement for obtaining the PhD degree at the Department of Micro- and Nanotechnology, Technical University of Denmark. The PhD project was funded by the Danish Council for Strategic Research and the Technical University of Denmark. The experimental work was carried out in the Colloids & Biological Interfaces (CBIO) Group at DTU Nanotech in the period from August 2011 to November 2014 under the supervision of Professor Thomas L. Andresen.

There are many people without whom this project would not have been possible. First and foremost, I would like to thank my supervisor Thomas L. Andresen for the opportunity to work in his group and benefit from his knowledge, guidance and encouragement.

I have enjoyed the direct collaboration with a number people, and I would like to express my sincere gratitude to Torben Gjetting for his advice and inspiration on the siRNA delivery project and to Susanne Brix Pedersen and Simon Skjøde Jensen for their invaluable guidance on the cancer immunotherapy project. Further, I have had the pleasure of the insight and practical directions on flow cytometry from Janne Marie Lauersen, and on synthetic chemistry from Rasmus Irming Jølck and Lise Nørkjær Bjerg. Rikke Søndergaard deserves great thanks for providing the ratiometric pH measurements in the siRNA delivery project and general advice in her capacity as team leader, and Jonas Bruun deserves thanks for being a vital source of practical instructions on both projects as well as always being up for a discussion on the elucidation of the mysteries of siRNA delivery and – last but not least – helping me raise the aesthetic level of this dissertation.

Also, of course, I thank all my fantastic colleagues in the CBIO group for providing an inspiring working atmosphere, where help and high spirits are never in short supply.

Finally, I wish to extend a sincere thank you to my lovely girlfriend, who throughout my work, but particularly in the last phase, has demonstrated patience of Olympic proportions.

# Abstract

In the recent decade, two strategies in particular have attracted attention due to the prospect of significantly improving cancer treatment: Gene silencing therapy and immunotherapy. Both strategies work by manipulating endogenous mechanisms and theoretically promise very strong effect on the diseased cells and minimal effect on the healthy ones. This thesis regards the investigation of important mechanistic aspects of gene silencing mediated by delivery of small interfering RNA (siRNA) using synthetic vectors (Project I) as well as the development of a delivery platform for targeted immunotherapy (Project II).

Transfer into the clinic of therapies based on gene silencing by siRNA delivered by synthetic vectors has yet to happen. A major reason is the lack of efficiency in the delivery process, partly due to insufficient understanding of cellular uptake and processing of the siRNA-containing particles.

Project I aims to provide new mechanistic understanding of intracellular processing and vector interaction with target cells by investigating siRNA delivery using branched polyethyleneimine (bPEI), which is a well-known synthetic vector for DNA delivery, and comparing the properties of bPEI with a lipid derivative thereof (DOPE-PEI).

We demonstrate mechanistic differences between the bPEI conjugate and conventional bPEI with respect to siRNA condensation and intracellular processing and also show that lipid conjugation of bPEI results in markedly different formulation requirements compared to the conventional PEIs. However, lipid conjugation did not sufficiently reduce the inherent toxicity associated with high molecular weight PEI, and lipid conjugation of bPEI did also not change the ability of bPEI to affect lysosomal pH as a function of time.

In contrast to gene silencing therapy, cancer immunotherapy is starting to produce positive results in the clinic. A major target in cancer immunotherapy is the immunosuppressive tumor microenvironment generated directly or indirectly by the tumor. Tumor tissues have been shown to be heavily infiltrated by macrophages and DCs but due to the immunosuppressive environment they frequently adopt an in-active or tumor-promoting phenotype.

Project II describes the development of a platform which enables the highly specific targeting of monocytes and DCs in the bloodstream. Using this platform to deliver a TLR7 agonist, we were able to demonstrate activation of the targeted cells and increased potency of the agonist. While the described platform targets selected immune cells in the blood and not in itself targets the

tumor tissue, we believe that because tumor associated inflammation has been shown to recruit monocytes and DCs to the tumor tissues, our strategy could be an elegant and efficient way of providing activated monocytes, monocyte-derived macrophages, and DCs to the tumor site. If the duration of cytokine secretory activity extends post-extravasation, this will not only provide activated innate immune cells to the tumor site, but may also contribute to the re-polarization of the tumor microenvironment thereby promoting antitumor immunity.

# Dansk resumé

To eksperimentelle cancerbehandlingsstrategier har fået særlig meget opmærksomhed inden for det sidste årti: Knockdown genterapi og immunterapi. Begge fungerer via manipulation af endogene systemer og begge lover i teorien meget høj og meget specifik effekt på sygdomsramte celler. Denne afhandling omfatter en undersøgelse af vigtige mekanistiske aspekter af knockdown terapi baseret på small interfering RNA (siRNA) leveret af non-virale vektorer (Projekt I), samt design og undersøgelse af et system til målrettet immunterapi (Projekt II)

Bred klinisk brug af siRNA-baseret genterapi leveret af syntetiske vektorer er endnu urealistisk. En vigtig grund er ineffektiv levering af siRNA til de sygdomsramte celler, til dels på grund af mangelfuld viden om cellernes internalisering og intracellulære behandling af siRNA partiklerne. Projekt I søger at forbedre forståelsen af cellernes interaktion med vektorerne. Vi undersøgte siRNA-medieret knockdown med forgrenet polyethyleneimine (bPEI) og sammenlignede bPEIs egenskaber med et lipidkonjugeret derivat af bPEI. Vi viser, at der er forskel på bPEIs og lipidkonjugeret bPEIs egenskaber med hensyn til kondensering, og at lipidkonjugering påvirker virkemåden og formuleringsparametrene. Endvidere viser vi, at lipidkonjugering ikke i tilstrækkelig grad reducerer bPEIs cytotoxicitet eller ændrer bPEIs evne til at påvirke lysosomal pH som funktion af tid.

I modsætning til knockdown terapi, så er immunterapi begyndt at vise positive resultater til kræftbehandling. Det immunundertrykkende nærmiljø omkring en tumor er et vigtigt mål inden for immunterapi til kræftbehandling, og det er blevet vist, at selvom makrofager og dendritiske celler (DC) er stærkt repræsenteret i tumor vævet, så antager de ofte en inaktiv eller direkte immunundertrykkende fænotype. Project II beskriver et system, som muliggør målrettet levering til monocytter og DC'er i blodet. Vi brugte systemet til at levere en Toll-like receptor-7 agonist og kunne demonstrere aktivering af monocytter og DC'er samt en væsentligt forøget effekt i forhold til ikke-målrettet levering. Selvom det beskrevne system er målrettet mod udvalgte immunceller i blod og ikke mod (celler i) tumor vævet, mener vi, at fordi monocytter og DC'er bliver rekrutteret til tumor vævet via den tumor-associerede inflammation, så kan den beskrevne strategi være en måde til dels at opnå aktiverede monocytter, makrofager og DC'er i tumor vævet, dels at levere cytokiner med antitumor effekt til tumor nærmiljøet og dermed bidrage til at polarisere tumor vævet i en retning, der favoriserer tumor eliminering.

# Abbreviations

| | |
|---|---|
| API | Active pharmaceutical ingredient |
| Ab | Antibody |
| Ag | Antigen |
| APC | Antigen presenting cell |
| BDCA | Blood dendritic cell antigen |
| bPEI | Branched Polyethyleneimine |
| Chol | Cholesterol |
| CLEC | C-type lectin |
| CLR | C-type lectin receptors |
| CRD | Carbohydrate recognition domain |
| CTLA | Cytotoxic T-lymphocyte associated protein 4 |
| DC | Dendritic cell |
| DCAR | Dendritic cell immunoactivating receptor |
| DCIR | Dendritic cell immunoreceptor |
| DLS | Dynamic light scattering |
| DOGS | Dioctadecylamidoglycyl-spermine |
| DOPE | Dioleoylphosphatidylethanolamine |
| DOSPA | 2,3-dioleyloxy-N-[2(sperminecarboxamido)ethyl]-N,N-dimethyl-1-propanaminium-trifluoroacetate |
| DOTAP | 1,2-dioleoyl-3-trimethylammonium-propane |
| DOTMA | 1,2-di-O-octadecenyl-3-trimethylammonium-propane |
| DPPC | 1,2-dipalmitoyl-sn-glycero-3-phosphocholine |
| DPPE-RhB | 1,2-dipalmitoyl-*sn*-glycero-3-phosphoethanolamine-N-(lissamine rhodamine B sulfonyl) |
| DSPE-mal | 1,2-distearoyl-sn-glycero-3-phosphoethanolamine-N-[maleimide(polyethylene glycol)-2000] |
| DSPE-$PEG_{2000}$ | 1,2-distearoyl-*sn*-glycero-3-phosphoethanolamine-N-[methoxy(polyethylene-glycol)-2000] |
| dsRNA | Double stranded RNA |
| EDTA | Ethylenediaminetetraacetic acid |
| EMA | European Medicines Agency |
| EPR | Enhanced permeability and retention |
| FBS | Fetal bovine serum |
| FDA | Federal Drug Administration |
| GAG | Glycosaminoglycans |
| GFP | Green fluorescent protein |
| HBG | Hepes buffered glucose |
| Hepes | 5,5 '-dithio-bis(2-nitrobenzoic acid) (DTNB) and 4-(2-hydroxyethyl)-1-piperazineethanesulfonic acid |
| HPLC | High performance liquid chromatography |
| HuS | Human serum |
| IFN | Interferon |
| IL | Interleukin |
| IRM | Immune response modifier |
| lPEI | Linear Polyethyleneimine |
| Luc | Luciferase |
| mDC | Myeloid dendritic cell |

| | |
|---|---|
| MDSC | Myeloid-derived suppressor cell |
| MHC | Major histocompatibility complex |
| MPS | Mononuclear phagocyte system |
| mRNA | Messenger RNA |
| MTS | 3-(4,5-dimethylthiazol-2-yl)-5-(3-carboxy-methoxyphenyl)-2-(4-sulfophenyl)-2H-tetrazolium |
| MW | Molecular weight |
| N/P | Nitrogen to phosphate ratio |
| NK cell | Natural killer cell |
| nt | Nucleotide |
| ODN | Oligodeoxyribonucleotides |
| PBMC | Peripheral blood mononuclear cell |
| PBS | Phosphate buffered saline |
| PD | Programmed cell death protein |
| pDC | Plasmacytoid dendritic cell |
| PDI | Polydispersity index |
| PEG | Poly(ethyleneglycol) |
| PEI | Polyethyleneimine |
| Pen | penicillin |
| PLL | Poly-L-Lysine |
| PRR | Pathogen recognition receptor |
| RhB | Rhodamine B |
| RISC | RNA-induced silencing complex |
| RNAi | RNA interference |
| RPMI | Roswell Park Memorial Institute |
| SD | Standard deviation |
| SEM | Standard error of the mean |
| siRNA | Small interfering RNA |
| Strep | streptomycin |
| TAM | Tumor associated macrophage |
| Th2 | T-helper cell, type 2 |
| THF | Tetrahydrofuran |
| TLR | Toll-like receptor |
| TNF | Tumor necrosis factor |
| TAA | Tumor associated antigen |

# Table of Contents

Introduction ..... 1
Project I - Non-Viral delivery of siRNA ..... 5
1 Background ..... 5
1.1 Gene therapy - concept, discovery and early development ..... 5
1.2 The discovery of gene silencing ..... 5
1.3 RNA interference in the cell ..... 6
1.4 Delivery of siRNA to the target cells ..... 7
1.4.1 Stability in the circulation ..... 8
1.4.2 Egress from the bloodstream ..... 8
1.4.3 The extracellular matrix ..... 9
1.4.4 Cellular entry ..... 9
1.4.5 Endosomal escape and intracellular trafficking ..... 10
1.5 Viral and Non-Viral vectors ..... 12
1.5.1 Cationic polymers ..... 12
1.5.2 Cationic lipids ..... 13
1.6 Polyethyleneimine (PEI) ..... 14
1.6.1 How does PEI facilitate transfection? ..... 15
1.6.2 Structure of PEI polyplexes ..... 16
1.6.3 Modifications of PEI ..... 17
2 Aim of Project I ..... 18
3 Article 1: Elucidating the role of free polycations in gene knockdown by siRNA polyplexes 19
3.1 Abstract ..... 19
3.2 Introduction ..... 20
3.3 Materials and Methods ..... 22
3.3.1 Materials and Cell Lines ..... 22
3.3.2 Methods ..... 23
3.4 Results ..... 27
3.4.1 Cytotoxicity of vector polymers and polyplexes ..... 27
3.4.2 Lysosomal pH ..... 29
3.4.3 Size and ξ-potential of the polyplexes ..... 31
3.4.4 Condensation and decondensation properties of the polypolexes ..... 32

3.4.5 *In vitro* knockdown studies ..... 33
3.4.6 Uptake ..... 36
3.5 Discussion ..... 37
3.6 Conclusions ..... 41
3.7 Supplementary Figures ..... 42
4 Concluding remarks on Project I ..... 45
Project II – Cancer Immunotherapy ..... 47
5 Background ..... 47
5.1 Cancer immunotherapy - concept and current state ..... 47
5.2 Mechanisms of cancer immunity and opportunities for intervention ..... 48
5.3 Dendritic cells and macrophages in cancer immune therapy ..... 51
5.3.1 Dendritic cells in cancer ..... 51
5.3.2 Macrophages in cancer ..... 53
5.3.3 Myeloid-derived suppressor cells ..... 53
5.4 Macrophages and DC as targets of cancer immunotherapy ..... 54
5.4.1 Toll-like receptors ..... 54
5.4.2 Toll-like receptor agonists ..... 55
5.4.3 Targeted delivery ..... 56
5.4.4 Immunoliposomes ..... 57
5.4.5 Targeting monocytes, macrophages or DCs ..... 59
6 Aim of Project II ..... 61
7 Article 2: Activation of dendritic cells and monocytes by targeted delivery of a TLR7 agonist 63
7.1 Abstract ..... 63
7.2 Introduction ..... 64
7.3 Materials and Methods ..... 66
7.3.1 Materials ..... 66
7.3.2 Methods ..... 67
7.4 Results ..... 72
7.4.1 Preparation of immunoliposomes ..... 72
7.4.2 Characterization of liposomes – size, ξ-potential and polydispersity index (PDI) . 73
7.4.3 Characterization of liposome preparations ..... 74
7.4.4 Liposome association to peripheral blood mononuclear cell (PBMC) subsets ..... 75

7.4.5 Cytokine secretion from *in vitro* stimulated PBMCs ..... 77
7.5 Discussion ..... 80
7.6 Supplementary Figure 7.1 ..... 86
8 Concluding remarks on Project II ..... 87
9 Final concluding remarks and perspectives ..... 89
References ..... 93

# Introduction

Cancer is a leading cause of mortality in the world, counting 14 million diagnosed adults and 8.2 million fatal outcomes in 2012[1]. Consequently, there is a continued search for improved strategies in cancer treatment. The current types of treatment are often divided into the following main categories: Surgery, radiotherapy, chemotherapy, and biological therapies. Biological therapies are variously defined as a. therapies that stimulate the body's own healing mechanism or use biologics (e.g. gene therapy or antibody therapy), or b. therapies that arrest or regress cancer growth through interference with biological processes (e.g. inhibition of angiogenesis). Regardless of the definition, biotherapies are thus different from chemotherapeutic drugs that directly kill malignant cells through cytotoxicity.

While surgery has proven efficient in treating some cancers, it is clearly limited to localized and early-stage cancers, and cancers with limited metastatic activity. The current view is that no tumors are inherently non-metastatic[2], so most therapeutic strategies include some form of chemotherapy or biological therapy even when complete removal of the tumor is deemed feasible.

With very few exceptions, current chemo- and biotherapeutics do not employ any mechanisms to ensure tissue- or cell-specific accumulation of the active pharmaceutical ingredients (API)[3]. Whereas biotherapeutics typically target biological parameters, which afford some level of functional differentiation between healthy and malignant cells, the mode of action of traditional chemotherapeutics is non-specific and results in killing of all (rapidly) dividing cells primarily through interference with DNA management (synthesis, structural maintenance, repair or replication). One example of a biotherapy with some level of specificity for tumor cells, is breast cancer treatment with Trastuzumab (a humanized monoclonal antibody (Ab) against the HER2/neu receptor), which bases its discrimination on the relative (but not exclusive) overexpression of the target antigen in ≈25% of breast cancers[4].

The lack of targeted delivery of chemo- and biotherapeutics has several undesirable consequences. Usually, the API becomes distributed quite evenly within the body, proportionally to the regional blood flow, and has to cross many biological barriers (other organs, cells and intracellular compartments). Accordingly, it has ample opportunity to interact with and induce side effects in organs, tissues and cells that are not involved in the pathological process. Further, the drug has to be administered in large quantities in order to achieve the required therapeutic

concentration of the API in the target compartments or tissues (which greatly increase the cost of the therapy) and the drug may also become inactivated or degraded en route to the target tissue[3]. Finally, due to insufficient specificity of the drug mode-of-action, the impact on the non-pathological cells may be quite severe, as in many cases the targeted biological parameter is also essential for the non-pathological cells.

Conversely, the ideal drug employs targeted delivery to ensure minimal impact in non-pathological tissues, thus minimizing the side effects as well as the administered drug dose, and combines this with an effector mechanism, which exclusively causes damage to the malignant cells thus ensuring that any interaction between drug and non-pathological cells has minimal impact on those cells.

Through the tremendous advances in areas such as genetics, molecular biology and immunology, new opportunities for intervention have emerged, which theoretically promise to come closer to the ideal drug principle described above. This thesis regards two of those strategies, namely gene knockdown therapy, the subject of Project I, and targeted cancer immunotherapy, which is the subject of Project II. The uniting core principle is the manipulation of endogenous mechanisms to control and combat disease.

The molecular machinery involved in gene expression and posttranscriptional regulation has extremely high specificity through the principle of base-pairing. Therefore, therapy based on RNA interference (RNAi) promises absence of unintended gene knockdown, which - if a suitable oncogene is targeted - eliminates API-specific effects on non-cancerous cells. However, the challenge of targeted and efficient delivery of the therapeutic small interfering RNAs (siRNAs) remains, the more so because unprotected/unmodified siRNA is extremely susceptible to degradation in the bloodstream and interstitial space. Project I of this thesis is an investigation of non-viral siRNA delivery with one of the most commonly used vector polymers, polyethyleneimine (PEI). As lipid conjugation has been pursued as a promising strategy to increase the delivery efficiency and/or reduce the cytotoxicity of various polymers, the study includes a lipid conjugate of PEI. Using a combination of biophysical characterization and *in vitro* assays, we compare the polymers with respect to the interaction of the siRNA-containing particles with the target cells; how crucial formulation parameters influence the interplay between uptake and gene silencing effect and whether lipid conjugation fundamentally improves the potential of PEI as a siRNA delivery agent.

The results obtained in the study are presented in section 3 in the form of a manuscript, which has been prepared for submission to *Biomaterials*. Section 1 provides a detailed introduction to siRNA based gene therapy and the major obstacles faced by non-viral siRNA delivery.

Where Project I focuses on cellular interaction, Project II regards true targeted delivery to a subset of immune cells with the intent to stimulate the immune system to respond more vigorously to the presence of malignant cells.

As mentioned, a few cancer therapies do employ some level of direct targeting to cancerous cells. However, while Trastuzumab therapy is based on an Ab, it is believed to primarily work by antagonizing oncogenic pathways and only to a limited extent - if at all - through actual stimulation of antitumor immunity[4]. A more powerful, elegant and potentially more durable type of immunotherapy is the sensitization of the immune system to the presence and nature of the cancerous cells. Not only will such a strategy leave the actual disease elimination to the immune effector cells, which have been matured through millennia of evolution for exactly this task, but it will – in its most successful form – lead to the generation of memory cells capable of a rapid anti-cancer response should the cancer reappear after initial elimination. In Project II of this thesis, we attempt to develop a targeted, liposomal formulation of an immunomodulator and investigate whether targeted delivery of the compound to monocytes and dendritic cells improves the potency compared to non-targeted delivery. As the targeted cells are all present in the bloodstream, the obstacle of extravasation of our delivery vehicle becomes irrelevant, and the process of migrating to the diseased tissue to interact with the tumor cells is left to the stimulated immune cells working in concert with the vessel endothelia in and around the diseased tissues.

Section 5 of this thesis provides an introduction to cancer immunotherapy, and section 7 describes the work and results of Project II in the form of a manuscript in preparation for submission to *Nanomedicine: Nanotechnology, Biology and Medicine*.

# Project I - Non-Viral delivery of siRNA

## 1 Background

### 1.1 Gene therapy - concept, discovery and early development

Gene therapy is the use of nucleic acids as APIs to treat disease. The aim is to introduce or manipulate the expression of the genetic information contained in the targeted cells to influence their behavior or survival in a way that can treat or cure disease[5]. Initially, the vision of gene therapy was the treatment of hereditary diseases with genetic basis[6]; today the scope has expanded to include acquired disorders, such as cancer, heart diseases and immunodeficiency syndromes[6,7]. The following sections provide an introduction to gene therapy with emphasis on gene silencing.

The concept of gene therapy arose in the early 1970s when it was found that exogenous DNA could be introduced into and subsequently expressed by mammalian cells[5]. Owing to the enormous potential of gene therapy, huge efforts have gone into its development but so far very few therapies have been approved. This is mainly due to the lack of efficient and safe delivery of the nucleic acid to target cells *in vivo*[8–10]. As of 2013, no gene therapies have been approved in the US[11] or EU for treatment of cancer[12], while the first and so far only gene therapy product was recommended for approval by the European Medicines Agency (EMA) in July 2012 for treatment of lipoprotein lipase deficiency using recombinant lipoprotein lipase in an adeno-associated virus vector[12].

### 1.2 The discovery of gene silencing

Whereas DNA-based gene therapy attempts to achieve expression of exogenously introduced DNA, the objective of gene silencing is to cancel the expression of the targeted gene and

eliminate the production of disease-causing proteins which would otherwise arise as a result of gene transcription and mRNA translation.

Specific inhibition of gene expression using DNA-based antisense oligonucleotides (ODN) was first described in the late 1970s[13,14]. Upon transfection into a cell, antisense ODNs were able to hybridize to their target mRNA leading to the degradation of the mRNA-DNA hybrid strands. However, the crucial breakthrough came when it was discovered that double-stranded RNA could silence gene expression in the model organism C. elegans[15]. This mechanism for post-transcriptional gene silencing was termed RNA interference (RNAi), and its discovery earned C. Mello and A. Fire the Nobel Prize. The observations from C. elegans were rapidly extended to mammalian cell lines[16] and mice[17], after which the biotech community has worked hard to translate the technology into a working therapy for the treatment of various diseases, notably cancer.

## 1.3 RNA interference in the cell

RNAi is an evolutionarily conserved, post-transcriptional gene-silencing mechanism, which is present in most eukaryotic cells and regulates cellular transcriptional activity through degradation or translation-arrest of the target mRNA in a sequence-specific manner[16]. The effector molecules of RNAi are small double stranded RNA (dsRNA) molecules of ≈22 nucleotides (nt). Two pathways exist; one wherein the effector RNA molecule may be of endogenous origin and the final effector RNA has 1-3 mismatches with the target sequence. In this pathway, the effector RNAs are called miRNAs. In the other pathway, which is the one relevant to this dissertation, the effector RNAs are called small interfering RNAs (siRNA), are of exogenous origin, and has complete complementarity with the target mRNA sequence[18–20] (Fig. 1.1). siRNAs may be introduced into the cytosol in their final form of ≈22 nucleotide (nt) double stranded RNAs (dsRNAs) with a symmetric 2-nt overhang at the 3'-end of each strand[21], or as larger dsRNAs. dsRNAs larger than ≈22 nt will be trimmed to the short ≈22 nt form upon entry into the cytosol by a ribonuclease III-type protein called Dicer[22]. After generation of the ≈22 nt duplexes, the siRNAs are incorporated into a protein complex called the RNA-induced silencing complex (RISC), where the siRNA is unwound and the sense strand (or passenger strand) is cleaved. The activated RISC, which now only contains the antisense strand (or guide strand) of the original siRNA duplex, selectively pairs with and degrades mRNA that is complementary to the antisense strand, and as each activated RISC complex can perform many targeted degradations, siRNA-mediated RNAi is extremely potent[23]. This potency ensures a therapeutic effect for 3–7 days in

rapidly dividing cells, and for several weeks in non-dividing cells[24]. Eventually, the siRNAs are diluted below a certain critical threshold or degraded within the cell, and so – in a therapeutic setting – repeated administration is necessary to achieve a persistent effect. Theoretically, when using appropriately designed siRNA, the RNAi machinery can be exploited to silence nearly any gene in the body, giving it a much broader therapeutic potential than typical small-molecule drugs. As cancers are characterized by upregulated or inappropriately expressed genes that lead to uncontrolled cell growth, RNAi represents an attractive treatment strategy for many types of cancer.

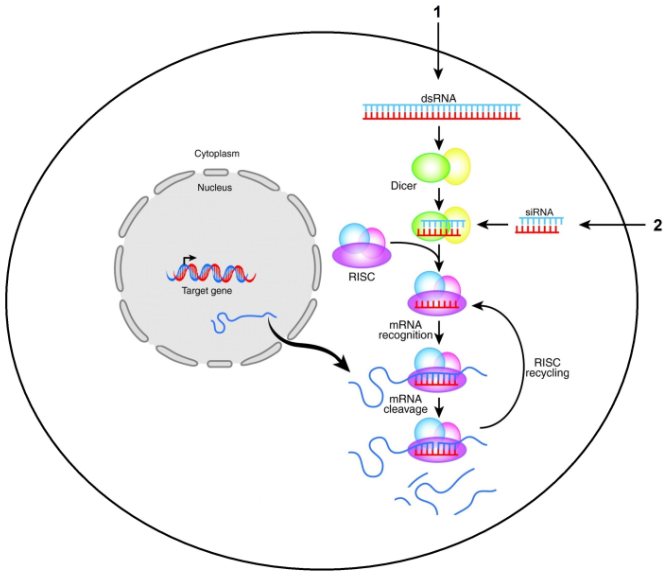


**Figure 1.1.** Cartoon of the mechanism of RNAi by siRNA in mammalian systems. Long double-stranded RNA molecules (dsRNA) enter the cell (arrow 1), are processed by the Dicer complex resulting in the formation of small interfering RNAs (siRNAs). Alternatively, siRNAs of ≈22 nt duplexes are delivered directly into the cell (arrow 2). The siRNAs are incorporated into the RNA-induced silencing complex (RISC), which becomes activated upon the ATP-dependent unwinding of the siRNA duplex. The passenger strand (blue) is cleaved and the now single-stranded siRNA guide strand (red) guides RISC to its complementary target mRNA. After base-pairing with the target mRNA sequence, the mRNA molecule is cleaved by the endonucleolytical activity of RISC. While RISC is recovered for further cycles, the cleaved targeted mRNA molecule is rapidly completely degraded due to its unprotected ends. Figure modified from[25].

## 1.4 Delivery of siRNA to the target cells

While siRNA therapy takes advantage of cellular machinery located in the cytosol and avoids transport of the nucleic acid cargo into the nucleus, the many barriers between the cytosol of the cell and the point of administration remain a formidable challenge to systemically administered siRNA, and the delivery obstacles have turned out to be rate-limiting in the development of RNAi-based therapies[23]. To overcome the challenges posed by the many

barriers, a delivery vehicle (termed a vector) is employed, and the field is separated according to the type of vector; whether it is a lipid or polymer (non-viral delivery), or a genetically modified virus (viral delivery). The pros and cons of both types of delivery are briefly discussed in section 1.5 and an overview of the barriers to non-viral siRNA delivery is provided immediately below.

### 1.4.1 Stability in the circulation

Upon entry into the blood stream, the stability of the siRNA and vector-siRNA complex is challenged by a variety of blood components. The most important and abundant threat comes from ribonucleases, which are present ubiquitously as part of the defense against retroviruses, and degrade unprotected nucleic acids with high efficiency[26]. Accordingly, the siRNA needs protection against nucleolytic attack.

Electrostatic interaction with blood components is another obstacle to successful non-viral delivery of siRNA. Particles with a net cationic charge will interact with negatively charged blood components, such as serum proteins, which may lead to recognition by phagocytes and fast clearance from the circulation[26]. Particles with an overall charge, positive or negative, may aggregate in the bloodstream due to the presence of ions in the blood, which can shield the electrostatic repulsion between charged particles (a phenomenon known as salt-induced aggregation). Aggregation may increase phagocytic clearance as well as cause blocking of microvessels[27]. Conversely, particles with a diameter below 5 nm will be cleared rapidly by the glomerular filtration[28] highlighting that size and surface charge are very important properties for successful siRNA delivery.

### 1.4.2 Egress from the bloodstream

To exit the blood stream and accumulate in the target tissue, the siRNA-particles need to cross the vessel endothelium. While most capillary endothelia are impermeable to large molecules, vessels in inflamed and tumorous tissue have been shown to be “leaky” due to inflammation, rapid growth and/or angiogenesis. Combined with the lack of lymphatic drainage in tumor tissues, this permeability facilitates non-specific egress of macromolecules from the bloodstream into the tissue[6,28]. The phenomenon is known as the enhanced permeation and retention effect (EPR effect), and has been used to explain the increased accumulation of nanosized particles in tumorous tissues compared to other tissues. However, the EPR effect has also shown to be highly variable between different types of cancer and tissue, and evidence also suggests that the EPR effect is much more pronounced in mice and dogs than in humans[29]. In the absence of EPR-

like conditions, accumulation of nanoparticles in the tissues requires passive trans- or paracellular transport or the exploitation of active transport mechanisms[28].

### 1.4.3 The extracellular matrix

Following exit from the circulation, the transfection particles must diffuse through the extracellular matrix to the target cells in order for cellular uptake to occur. However, the extracellular matrix consists of a dense layer of polysaccharides and fibrous proteins and may slow down diffusion dramatically. A major component of the extracellular matrix is the proteoglycans, which consist of a core protein covalently linked to one or more anionic glycosaminoglycans (GAGs). The GAGs may interact with positively charged transfection particles, causing reduced mobility. They may also compete for binding to the vector, thus causing decondensation or release of the nucleic acid[30]. Finally, the extracellular matrix is particularly rich in nucleases, underlining the importance of nucleolytic protection of the siRNA. Unsurprisingly, it has been shown that the cellular uptake decreases with the amount of extracellular matrix needing to be traversed[31].

### 1.4.4 Cellular entry

To enter into the target cell, the transfection particles have to cross the plasma membrane. As passive diffusion across the plasma membrane is restricted to very small and hydrophobic entities[6], entry into the cell must follow other routes. While a recent interesting report hypothesized that a very small fraction of siRNA-lipoplexes (transfection particles consisting of cationic lipids and siRNA) was taken up through some form of direct membrane fusion and was responsible for all of the observed knockdown[32], most investigators currently believe that the internalization occurs through some form of endocytosis. Endocytosis is a cellular mechanism for uptake of macromolecules and solutes into membrane-bound vesicles derived by invagination and pinching off pieces of the plasma membrane[33]. Several different endocytic routes are known and the specific type of endocytosis employed for the uptake of a given transfection particle appear to depend on the biophysical characteristics of the particle, the cell in question and the possible presence of targeting ligands on the surface of the particles[33]. Some gene delivery vectors are believed to facilitate endocytosis unspecifically. For instance, it appears that endocytosis can be triggered by non-specific electrostatic interactions between positively charged transfection particles and negatively charged glycoproteins and proteoglycans on the cell surface in a process termed adsorptive pinocytosis[34]. However, while several groups have attempted to elucidate which type of non-viral transfection particle is preferentially taken up by

a given subform of endocytosis, the picture remains diffuse. The matter is further complicated by disagreement on the types of endocytosis possible – several groups remain skeptical towards the existence of caveolar endocytosis, claiming microscopic artefacts and physiologically irrelevant experimental circumstances to be at fault[35].

Regardless of the route of endocytosis, it has been shown that the size of the particle strongly affects cellular uptake and the optimal particle size using non-targeting vectors is assumed to be between 70 and 100 nm[26,29].

Other approaches to improve cellular internalization than receptor targeting have been examined, including the application of physical stress to the tissue in question in order to transiently disrupt the plasma membrane. However, these methods are highly invasive, damage the cells and the treatment cannot be utilized in deeper tissues. The use of cell penetrating peptides is another approach that has received some attention, but this strategy has also been associated with substantial unintentional cell damage[6].

### 1.4.5 Endosomal escape and intracellular trafficking

After internalization by endocytosis, the polyplexes are trapped in the endosomal compartment, specifically in the early endosome (Fig. 1.2). The early endosomes undergo a series of fusion processes during which some level of sorting of the internalized material takes place. Some of the internalized material, e.g. some internalized cell surface receptors, is recycled to the plasma membrane. Material which is not redirected to the plasma membrane remains in the endosome, which undergoes further vesicular fusions during which the internalized material reaches first the late endosomal compartment and finally the lysosomal compartment. During the course of this journey, the interior pH of the vesicle is gradually lowered because the V-ATPase pumps $H^+$ into the vesicle under the consumption ATP, followed by the passive influx of $Cl^-$[26]. The pH decrease culminates at pH 4.4 after fusion with the lysosomes, which also introduces a cocktail of acid hydrolases[6,36]. The acid hydrolases are enzymes capable of degrading most bio-polymers and lysosomal degradation is therefore a major bottleneck for efficient gene delivery. Consequently, for transfection particles taken up by endocytosis, it is crucial that the particles are able to escape from the endosomes before fusion with the lysosomes, a phenomenon referred to as “endosomal escape”. Viruses are able to escape from endosomes due to their contents of peptides with pH-triggered fusogenic activity, which can destabilize the endosomal vesicles[37], but only a subset of non-viral vectors possess this ability. For polycations, this ability has been shown to correlate with their buffering capacity in the pH range 5-7[37].

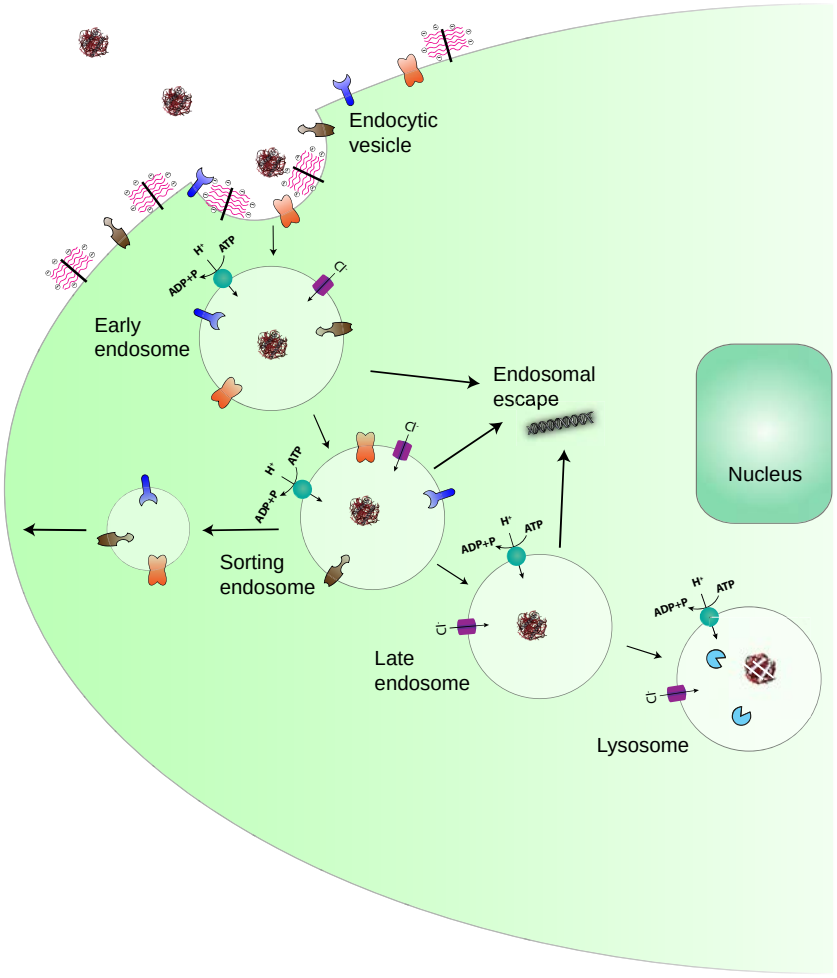


**Figure 1.2.** Intracellular trafficking of an siRNA transfection particle. An siRNA transfection particle is taken up into the cell by endocytosis, with cellular association mediated by interaction with a negatively charged proteoglycan. The endocytic vesicle is pinched off and fuses with the early endosomal compartment. The contents of the early endosome are trafficked to the sorting endosomal compartment, where recycling of selected cargo takes place. Then follows fusion with the late endosomal compartment and finally the lysosomal compartment, which is the site of hydrolysis of proteins and nucleic acids. Throughout the journey, the pH of the endosomal interior is gradually lowered through the action the V-ATPase culminating at pH 4.4 in the lysosomes. To direct silencing of the target gene, siRNAs must escape from the endosome into the cytoplasm before fusion with the lysosomal compartment and introduction of the acid hydrolases to avoid degradation. Modified from[25].

Following escape from the endosomes, the siRNA has to reach the RNAi machinery intact and be loaded into the RISC. As the cytosol contains numerous nucleases, the protection afforded by the vector is again of great importance, especially since diffusion in the cytosol is slow[38]. Further, for loading of the siRNA into the RISC protein assembly to be possible, the siRNA needs to dissociate from the vector at just the right place, which means that there is a delicate balance between a vector-siRNA association that is of exactly the right strength, and associations that are too weak/unprotective or too strong.

## 1.5 Viral and Non-Viral vectors

Some experimental treatments with DNA have achieved positive results using electroporation-assisted delivery[39] or "gene guns"[40] to force naked nucleic acids into cells. However, due to the barriers described in the previous sections, systemic and efficient delivery of siRNA necessitates some form of delivery vehicle, which is termed a vector.

Most clinical trials and experimental treatments use viral vectors[41], which are attenuated viruses. Virus propagation rely on the manipulation of host cells to produce new viral proteins by introducing nucleic acids into the host protein machinery, and evolution has perfected parameters such as stability towards the environment, efficiency of transfection and methods to ensure high volume expression of the cargo.

However, application of viral vectors has so far been restricted by a number of factors[42–44]:

- high complexity of vector preparation which greatly increases the therapeutic costs
- limited loading capacity of the viral vectors
- safety concerns due to the oncogenic potential of viral delivery
- risk of reversion to wild-type with restoration virulence due to the large amounts of ancient viral DNA material present in the human genome
- inflammatory and immunogenic effects which prevent repeated administration

In light of these concerns and challenges, synthetic vectors have been developed. They are oligo- or polycations of various types, which are able to form stable complexes with the negatively charged siRNA resulting in particles with varying biophysical properties (e.g. particle size and ξ-potential), which are important in determining the delivery capability of the vector. Non-viral vectors are less immunogenic and show much better overall safety profiles than viral vectors. Unfortunately, this comes at the expense of efficiency and many non-viral vectors also show substantial cytotoxicity. Thus, much of the research into non-viral siRNA delivery has focused on improving these parameters.

The major classes of non-viral vectors are cationic lipids and cationic polymers[37] and before focusing on the cationic polymer PEI, both classes will be described in overview immediately below.

### 1.5.1 Cationic polymers

Cationic polymers are synthetic compounds, which are easily modified with respect to average Mw and attachment of ligands[45]. The complexes formed between nucleic acids and polymers are

known as polyplexes. While rarely used unmodified in clinical trials, polymers are frequently used experimentally both *in vitro* and *in vivo*. Polyethylenimine (PEI) and various forms of poly-L-lysine (PLL, Fig. 1.3) are commonly used cationic polymers for gene delivery, but also polymers such as chitosans[46] (linear aminopolysaccharides) and dendrimers[45] such as highly branched polyamidoamines have been used. A detailed introduction to PEI is given in section 1.6.

PLL was one of the first polycations used for gene delivery and is a biodegradable linear polypeptide, with lysine as the repeating unit[26]. Importantly and in contrast to PEI, PLL itself is unable to facilitate endosomal escape. At physiological pH, all the primary amine groups of PLL will be protonated and therefore the polymer has no significant buffering capacity. Consequently, transfection using PLL requires co-administration of a lysosomotropic agent, such as chloroquine, or a fusiogenic peptide, which can facilitate the crucial endosomal escape[47]. As for PEI, the Mw of PLL has great influence on PLL's properties as gene delivery vector and in general PLL with Mw above 3 kDa is required for formation of stable transfection particles. The transfection efficiency increases with increasing Mw, but – unfortunately – so does cytotoxicity[48].

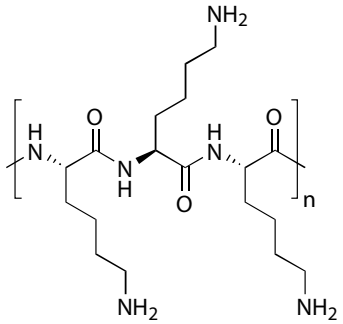


**Figure 1.3.** Structure of poly-L-lysine homo-polymer fragment (PLL).

### 1.5.2 Cationic lipids

Transfection using cationic lipids is often called lipofection and was described in as early as 1987[49]. The cationic lipids used for lipofection all contain a hydrophilic cationic head group and fatty acid side chains[26]. Owing to their amphiphilic properties, the lipids may self-assemble in aqueous environments. When mixed with siRNA, a variety of structures may be formed, the most common of which appear to be siRNA sandwiched between the layers of multilamellar vesicles (lamellar phase) or siRNA inserted within inverse lipid tubules, arranged on a hexagonal lattice (inverted hexagonal phase)[50].

A number of commercially available lipofection reagents exist (Fig. 1.4) and clinical studies have also been performed using cationic lipids, but so far no systems have reached the clinic due to cytotoxic effects and insufficient transfection efficiency[41]. Rapid clearance of particles which carry a net cationic charge is a major reason for the low efficiency, and accordingly several strategies have been devised to produce transfection particles which carry a neutral charge in the circulation. One strategy has been to use titratable cationic lipids enabling the charge of the formulated transfection particles to be adjusted to neutral at physiological pH after complex formation[51]. As positive charges facilitate cellular internalization, another promising strategy has been shielding the positive charges when the transfection particle is in the circulation followed by de-shielding in the target tissue through the action of tissue-specific proteases[52].

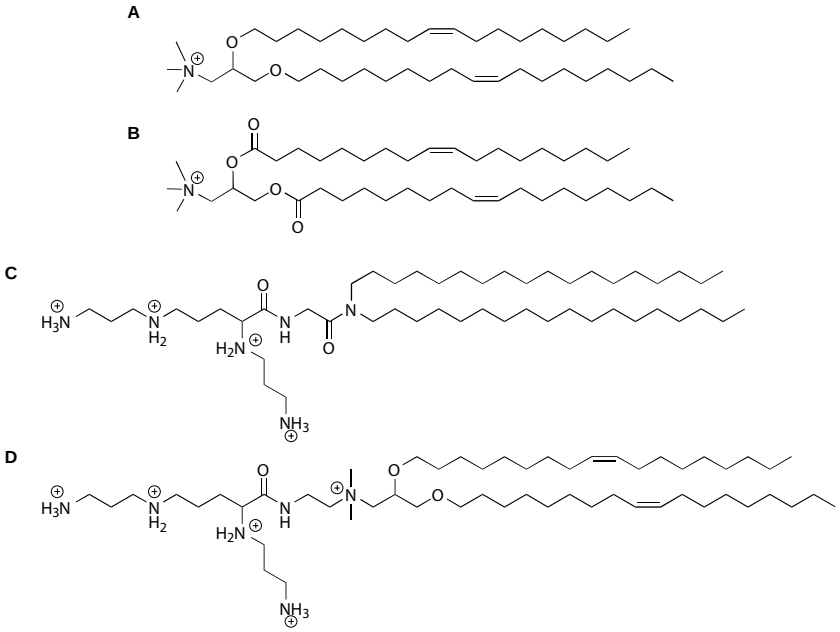


**Figure 1.4.** Structures of some commercially available lipofection reagents[26]. A. DOTMA, (Lipofectin®, 2-di-O-octadecenyl-3-trimethylammonium-propane), B. DOTAP (1,2-dioleoyl-3-trimethylammonium-propane), C. DOGS (Transfectam®, Dioctadecylamidoglycyl-spermine), D. DOSPA (Lipofectamine®, 2,3-dioleyloxy-N-[2(sperminecarboxamido)ethyl]-N,N-dimethyl-1-propanaminium-trifluoroacetate).

## 1.6 Polyethyleneimine (PEI)

PEI is a synthetic polymer, which has been widely used for various industrial applications for more than 40 years. PEI exists in linear and branched forms (abbreviated lPEI and bPEI, respectively, Fig. 1.5), each covering a wide range of average molecular weights, ranging from 100 Da to 1500 kDa[53,54]. As every third atom is an N, potentially capable of protonation, PEI has a very high charge density potential[55]. Importantly, the charge density is highly pH-dependent: At physiological pH (pH 7.4), only ≈20% of the nitrogens are protonated, while a decrease to pH 5

increases this percentage to ≈45[56]. Combined, the many proton-accepting groups and the wide range of apparent pKa values provide PEI with high buffering capacity over a wide pH range[53,57], which has been used to explain the efficiency of PEI as a transfection agent. lPEI and bPEI differ in the nature of their amines with lPEI containing almost exclusively secondary amines and bPEI containing a mixture of primary, secondary and tertiary amines. The ratio of the different amines on bPEI depends on the details of the synthesis, with most commercially available bPEI polymers having a ratio of primary to secondary to tertiary amines of 1:1:1[56]. PEI polymers have maximum buffer capacity between pH 8-10, and at a given pH in this range bPEI will show a higher charge density than lPEI, but at the endosomal pH range (pH 4-6), no effect of polymer structure on protonation has been demonstrated[53,58].

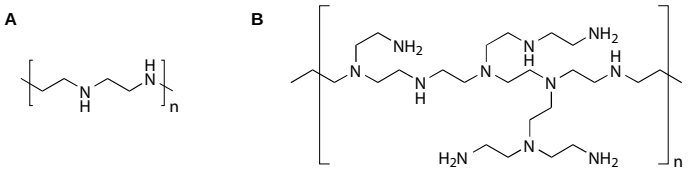


**Figure 1.5.** Structures of A. a typical linear PEI fragment (lPEI) and B. a typical branched PEI fragment (bPEI).

PEI forms the basis for a number of commercially available transfection agents for non-clinical use, and remains the "gold standard" for non-viral gene delivery vectors. However, while PEI is a potent transfection agent, the delivery efficiency of PEI-based transfections agents is still unable to compete with viral vectors[54,59].

### 1.6.1 How does PEI facilitate transfection?

Due to the high charge density, PEI is excellent at condensing the siRNA into small, compact transfection particles with an overall positive charge and protecting the siRNA against degradation by nucleases. Excess cationic charges have the ability to interact non-specifically with negatively charged glycoproteins and proteoglycans on the cell surface and may thus facilitate the uptake process[54,60]. Some reports claim to demonstrate internalization specifically though caveolar endocytosis[54], which should be beneficial as this pathway may avoid fusion with the lysosomes[33]. Regardless of internalization route, PEI is hypothesized to be able to facilitate endosomal escape although the mechanism for this is not fully understood. The dominant hypothesis is termed the "proton sponge effect" and states that PEI, through the many unprotonated amines left over from polyplex formation with the cargo, is able to absorb protons when the complex travels through the gradually more acidic endolysosomal compartments. This will then lead to excessive $H^+$ influx as the V-ATPase attempts to compensate for the $H^+$

absorption of PEI, leading to increased co-influx of $Cl^-$ and water[61], which in turn leads to osmotic swelling, destabilization and/or rupture of the lysosomal membrane and release of the siRNA into the cytosol[62]. However, the proton sponge effect is debated and incontrovertible experimental evidence remains elusive. As theoretical assessments have indicated that internalization of realistic amounts of bPEI-polyplexes is insufficient to cause rupture of the endosomal membrane, it has been hypothesized that the proton sponge effect is only a contributor to endosomal escape, possibly through local destabilization of the endosomal membrane[63]. The latter is viewed as congruent with observations of pore formation in the endosomal membrane after treatment with PEI[64]. As the endosomal escape properties of PEI by some has been viewed as the most important factor limiting PEI mediated transfection, several attempts have been made to enhance this property e.g. using membrane-destabilizing proteins or peptides[25]. However, these attempts have not been successful, which have led some to conclude that the inherent endosomal escape properties of PEI itself are not the bottleneck to the overall performance of PEI[54].

It remains unclear, exactly when de-complexation of the polyplexes takes place once endosomal escape has occurred, and how siRNA in condensed or de-condensed form is loaded into the RNAi machinery. While post-endosomal escape activities are not regarded as rate-limiting in the delivery process[65], it is intuitive that a balance between tight binding of the cargo and facile release exists.

The physical, chemical and biological properties of PEI has been found to depend highly on its structure[59,66]. A wide variety of PEI polymers have been tested, but no structure has been found unequivocally superior[54] and the structure-activity relationship is still not fully understood - including whether lPEI or bPEI provides the best results[60]. As seen for PLL, the transfection efficiency of PEI increases with MW, but so does cytotoxicity and an average MW of 25kDa is generally considered the upper limit for usability of PEI for transfection.

### 1.6.2 Structure of PEI polyplexes

PEI polyplexes have not been characterized to the same detail as lipopolexes in terms of structure, with most studies using PEI focusing on the fate of the complexed siRNA. As mentioned, it has been shown that PEI is able to condense siRNA into transfection capable particles in which the siRNA is protected against degradation by nucleases. In addition, experiments on bPEI and sRNA[67] indicate that in the presence of a long-chain polycations (bPEI 25kDa), the polyanion is neutralized and totally surrounded by the oppositely charged chains,

while with the shorter polycation chains (bPEI 2.7kDa), the siRNA is condensed but more exposed to the outside. In both cases the formed particles were spherical[67].

### 1.6.3 Modifications of PEI

Since the emergence of PEI as an efficient transfection agent, many diverse strategies have been employed attempting to reduce the toxicity while retaining the delivery efficiency: PEGylation (conjugation to poly(ethyleneglycol)) with or without addition of a targeting moiety[53], cross-linking of bPEI 2kDa and lPEI 423Da via ester- and/or amide- linkages[68], acylation with oleic acid[69], acylation and crosslinking using PEG as crosslinker[70] and lipid conjugation[71–73]. Lipid conjugation is a highly promising strategy as lipid-lipid interactions are orthogonal to the interaction sequestering the siRNA in the polyplex and thus may be exploited and manipulated separately. In addition, possible cell entry / endosomal escape mechanisms may work independently of the siRNA condensation, which could be an advantage. Finally, while lipid-conjugated cations cannot be assumed to behave similarly to cationic lipids due to the different ratio between charged and lipid moieties, a lot of information regarding the structure of lipoplexes and siRNA exist[50,74–77], and this may prove a useful starting point for the rational development of future lipid-conjugated PEI-based vectors for siRNA delivery.

# 2 Aim of Project I

The aim of Project I was to investigate mechanistic and biological aspects of siRNA delivery using bPEI and one of the most promising types of PEI modification, namely a lipid conjugate of bPEI. Project I focused on the vector-to-cargo ratio and examined whether a free vector fraction exists when bPEI and bPEI-lipid conjugates are used for siRNA delivery. Further, Project I investigated the impact of the free fraction on the ability of bPEI and the bPEI-conjugate to facilitate siRNA internalization and knockdown of reporter gene expression as well as the importance of the free fraction for the cytotoxicity of the vectors and polyplexes. Finally, Project I examined the potential effect on pH in the lysosomes induced by these polycations to elucidate the differences in the proton sponge effect between lipid-conjugated PEI and conventional PEI.

# 3 Article 1: Elucidating the role of free polycations in gene knockdown by siRNA polyplexes

This section contains the manuscript prepared for submission to *Biomaterials*.

Thomas C. B. Klauber[1], Rikke V. Søndergaard[1], Rupa R. Sawant[2], Vladimir P. Torchilin[2], Thomas L. Andresen[1]

[1]DTU Nanotech, Department of Micro-and Nanotechnology, Center for Nanomedicine and Theranostics, Technical University of Denmark, Building 423, 2800 Lyngby, Denmark

[2]Center for Pharmaceutical Biotechnology and Nanomedicine, Northeastern University, Boston, MA 02115, USA

## 3.1 Abstract

Future improvements of non-viral vectors for siRNA delivery require new mechanistic understanding of intracellular processing and vector interactions with target cells. In the present work, we have compared the siRNA delivery properties of a lipid derivative of bPEI 1.8kDa (DOPE-PEI) with branched polyethyleneimine (bPEI) with average molecular weights of 1.8kDa (bPEI 1.8kDa) and 25 kDa (bPEI 25kDa). We have investigated the potential effect on pH in lysosomes induced by these synthetic vectors in order to elucidate the differences in the proton sponge effect between lipid conjugated PEI and conventional PEI. We find mechanistic differences between the DOPE-PEI conjugate and bPEI with respect to siRNA condensation and intracellular processing. bPEI 1.8kDa and bPEI 25kDa have similar properties with respect to condensation capability, but are very different with respect to siRNA decondensation, cellular internalization and induction of reporter gene knockdown. Lipid conjugation of bPEI 1.8kDa improves the siRNA delivery properties, but with markedly different formulation requirements and mechanisms of action compared to conventional PEIs. Furthermore, cellular incubation with either DOPE-PEI or bPEI 25kDa did not affect lysosomal pH as a function of time, underlining that the possible proton sponge effect is not associated with changes in pH.

**Keywords:** siRNA, Polyethyleneimine, PEI, Non-viral gene delivery, Proton sponge effect, Polycation

## 3.2 Introduction

RNA interference (RNAi) based drugs are currently under intense investigation for treating viral infections, cancer and neurological disorders[78]. RNAi is a naturally occurring post-transcriptional gene-silencing mechanism for regulating cellular transcriptional activity through degradation or translation-arrest of the target mRNA[65]. The most extensively described form of RNAi acts through small interfering RNAs (siRNAs), which have complete sequence complementarity with the target mRNA. The siRNAs can be transfected into cells in their short active form or generated intracellularly from longer double stranded RNAs (dsRNAs)[22,79].

The safe and efficient delivery of siRNA specifically to target cells is essential to RNAi-based therapy, but remains a major challenge[80]. Many attempts have relied on modified viruses, which - while very efficient - are challenged by the possibilities of insertional mutagenesis, immune responses or severe systemic toxicity as well as scalability issues and the possibility of reversion to transmissible forms[8]. As a consequence, non-viral vectors, which are characterized by low host immunogenicity and easy manufacturability, have attracted considerable attention and successful development of a safe and efficient non-viral delivery system would be one of the most important achievements in medicine today[26,81].

Cationic polymers are attractive for delivery of siRNA (and DNA) since they are particularly easy to formulate with poly-anionic nucleic acids. The electrostatic interactions between the anionic phosphates in siRNA and the cationic moieties in the polymers can assemble the siRNA into nanoparticles - polyplexes - suitable for cellular uptake. Vectors based on polyethylenimine (PEI) were among the first to emerge and are still considered the gold standard in polymer based DNA delivery[53–55,60] and have also turned out to be efficient siRNA delivery agents *in vitro*[82–84].

In spite of the huge activity in the field and the broad use of cationic polymers as siRNA delivery agents, several aspects about their mode of action remain unclear. Polyplexes are generally believed to enter the cell via endocytosis, thus a primary research focus has been to ensure endosomal escape to avoid degradation in the lysosomes[85,86] and achieve release of the cargo into the cytosol. One of the key advantages of cationic polymers is their alleged ability to facilitate the so-called proton sponge effect[55], which is believed to be associated with endosomal/lysosomal escape of the polyplexes or their components. In PEI, the many protonated amines facilitate strong binding to siRNA to form polyplexes, while the unprotonated amines of PEI are able to absorb protons when the complex enters acidic compartments

(endosomes and lysosomes). The proton sponge effect is believed to result in excessive V-ATPase mediated $H^+$ influx, which leads to increased influx of $Cl^-$ and water, and in turn this may lead to osmotic swelling, destabilization and/or rupture of the lysosomal membrane and release of the siRNA into the cytosol[62]. However, the proton sponge effect is debated and incontrovertible experimental evidence remains elusive. An alternative hypothesis is that polyplexes are internalized via the caveolar pathway that bypasses the endolysosomal pathway altogether[87], but the existence of a physiologically relevant caveolar pathway with a role in constitutive endocytic trafficking is equally debated[35,88,89].

One limitation of PEI as a transfection agent has been the necessity to use PEIs of high average molecular weight (Mw) to achieve efficient transfection. Unfortunately, there is a direct correlation between the Mw and the toxicity of PEI[90]. Several approaches to circumvent this have been explored, one of the more promising being to use low-Mw PEI with low toxicity, e.g. PEI 2kDa[91], and improve the otherwise poor transfection efficiency of such PEIs by incorporating hydrophobic moieties onto the polymer amines. The hydrophobic substituents are expected to increase the ability of the PEIs to form polyplexes and increase the interaction of the polymer with the cell membrane. Such a beneficial effect of lipid substitution has been established in the context of plasmid DNA delivery for several cationic carriers[72,92] and more recently for delivery of siRNA[71,91,93,94].

An important aspect of polycation based gene delivery is the polymer/siRNA ratio necessary to obtain high transfection efficiency. This issue has been addressed thoroughly for PEI mediated DNA transfection[95–97], where it was found that a free (non-condensed) fraction of PEI is very important for achieving high transfection levels. However, as size, electrostatic charge and intracellular compartment of action differ for siRNA compared to DNA, it is not clear how a free fraction of PEI influences gene silencing. For *in vivo* use, a potential requirement for a free fraction for achieving high gene silencing efficiency is a major obstacle for the use of PEI and other polycations for non-viral gene delivery. Such systems are challenged by the fact that highly cationic entities will interact strongly with anionic blood constituents, the immune system and cells in general, and will therefore not allow for targeting of diseased tissue. In order to rationally develop efficacious siRNA carriers, it is essential that the interplay between the above-mentioned properties is understood.

In the present study we compare lipid derivatized PEI in the form of a dioleoylphosphatidyl-ethanolamine (DOPE)-bPEI 1.8kDa conjugate (DOPE-PEI) with conventional bPEI 1.8 kDa and bPEI 25kDa to establish to what extent the lipid conjugation alters the condensation properties of siRNA, cellular delivery and silencing of a reporter gene as well as to what extent the toxicity of the transfection agent is reduced. We further investigate and compare how PEI and lipid conjugated PEI affects the pH in the lysosomes, as an increase in lysosomal pH has been associated with the proton sponge effect. Lastly, we have systematically investigated the impact of lipid conjugation to bPEI in relation to the use of excess transfection agent beyond the requirement for full condensation of the siRNA (termed the "free fraction") and the silencing efficiency in comparison to bPEI itself.

## 3.3 Materials and Methods

### 3.3.1 Materials and Cell Lines

Branched PEI with a weight-averaged molar mass of 25,000 g/mol (bPEI 25kDa) and 1,800 g/mol (bPEI 1.8kDa) were purchased from Sigma-Aldrich (US) and used without further purification. Before use they were dissolved in MQ water to a concentration of 15.4 mM with respect to nitrogen and further diluted in Hepes buffed glucose (HBG: 10 mM Hepes, 5% w/v glucose, pH 7.4) as needed. DOPE-PEI was synthesized as described by Sawant et al.[72] and kindly supplied by Professor Vladimir Torchilin's laboratory as a lyophilized powder and dissolved in MQ water to a concentration 1 mg/mL and further diluted in HBG as needed. All siRNA duplexes were purchased from Eurofins MWG Operon (Germany): siRNA targeting green fluorescent protein (GFP-siRNA): 5′-GGCUACGUCCAGGAGCGCACC(dTdT)-3′ (sense) and siRNA targeting Luciferase (5′-CUUACGCUGAGUACUUCGA(dTdT)-3′ (sense). PicoGreen and Lipofectamine® RNAimax were purchased from Invitrogen (US) and Na-Heparin from porcine intestinal mucosa was purchased from Sigma-Aldrich (US). The CellTiter 96® AQueous Non-Radioactive Cell Proliferation Assay (MTS) was purchased from Promega (US).

The cell line HT1080 (human fibrosarcoma, ATCC no. CCL-121) was transfected to stably express luciferase and is referred to as HT1080pLUC. The cells were cultured at 37°C, 5% $CO_2$ in RPMI 1640 (Sigma-Aldrich) supplemented with 10% fetal bovine serum (FBS, heat-inactivated, Fisher Scientific), penicillin at 100 units/mL (pen), streptomycin at 100 mg/mL (strep), and Genticin

(G418) at 0.8 mg/mL (all from Sigma-Aldrich). For knockdown experiments the selection antibiotic, G418, was omitted from the culture medium.

### 3.3.2 Methods

*Preparation of polyplexes*

The N/P ratio of the present polyplexes is defined as the molar ratio of the total number of nitrogen atoms in the PEI segment of the polymer or lipid-cojugated polymer to the number of siRNA phosphates. Polyplexes with varying N/P ratios were formulated by adding a volume (≈35 µL) from an siRNA solution in water to an equal volume of a solution of cationic polymer diluted in HBG. The final siRNA concentration was kept constant while the bPEI concentration was varied with the different N/P ratios. Each resulting formulation mixture was first mixed by pipetting up and down 10 times, then vortexed gently for 15 s and then incubated for 45 min at RT before further use. The final concentration of siRNA in all formulation mixtures was 0.039 µg/µL.

*Size and ξ-potential of polyplexes*

The hydrodynamic diameter (particle size), polydispersity and ξ-potential of the polyplexes were determined using dynamic light scattering (DLS) on a ZetaPals (Brookhaven Instrument Corporation, Holtsville, NY, USA) at 25°C with an angle of 90°. Before ξ-potential measurements the electrode was conditioned in a 1 M KCl solution. Polyplexes were prepared as described above and diluted up to a volume of 1.75 mL in HBG and measured immediately after preparation. The particle size was determined by five runs of 30 s each on three separate preparations. ξ-potential determination of each sample was carried out by 10 runs with a target residual of $3.5 \times 10^{-2}$, three separate preparations per N/P ratio.

*PicoGreen exclusion assay and heparin competition assay*

The complex formation between siRNA and the cationic polymers was studied in an exclusion assay using the fluorescent intercalating dye PicoGreen. PicoGreen shows maximum fluorescence at 535 nm when it intercalates between the bases in double stranded RNA (and DNA) while showing virtually none in the absence of intercalation, and is thus a highly sensitive detector of accessible siRNA, in this case meaning uncomplexed siRNA. Polyplexes were prepared at different N/P ratios at RT as described above and transferred to a dark microtiter plate and PicoGreen solution was added. The fluorescence of the polyplex dispersions was measured 10 min after addition of PicoGreen. A Victor 3 plate reader (Perkin-Elmer, US) was used to measure the fluorescence ($\lambda_{ex}$ = 485 nm, $\lambda_{em}$ = 535 nm).

To study the dissociation of the polyplexes when exposed to a competing polyanion, increasing amount of heparin was added to the polyplex dispersions after 45 min incubation. When the negatively charged heparin is added to the dispersions of the polyplexes, it competes with the siRNA for binding to the cationic bPEI, potentially leading to the displacement of siRNA from the polyplex. The resulting mixtures were incubated for 30 min at RT and measured on the Victor 3 plate reader. The relative fluorescence values and thus the percentage of accessible (= uncondensed) siRNA were determined and reported as percent fluorescence of free siRNA in the absence of vector. All results are corrected for fluorescence quenching by heparin and each experimental condition was done in triplicates.

*Gel electrophoresis visualization of the siRNA condensation*

The polyplex formation between siRNA and the polycations was further evaluated using agarose gel electrophoresis; exploiting the fact that naked siRNA readily migrates in an agarose gel while polyplexes are retained in the wells. Each preparation of polyplex with a desired N/P ratio was loaded onto a 2% (w/v) agarose gel containing ethidium bromide (Sigma-Aldrich) in Tris-Acetate EDTA buffer. The amount of siRNA loaded into each well was 69 pmol in a total volume of 12 µL including loading buffer (1 mM cresol red in 0.6 M sucrose). The electrophoresis was performed at 50 V for 35 min and siRNA bands were visualized using a BioSpectrum® Imaging System (excitation at 480 nm, emission filter at 570-640 nm.)

*Knockdown of luciferase expression*

HT1080 pLuc cells, which stably expressed luciferase, were seeded in RPMI 1640 medium with 10% FBS, 5% pen/strep (complete medium) in 24-well plates 24 h prior to transfection (50,000 cells per well). The cells were washed with PBS, polyplexes formulated as described above were further diluted in RPMI 1640 medium with 5% pen/strep (serum free medium) and added to the cells resulting in a final concentration of 120 nM siRNA per well. The cells were incubated with polyplexes for 6 h, transfection medium was removed, and the cells were washed with PBS and incubated for an additional 22 h in complete medium. The cells were then washed once with PBS and lysed using 125 µL Reporter Lysis Buffer (Promega, US). Luciferase activity was measured using a luciferase assay[98] with D-luciferin (Caliper Life Sciences, US). Each sample was measured for 10 s on a luminometer (Lumat LB9507, Berthold, Germany). The total lysate protein concentration was determined using the BCA kit (Pierce, US) and the gene expression was normalized to the total protein concentration in the cell lysate and described as luciferase activity (relative light units) per µg protein. All knockdown assays comprised, as a positive

control, Lipofectamine® RNAimax using 30 pmol of siRNA. In addition, all assays comprised a non-sense control using siRNA directed against GFP as well as anti-luciferase siRNA administrated unassociated to vector. The non-sense control was prepared using N/P16 for DOPE-PEI and N/P3 for bPEI 25kDa and PEI 1.8kDa. Each experimental condition was done in triplicates.

In order to examine the importance of the free fraction, the extra vector material was diluted in serum free medium and added to cell cultures which had already been incubated for 2 h with polyplexes formulated for full condensation of the siRNA. Specifically, HT1080pLuc cells were incubated with polyplexes formed at the N/P ratio of full condensation for 2 h (N/P2 for bPEI 25kDa and N/5 for DOPE-PEI). Then, the free fraction was added to the incubations, resulting in a total N/P ratio of 3 for bPEI 25kDa and 16 for DOPE-PEI. The cultures were then incubated with the mix of fully condensed polyplexes and separately added free fraction for 1, 2, or 4 h resulting in a total incubation time of 3, 4 or 6 h. After end of incubation with the mix of polyplexes and separately added free fraction, the cells were washed in PBS, fresh complete medium was added and the cells were incubated to a total of 28 h until lysis and analysis of knockdown. Control cells were incubated in parallel with fully condensed polyplexes or optimally formulated polyplexes. Each experimental condition was done in triplicates.

*Radiolabeling of siRNA*

Luc siRNA (MWG Eurofins Operon, Germany) was labeled with radioactive $^{33}P$ using the kit for phosphorylation of DNA with T4 Polynucleotide Kinase (Fisher Scientific, US). The T4 Polynucleotide Kinase was used to catalyze the transfer of $^{33}P$ from [γ-$^{33}P$]-ATP (Perkin Elmer, US) to the free hydroxyl end (5') of luciferase siRNA. The reaction was stopped by addition of EDTA and the product was purified using the QIAquick nucleotide removal kit (Qiagen, Germany). Care was taken not to damage any secondary structure of the siRNA, accordingly the reaction mixture was never heated above 40°C.

*In vitro cellular uptake*

For experiments with parallel determination of uptake and knockdown, the siRNA was spiked with $^{33}P$ labeled siRNA. Knockdown assays were performed as described above and the experiments were terminated by removal of the medium, and the cells were washed with PBS containing 0.11 mg/mL heparin in order to remove polyplexes bound to the plasma membranes and once with PBS. The cells were then lysed as described above, luciferase and BCA assays were

performed, 65 µL lysate per population was mixed with 5 mL scintillation liquid (UltimaGold, Perkin Elmer, US), and radioactivity was measured as counts per minute using a scintillation counter (Beckman Coulter, US). Each experimental condition was done in triplicates.

*Cytotoxicity assay of polymers and polyplexes*

The cytotoxicity of free vector polymers and the corresponding polyplex dispersions was evaluated on HT1080 pLuc cells using the MTS assay (CellTiter 96® AQueous Non-Radioactive Cell Proliferation assay, Promega, USA). Cells were seeded in a 96-well plate at an initial density of 10,000 cells per well in complete medium. After 24 h, free vector polymers or polyplexes were added to the cells at varying concentrations in serum free medium. The cells were incubated at 37°C, 5% $CO_2$ for 24 h. The MTS working solution was then added to each well (20 µL). The cells were further incubated for 1 h at 37°C and absorbance was measured (490 nm, Victor 3 plate reader). Cytotoxicity was reported as percent cell viability using untreated cells as 100% (triplicate measurements).

*Ratiometric pH measurements in the endolysosomal compartment*

Measurements of endolysosomal pH was performed largely as described in[57,99]. Briefly, HT1080 cells were plated in Ibidi 8-well µ-slides (27,000 cells/well in 300 µL/well) in complete medium and incubated over-night. On day 2, medium was changed to complete medium with 25 µg/mL nanosensor. On day 3, cells were carefully washed once in PBS-Heparin (0.111 µg/mL heparin in PBS) and once in PBS in order to remove un-internalized nanosensor. Then vector polymers were added in the following concentrations: 0.73 µg/mL (bPEI 1.8kDa, bPEI 25kDa) and 5.7 µg/mL (DOPE-PEI) in imaging medium (full growth medium without phenol red). These concentrations are 10% higher than for any *in vitro* cell assay with polyplexes, but below a level where significant cytotoxicity is observed. Confocal images were recorded at 0, 2 and 6 h, where after the cells were washed once in PBS-Heparin and once in PBS. Additional images were then acquired 10 and 24 h after addition of bPEI. Images were captured by a Leica TCS SP5 confocal microscope with a 63x water-immersion objective. The microscope is equipped with an incubator box and $CO_2$ supply for optimal growth conditions during imaging. Images were acquired with fixed settings for all samples and the corresponding calibration curve. Two-color images were obtained by sequential line scanning with the following excitation/emission wavelengths: 488/493-560 nm and 561/566-680 nm. At each time point, before imaging the PEI treated cells, a control experiment was performed in order to optimize the microscope settings. One well containing cells unexposed to bPEI or PEI-derivative, but with nanosensor, was treated

with 200 nM Bafilomycin $A_1$ for 40 min and used to optimize microscope settings. This treatment increases the pH of the lysosomes and adjusting the imaging settings to achieve maximum signal for this sample, ensures optimal use of the dynamic range of the nanosensor. Ten images were acquired of this sample and of an untreated sample (no PEIs or Bafilomycon $A_1$, but with nanosensor) where after 15 images were acquired of each of the three PEI samples (per time-point). A calibration curve was prepared by diluting the nanosensor in buffers (20 mM phosphate/20 mM citrate/20 mM malate/100 mM NaCl) from pH 2.8-7.5 with a final nanosensor concentration of 10 mg/mL. Each solution (2.5 µL) was transferred to a diagnostic microscope slide, sealed with a cover glass and imaged. Image analysis was performed as described previously using a pixel based method[99]. Briefly, image processing was used in order to determine which pixels are actual signal from the nanosensor and the included pixels were then converted to pH via the calibration curve. pH histograms are presented as mean ± SEM. pH images were generated by coloring single pixels according to a linear pH color scale. Additionally, phase contrast images were acquired at 2, 6, 10 and 24 h time-points to confirm cell viability and illustrate non-toxic footprint of nanosensor.

## 3.4 Results

### 3.4.1 Cytotoxicity of vector polymers and polyplexes

To establish the toxicity profiles of bPEI 25kDa, bPEI 1.8kDa and DOPE-PEI, we used a cell viability assay (Promega's MTS kit) to investigate the free vector polymers (Fig. 3.1) and the siRNA containing polyplexes (Fig. 3.2).

Figure 3.1 shows that all three polymers are associated with some cytotoxicity with bPEI 25kDa being the most cytotoxic. Importantly, formulation of the vectors into polyplexes greatly diminishes this inherent cytotoxicity, most pronounced for bPEI 25kDa and DOPE-PEI (Fig. 3.2). The selected N/P ratios are those involved in subsequent *in vitro* knockdown studies as described later in detail.

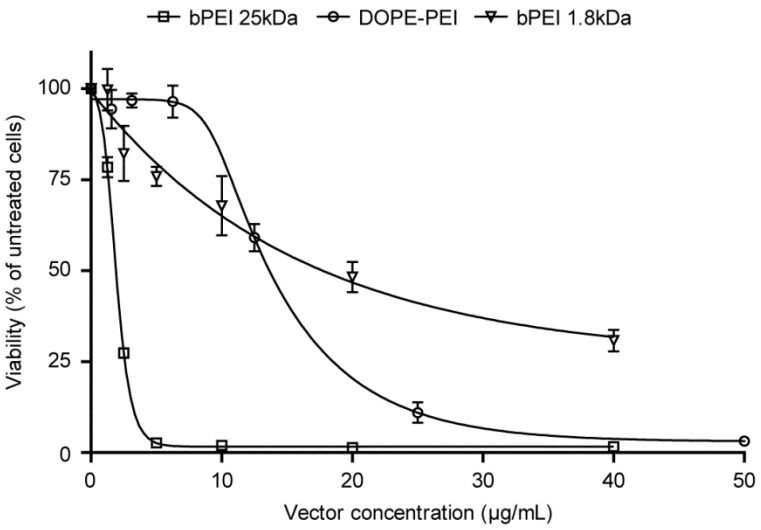


**Figure 3.1.** Cytotoxicity of vector polymers. The cells were treated with increasing concentrations of polymer for 24 h in serum-free medium before analysis by MTS assay. Results are presented as mean of triplicates ± SD. Trend lines are 5 parameter fits. Results are presented as mean of triplicates ± SD. Trend lines are 5 parameter fits. The figure is representative of three independent experiments.

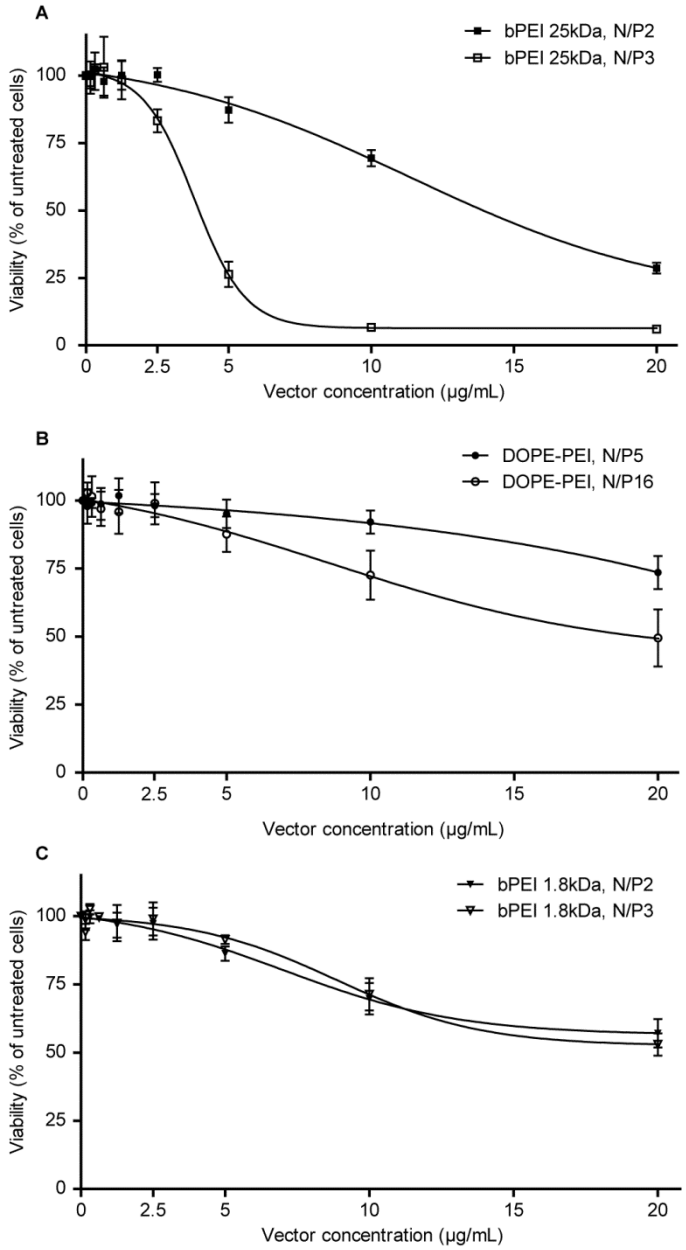


**Figure 3.2.** Cytotoxicity of polyplexes. A. bPEI 25kDa, B. DOPE-PEI, C. bPEI 1.8kDa. The cells were treated with increasing concentrations of polymer for 24 h in serum-free medium before analysis by MTS assay. For reference, the total vector concentration in our *in vitro* assays at N/P3 is 0.667 µg/mL (bPEI 25kDa, bPEI 1.8kDa) and 5.2 µg/mL at N/P16 (DOPE-PEI). Results are presented as mean of triplicates ± SD. Trend lines are 4 parameter fits. Representative of three independent experiments each.

### 3.4.2 Lysosomal pH

The proton-sponge effect remains the dominant hypothesis used to explain the ability of PEI to promote high transfection levels. We therefore measured the lysosomal pH in cells incubated with PEI 1.8kDa, DOPE-PEI, and bPEI 25kDa using a ratiometric nanosensor[57,99] to compare the lipid conjugated PEI with conventional PEIs.

Figure 3.3A shows that the pH distributions of the samples treated with bPEI 25kDa or DOPE-PEI do not differ from the untreated control cells, whereas the Bafilomycin A1 treated sample displays a significant increase in pH, confirming that the nanosensor is capable of measuring an increase in pH. The lysosomal pH is visually presented in Figure 3.3B which shows images from the 6 h time-point. A lack of change in color between the Control and DOPE-PEI treated cells indicates no change in pH. Finally, the pH as a function of time is presented in Figure 3.3C for the Control and DOPE-PEI treated samples under exactly the same conditions over a period of 24 h, and no change in pH is observed over time. Thus, we do not find that lipid conjugated PEI changes the pH in the endolysosomal compartment, which is thereby similar to our previous study evaluating the proton sponge effect of conventional PEI[57].

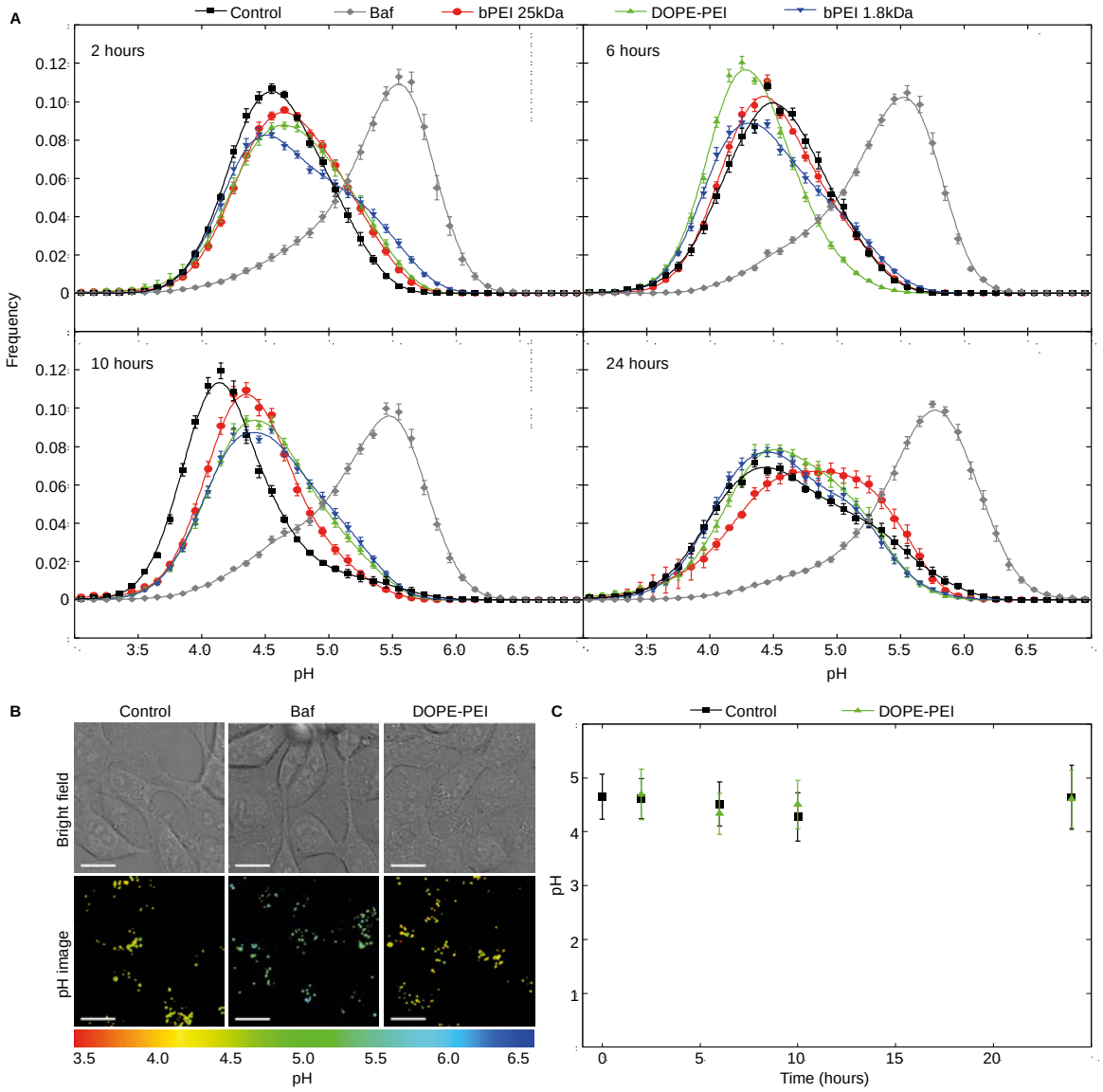

**Figure 3.3.** Lysosomal pH in response to bPEI 1.8kDa, bPEI 25kDa, DOPE-PEI or Bafilomycin A1. HT1080pLUC cells with internalized nanosensor for 16 h were treated with bPEI 1.8kDa, bPEI 25kDa or DOPE-PEI for 6 h and imaged at the indicated time points. A. Histograms showing pH distributions of nanosensor containing cells without further treatment (Control) or treated with bPEI 25kDa, bPEI 1.8kDa, DOPE-PEI or Bafilomycin A1 (Baf). Bafilomycin A1 was always added 40 min prior to measurement. Data points are mean values ± SEM. B. Representative images of cells obtained after 6 h of incubation. Top row: bright field images. Bottom row: pH images. The ratio of the original pH-sensitive and reference signals was converted to pH via a calibration curve and images color coded according to the linear pH scale. No difference is observed between the control cells and the DOPE-PEI treated cells, whereas a clear change in color from yellow/green to cyan can be observed between the control cells and the Bafilomycin A1 treated cells. C. Measurements of lysosomal pH in response to DOPE-PEI over time compared to untreated control cells. Presented is mean ± SD of the pH frequency distributions obtained in A. Time-point zero was collected just before addition of vector. Representative of three independent experiments.

Phase contrast images (Supplementary Fig. 3.1) indicate that the combined exposure to nanosensor and bPEI / bPEI-derivative has a minimal impact on cell viability at the concentrations used. Furthermore, we have previously established that the nanosensor does not affect cell viability[57,99].

### 3.4.3 Size and ξ-potential of the polyplexes

Size and charge of polyplexes greatly influence the efficiency of cellular uptake. Therefore, the complex formation of bPEI 1.8kDa, bPEI 25kDa and DOPE-PEI with siRNA was characterized. In HBG, all three vectors are able to condense the siRNA cargo into small particles with DOPE-PEI consistently forming the smallest particles (Fig. 3.4A). The ξ-potentials of the polyplexes are positive at N/P ≥ 3 for bPEI 1.8kDa and bPEI 25kDa, or at N/P ≥ 6 for DOPE-PEI (Fig. 3.4B). The slightly higher N/P ratio for transition from negative to positive ξ-potential for DOPE-PEI reflects the altered condensation properties of this vector due to the lipid conjugation.

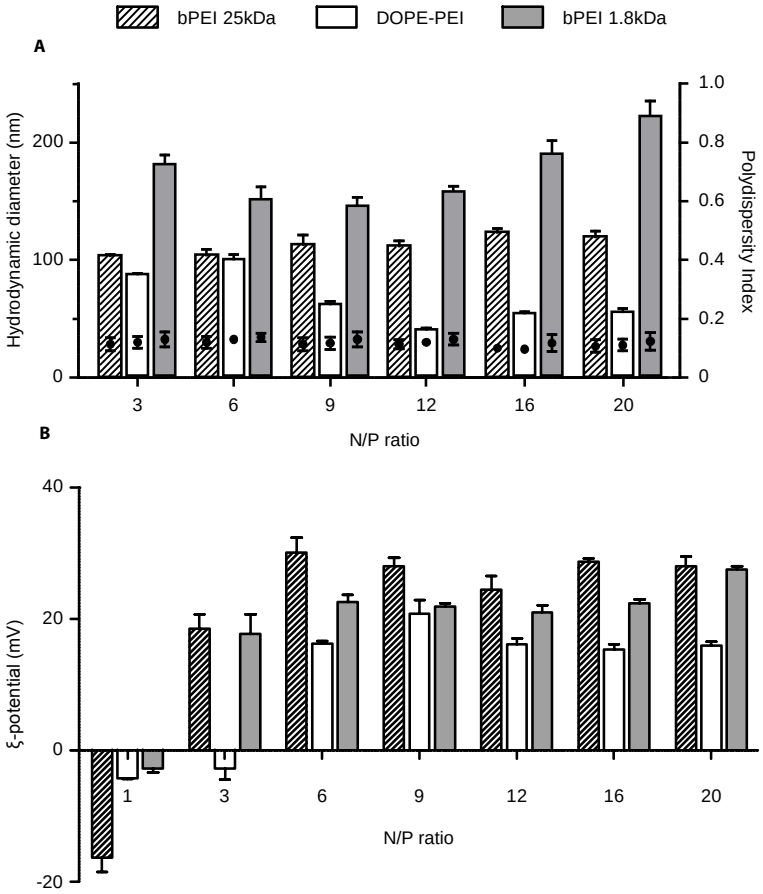


**Figure 3.4.** Size and ξ-potential as a function of N/P ratio. Scatter symbols represent polydispersity for the corresponding polyplex. A. Size measured in 10 mM Hepes, 5 % w/v Glucose, pH 7,4 (HBG). B. ξ-potential measured in HBG. Three separate preparations per N/P ratio, error bars represent SD.

### 3.4.4 Condensation and decondensation properties of the polypolexes

The balance between cargo condensation extracellularly and dissociation intracellularly is crucial for efficient transfection, and previous reports have indicated full condensation of siRNA cargo by bPEI 1.8kDa at N/P2 and DOPE-PEI at N/P3[94]. We examined the ability of all three polymers to condense siRNA using the PicoGreen exclusion assay as well as gel-shift assays. The differences in condensation behavior of the three polymers are depicted in Figure 3.5, which shows that bPEI 1.8kDa and bPEI 25kDa reaches full and similar condensation of the siRNA at N/P2 in agreement with literature[94]. In contrast, DOPE-PEI does not reach full condensation until N/P5. These results are supported by the gel-shift assays (Supplementary Fig. 3.2) as well as the ξ-potential measurements (Fig. 3.4B).

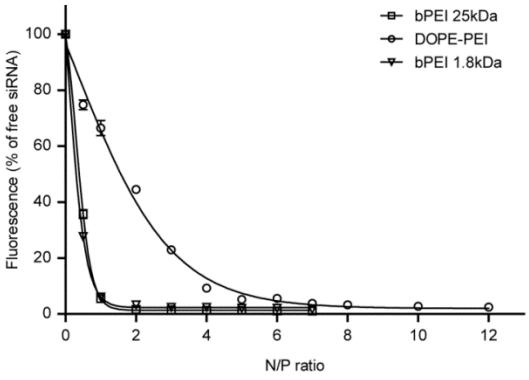


**Figure 3.5.** Condensation of siRNA by bPEI 25kDa, DOPE-PEI and bPEI 1.8kDa. Condensation assessed by PicoGreen exclusion following addition of increasing amounts of vector to a constant amount of siRNA. The PicoGreen fluorescence intensity for siRNA in the absence of any vector was set to 100%. Results are presented as mean of triplicates ± SD. Trend lines are 5 parameter fits. Representative of four independent experiments.

Anionic competition for binding to the vector polymers is one way to assess the strength of the siRNA-vector association, and we therefore monitored the heparin-induced release of siRNA or decondensation of the polyplexes through the fluorescence intensity of PicoGreen (Fig. 3.6). Surprisingly, bPEI 25kDa polyplexes were the most vulnerable to competition from heparin as they decondense to a level of 40% PicoGreen accessibility (percentage relative to free siRNA). In contrast, bPEI 1.8kDa and DOPE-PEI reaches plateaus of PicoGreen accessibility of only 5% and 10%, respectively.

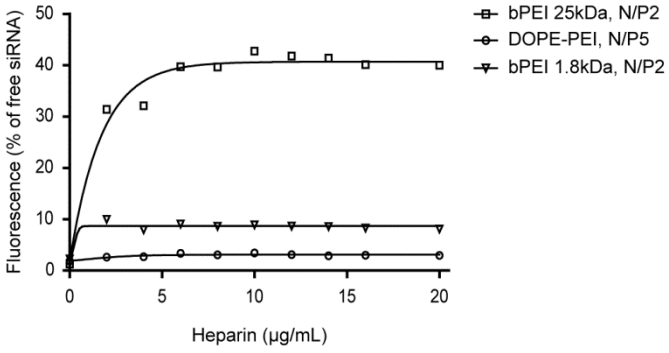


**Figure 3.6.** Heparin induced decondensation of polyplexes. Increasing amounts of sodium heparin was added to the polyplex dispersions and incubated for 30 min before PicoGreen assay. The PicoGreen fluorescence intensity for siRNA in the absence of any vector was set to 100%. Results are presented as mean of triplicates ± SD. Trend lines are 5 parameter fits. Representative of three independent experiments.

### 3.4.5 *In vitro* knockdown studies

To systematically analyze and compare the performance of bPEI 25kDa, bPEI 1.8kDa and DOPE-PEI as delivery agents of siRNA, we established the optimum balance between knockdown and induction of cytotoxicity in an HT1080pLUC cell line. bPEI 1.8 kDa was unable to suppress

expression of luciferase (Fig. 3.7C), while bPEI 25kDa showed efficient knockdown, reaching a plateau of maximum knockdown at N/P3 (Fig. 3.7A). Lipid conjugation of bPEI 1.8kDa transformed the polycation into an efficient transfection agent reaching a plateau of maximum knockdown at N/P16 (Fig. 3.7B). Above these N/P ratios the cytotoxic impact of the polyplexes gradually became apparent. We therefore conclude that bPEI 25kDa at N/P3 and DOPE-PEI at N/P16 strike an optimal balance between knockdown and absence of cytotoxicity and regarded these formulations as optimal. For referencing with Figure 3.1 and 3.2, these N/P ratios translate to 0.67 µg/mL (bPEI 1.8kDa and 25kDa) and 5.2 µg/mL (DOPE-PEI) in our *in vitro* assays, where none of the transfection systems show toxicity.

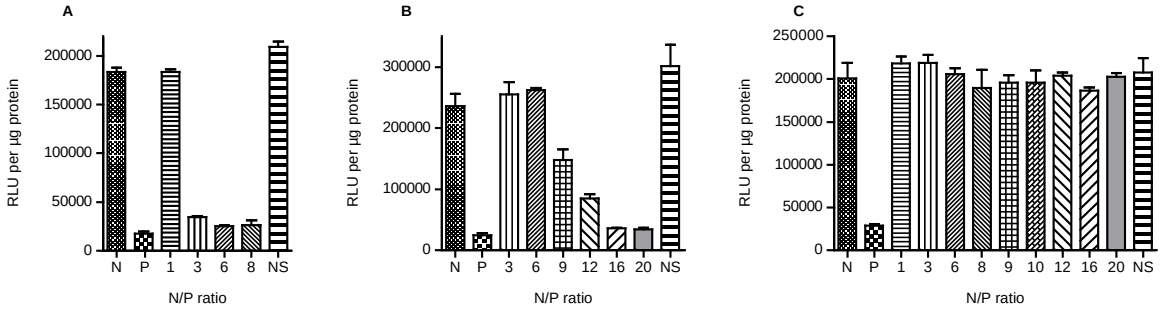


**Figure 3.7.** *In vitro* knockdown of luciferase expression. A: bPEI 25kDa, B: DOPE-PEI, C: bPEI 1.8kDa. N = Negative control cells, P = Positive control cells (RNAimax), NS = Non-sense siRNA (anti-GFP siRNA). Cells were incubated in serum-free medium for 6 h with polyplexes prepared at varying N/P ratios in serum-free medium, washed and incubated in complete medium for 22 h. RLU = relative light units. Results are presented as mean of triplicates ± SD. Representative of three independent experiments.

The results of Figure 3.3-3.7 demonstrate that excess of vector is also necessary in the case of siRNA cargo in order to realize the full transfection potential of each vector. However, compared to similar experiments with DNA using bPEI 25kDa[95], it is notable that the N/P ratio necessary to achieve maximum knockdown is much lower with siRNA than DNA cargo (N/P3 vs N/P8, respectively).

As efficient knockdown required use of vector material in excess of what was required for full siRNA condensation, we wanted to investigate the role and importance of this vector fraction (the “free fraction”) and how the lipid conjugation affected the behavior of the free fraction compared to the conventional bPEI 25kDa (Fig. 3.8). This was assessed as the ability of the free fraction to improve the knockdown capability of polyplexes formed at the N/P ratio for full condensation. We therefore incubated our reporter cell line with fully condensed polyplexes for two hours, added free vector, incubated further, washed to remove uninternalized material, and incubated to a total of 28 h before analysis of knockdown.

DOPE-PEI and bPEI 25kDa differ in the degree to which delayed addition of the free fraction results in as large a knockdown as optimal N/P ratios. For bPEI 25kDa, delayed addition of the free fraction results in a knockdown, which is statistically identical to the populations that were incubated with polyplexes formulated with the optimal N/P ratio (Fig. 3.8A-C). For DOPE-PEI, delayed addition of the free fraction increases the knockdown but not to the level of optimally formulated particles (N/P16) (Fig. 3.8D-F). This indicates that lipid conjugation does change the behavior of bPEI with respect to the mechanism of action.

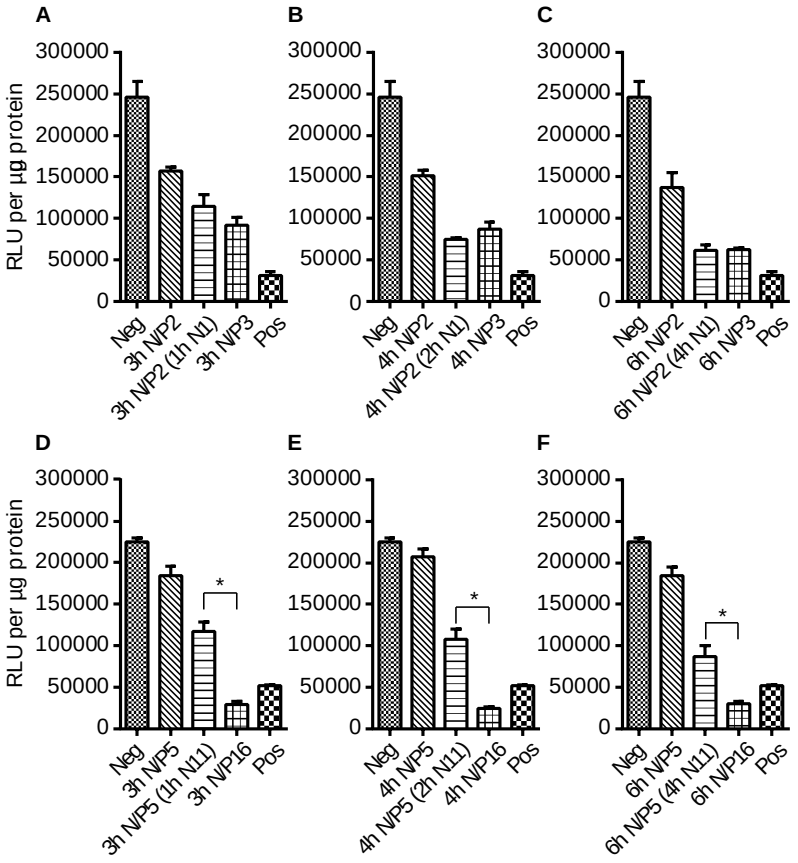


**Figure 3.8.** *In vitro* knockdown of luciferase expression with delayed addition of the excess fraction of vector. A-C: bPEI 25kDa, D-F: DOPE-PEI. The cells were incubated in serum-free medium with fully condensed polyplexes for 2 h, followed by addition of the free polymer and incubation for 1 h (A and D), 2 h (B and E), or 4 h (C and F) to a total incubation time with polyplexes and polymer of 3, 4 or 6 h. The cells were then washed and incubated to a total of 28 h in complete medium. Neg = Negative control cells, Pos = Positive control cells (RNAimax). For example (A and D): "3h N/P2" and "3h N/P5" = cells incubated for 3 h with fully condensed polyplexes – no free polymer added. "3h N/P3" and "3h N/P16" = cells incubated for 3 h with optimally formulated polyplexes – no free polymer added. "3h N/P2 (1h N1)" and "3h N/P5 (1h N11)" = cell incubated for 2 h with fully condensed polyplexes, where after free polymer was added to a total polymer amount corresponding to optimally formulated polyplexes, the cell were incubated for 1 h, washed and incubated until harvest and analysis. RLU = relative light units. Results are presented as mean of triplicates ± SD. Representative of three independent experiments. (*) = significantly different by t-test ($p < 0.005$).

### 3.4.6 Uptake

To elucidate how the N/P ratio influenced the uptake and concomitant knockdown, and to see if polyplexes of DOPE-PEI behaved differently than polyplexes of conventional bPEIs, we performed *in vitro* knockdown assays using radioactively labeled luciferase siRNA (Fig. 3.9).

The knockdown profiles in Figure 3.9 confirm the trends from Figure 3.8, i.e. a large knockdown by RNAimax (85%), bPEI 25kDa at N/P3 (77%) and DOPE-PEI at N/P16 (86%), a small knockdown by bPEI 25kDa at N/P2 (34%) and complete absence of knockdown from bPEI 1.8kDa at N/P2 and 3, DOPE-PEI at N/P5 and uncomplexed siRNA. These observations correlate well with the uptake data, to the extent that bPEI 25kDa at N/P3 and DOPE-PEI at N/P16 show relatively high siRNA uptake levels compared with very low uptake levels for bPEI 1.8kDa at N/P2 and 3 and uncomplexed siRNA. However, considerable complexity is added by the following observations: 1) bPEI 25kDa at N/P2 consistently induces a significantly higher siRNA uptake than bPEI 25kDa at N/P3 ($p < 0.001$), but bPEI 25kDa at N/P2 induces only a small knockdown, 2) DOPE-PEI at N/P5 is taken up to a considerable extent but induces no knockdown, and 3) RNAimax is never internalized to more than 2% of the available siRNA but remains as efficacious as DOPE-PEI at N/P16 and bPEI 25kDa at N/P3.

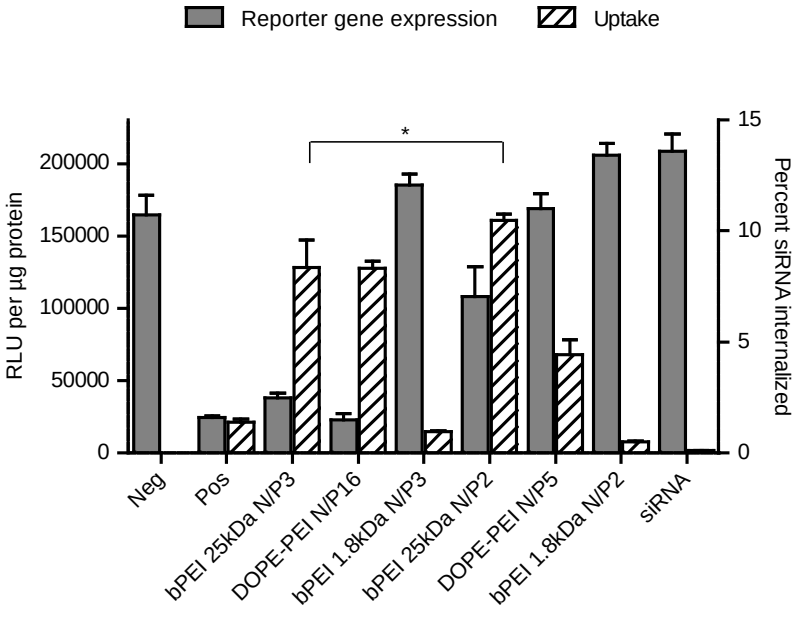


**Figure 3.9**. *In vitro* determination of siRNA internalization and knockdown of luciferase expression. The cells were incubated with polyplexes of the indicated N/P ratio for 6 h in serum free medium. The cells were then washed with PBS, incubated for 22 h in complete medium, washed 1x with PBS-heparin, 1x with PBS, and analyzed for both knockdown of luciferase expression and uptake of siRNA. Neg = Negative control cells, Pos = Positive control cells (RNAimax), siRNA = cells incubated with siRNA in the absence of vector, RLU = relative light units. Results are presented as mean of triplicates ± SD. Representative of three independent experiments. (*) = significantly different by t-test ($p < 0.001$).

## 3.5 Discussion

Safe and efficacious delivery of siRNA to the cytoplasm of target cells is a prerequisite for knockdown of a target gene. Detailed knowledge of the interaction between the vector polymers and the siRNA cargo as well as between the polyplexes and the cells is necessary, if rational and focused design of siRNA delivery systems shall become possible. PEI has been extensively characterized for DNA delivery on the mechanistic level[95–97,100]. For instance, it has been shown that high efficiency is achieved at N/P > 8[95,100], while full condensation of the DNA is reached at N/P3-4[95,96,101]. This indicates an important role of the fraction of vector that is in excess of the amount necessary to form the polyplexes, and the excess fraction has been speculated to be free in solution or at least only weakly associated to the nucleic acid-containing polyplex. siRNA delivery by PEI has been much less studied, but as size and electrostatic density of the cargo as well as intracellular compartment and molecular machinery of action differ for siRNA in comparison to DNA, it is not possible to directly extrapolate mechanistic results from DNA to the delivery of siRNA[102]. Therefore, the mechanistics of siRNA delivery using bPEI and a lipid conjugate of bPEI has been investigated in this study.

At similar polycation concentrations, fully condensed polyplexes based on DOPE-PEI display lower cytotoxicity than fully condensed polyplexes with bPEI 1.8kDa and bPEI 25kDa (Fig. 3.2, filled symbols). Further, at the concentrations relevant to our assays, lipid conjugation of bPEI 1.8kDa does not appear to have increased the inherent cytotoxicity of bPEI 1.8kDa (Fig. 3.1) in spite of DOPE having high membrane affinity and fusogenic capability[103,104]. However, comparing polyplexes of bPEI 25kDa and DOPE-PEI at the optimal N/P ratios (Fig. 3.2A and B) shows that there is no large beneficial effect of DOPE-conjugation in terms of a reduction of cytotoxicity. While DOPE-PEI based polyplexes are less cytotoxic than polyplexes based on bPEI 25kDa at corresponding vector concentrations, this benefit is eliminated by the larger amounts of DOPE-PEI necessary to achieve the same knockdown effect as with bPEI 25kDa. On the other hand, DOPE-PEI may have advantageous formulation properties; the hydrocarbon moiety of DOPE-PEI could be used to enable formulation into liposomes or establish otherwise impossible lipid-lipid interactions as described by Sawant et al. with DNA cargo[72].

One aspect where DNA and siRNA polyplexes formed using bPEI differ is the stability against polyanions such as heparin; siRNA polyplexes with bPEI 25kDa are much more sensitive to heparin mediated decondensation than siRNA polyplexes with bPEI 1.8kDa and DOPE-PEI. This was surprising since we have observed the opposite for DNA. Here, a heparin:DNA ratio of 10

results in 15% decondensation for bPEI 25kDa-polyplexes and 70% for bPEI 1.8kDa-polyplexes, showing that bPEI 25kDa-based DNA-polyplexes are far more resistant to heparin-induced decondensation than bPEI 1.8kDa DNA-polyplexes (unpublished results). This difference between DNA and siRNA is probably due to the smaller size of the siRNA duplexes compared to the much larger DNA plasmids. Thus - in the case of siRNA - bPEI 1.8 kDa and DOPE-PEI seem to have stronger interactions with the cargo than bPEI 25kDa, possibly due to the higher conformational rigidity of the latter[105].

The size measurements in HBG (Fig. 3.4A) demonstrate that all three polycations are able to condense siRNA and form particles that are smaller than 200 nm, which is believed to be the upper size limit of clathrin-mediated endocytosis[106]. Furthermore, the ξ-potential measurements, PicoGreen exclusion and gel shift assays (Fig. 3.4B, Fig. 3.5 and Supplementary Fig. 3.2, respectively) confirm that at the N/P ratio that gives optimal transfection efficiency (N/P3 for bPEI 25kDa and N/P16 for DOPE-PEI), excess free vector material is present. In addition, the cytotoxicity results (Fig. 3.1 and 3.2) show that the free vector polymers are much more cytotoxic than polyplexes containing an equivalent amount of polymer, and that the toxicity increases markedly when going from N/P2 to N/P3 for bPEI 25kDa or from N/P5 to N/P16 for DOPE-PEI. Combined, these data support that at the optimal N/P ratios two vector fractions exist, one that is tightly bound in the core polyplex and one which is less tightly associated (a free fraction), each fraction with potentially different functions in the transfection process.

The results demonstrate additional key differences between siRNA and DNA condensation as well as differences between the regular bPEIs and the lipid conjugate. Firstly, bPEI 25kDa condenses siRNA better than DNA[95,97], probably due to the smaller size of the siRNA duplexes compared to the DNA plasmid. Secondly, DOPE-PEI reaches maximum condensation at a much higher N/P ratio than the free bPEIs. This could be due to polyplex formation having to compete with the amphipathic DOPE-PEI's tendency to self-associate, which would lower the effective concentration of DOPE-PEI available for polyplex formation. Alternatively, it could be the consequence of DOPE-PEI not being able to pair as many of its charged nitrogens as regular bPEI due to its self-association properties and steric hindrance. The idea that lipid conjugation can diminish the effective charge of the PEI segment resembles experiences from studies on antimicrobial lipopeptides and their partitioning into cell membranes[107].

The observation that a free fraction of vector is necessary for efficient knockdown, led us to examine the role of the free vector. The results from simultaneous determination of knockdown and siRNA uptake and experiments with delayed addition of the free fraction, demonstrate the complexity of the process of siRNA delivery using bPEI 25kDa and DOPE-PEI as well as further important differences between bPEI 25kDa and DOPE-PEI.

For bPEI 25kDa, the delay experiments indicate that the free fraction is not associated to the siRNA-containing polyplexes. This observation is based on the results obtained from adding a free vector fraction to cells separately from the fully condensed siRNA-containing polyplexes formed at N/P2, where knockdown efficiencies were achieved that were similar to those achieved with optimally formulated polyplexes (Fig. 3.8A-C). DOPE-PEI does not fully share the behavior of bPEI 25kDa. Even though delayed addition of the free fraction does have a significant impact on the knockdown, it does not reach the level of knockdown of optimally formulated polyplexes (N/P16) (Fig. 3.8D-F). This is likely due to the amphipatic nature of DOPE-PEI, which gives it a tendency to self-associate and results in a different siRNA condensation behavior.

The siRNA uptake data (Fig. 3.9) demonstrate that the polyplexes based on bPEI 25kDa N/P3 and DOPE-PEI N/P16 are internalized to approximately the same extent, corresponding well with induction of comparable knockdown in our HT1080 cell line. Conversely, polyplexes based on bPEI 1.8kDa are unable to induce knockdown and show only limited uptake, demonstrating that lipid conjugation of low Mw bPEI with the intent to increase membrane interaction is a constructive strategy[71,72]. However, a puzzling and mechanistically interesting observation is the higher uptake of siRNA by bPEI 25kDa at N/P2 compared to bPEI 25kDa N/P3 ($P < 0.001$). This increased uptake occurs without resulting in a large knockdown. The presented data indicate that the free fraction exerts its influence separately from the siRNA-containing core polyplexes, and the higher uptake by N/P2 than N/P3 bPEI 25kDa polyplexes suggest that the free fraction plays a role after uptake, e.g. by facilitating endosomal escape through the proton sponge mechanism. Another possibility is that the free fraction activates an alternate route of uptake which bypasses the lysosomal compartment altogether, and thus - while resulting in a lower absolute uptake of siRNA - causes the siRNA to be taken up via a route which more efficiently directs the siRNA to its intracellular target location. This alternative route could be the proposed caveolar pathway[87], or it could be another form of internalization such as direct local destabilization of the plasma membrane influenced by cross linking of membrane glycoproteins and proteoglycans. Such a scenario was recently proposed for lipoplex uptake[32] where a small

*but efficacious* uptake of siRNA through a form of direct membrane fusion was hypothesized to induce the observed knockdown, while the siRNA taken up through clathrin-mediated endocytosis remained trapped in the lysosomes and thus had no effect.

It is widely reported that bPEI 1.8kDa is inefficient for DNA delivery while bPEI 25kDa is highly efficient[95], and we confirm this trend for siRNA. Many published reports on DNA transfection have compared polyplexes of these two polymers prepared at the same N/P ratio, which should provide the two polymers with equal proton-sponge capability. Our data shows that it is the internalization step that causes the efficiency gap between bPEI 1.8kDa and bPEI 25kDa, not necessarily the ability to induce endosomal escape. This hypothesis is in agreement with the work of Navarro and coworkers[108], who reported that the use of high N/P ratios and chloroquine did not enable bPEI 1.8kDa to induce knockdown. It is likely that it is the interaction with the plasma membrane that differs, although the specific mechanism for this membrane interaction remains to be elucidated. One structural advantage of bPEI 25kDa over bPEI 1.8kDa could be the ability to more efficiently cross-bind multiple anionic membrane proteins on the target cell plasma membrane, potentially influencing the uptake process through this interaction. Indeed, cross-binding of cell surface receptors has been shown to be able to induce clathrin-mediated endocytosis through signaling[109,110] and it would be compatible with the uptake improvement observed for lipid conjugated bPEI 1.8kDa, since lipid conjugation may increase membrane interactions and therefore potentially improve bPEI 1.8kDa's ability to induce endocytosis. Alternatively, it is possible that insertion of the lipid portion of DOPE-PEI into the plasma membrane induces membrane invaginations, which may facilitate endocytosis similar to observations by Cheng and coworkers[111].

The proton sponge effect has been hypothesized to cause an increase in the pH and osmotic swelling of PEI-containing lysosomes resulting in loss of membrane integrity and leakage of the nucleic acid cargo into the cytosol[55,62]. We have previously shown that no change in lysosomal pH can be observed for bPEI 25kDa[57]. However, DOPE-PEI shows different properties and behavior, and as the free fraction appears to play a role after polyplex uptake, we investigated if the lipid conjugation would change the ability of DOPE-PEI to influence lysosomal pH. We measured the pH in the lysosomes of cells exposed to the three vectors, but were unable to measure any perturbation of the pH by any of the PEIs compared to the untreated control cells. The positive control cells treated with Bafilomycin A1 displayed the expected increase in pH. However, even though we do not observe an increase in pH, the PEI polymer could still cause

influx of first $H^+$, then $Cl^-$ and water but with the V-ATPase being able to compensate and maintain the pH in the lysosomes. Osmotic swelling may then cause transient leakage events resulting in release of siRNA into the cytosol. The end result would be endosomal escape assisted by the proton sponge effect but without a concomitant drop in pH.

Finally, the efficiency of induced knockdown versus siRNA uptake is much lower for all the tested PEI vectors compared to the commercial control, RNAimax. The latter is noticeably more efficient than both bPEI 25kDa and DOPE-PEI with an uptake percentage that never exceeds 2% (of the siRNA) while inducing a knockdown comparable to bPEI 25kDa and DOPE-PEI. This high efficiency is attractive, as less interaction with both siRNA and vector polymers potentially lower the cytotoxicity.

## 3.6 Conclusions

Our experiments demonstrate the complexity of the cell-polyplex interactions. The importance of the free fraction for bPEI 25kDa and DOPE-PEI is evident - in its absence, the vectors are substantially less efficient. The considerable uptake of polyplexes of bPEI 25kDa at N/P2 and DOPE-PEI at N/P5 without concomitant knockdown indicates that the most important role of the free fraction is after internalization. Regardless of the specific role of the free fraction, future development of delivery systems for siRNA should consider the presence and potential role of a free vector fraction and how this can be controlled for *in vivo* delivery purposes. Lipid conjugation of bPEI 1.8kDa does not in itself provide the solution to the high cytotoxicity of bPEI 25kDa or the low efficiency of bPEI 1.8kDa. However, DOPE-PEI's ability to form lipid-based interactions may enable it or a similar compound to be formulated into e.g. liposomes that can have *in vivo* transfection potential.

## 3.7 Supplementary Figures

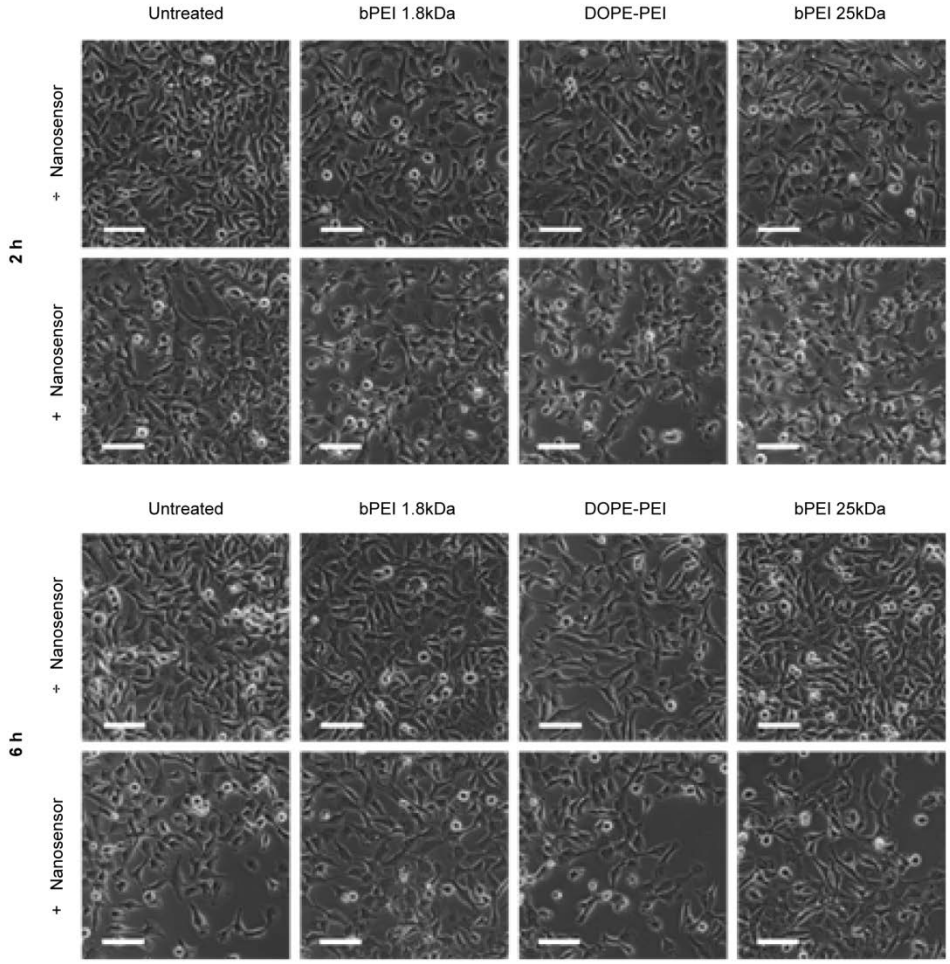


**Supplementary Figure 3.1.** Phase contrast images of HT1080pLUC cells exposed to pH-nanosensor and/or different bPEIs. HT1080 cells were either treated with nanosensor for 16 h (+Nanosensor) or left without nanosensor (÷Nanosensor) for the same time. Cells with and without nanosensor were then treated with either of the following PEIs: bPEI 1.8kDa, bPEI 25kDa or DOPE-PEI for up to 6 h or left untreated, followed by washing and incubation up to 24 h. Phase contrast images were captured of the cells after 2, 6, 10 and 24 h. Scale bars, 75 µm.

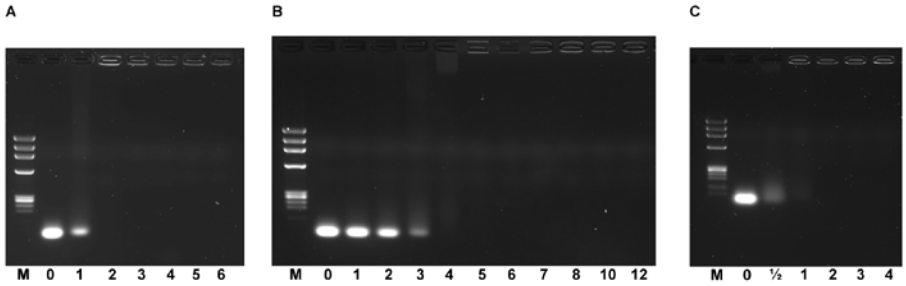


**Supplementary Figure 3.2.** Condensation of siRNA by bPEI 25kDa (A), DOPE-PEI (B), and PEI 1.8kDa (C), visualized by gel electrophoresis. Identical amounts of siRNA in all lanes. The numbers below the lanes refer to N/P ratios, 0 = free siRNA, M = MW marker.

# 4 Concluding remarks on Project I

Project I demonstrates some fundamental challenges facing siRNA delivery using polycations such as the bPEI 25kDa and DOPE-PEI. Both vectors are crucially dependent on the co-delivery of a free vector fraction to efficiently induce knockdown. Project I indicates that the free fraction exerts its influence quite independently of the fraction used for siRNA condensation, with this effect being clearest for the conventional bPEI 25kDa. Further, while lipid conjugation of PEI may introduce new formulation opportunities, Project I illustrates that cytotoxicity remains a challenge.

The need for controlled co-delivery of the free fraction necessitates some form of spatially restricted delivery vehicle which can encapsulate the core polyplex and the free fraction and provide this co-delivery capability. The extension of the delivery system with an encapsulating vehicle might also provide the opportunity to functionally separate the bound and the free vector fraction and enable the use of low MW PEI for siRNA condensation, which would be attractive in an effort to minimize cytotoxicity. Furthermore, as Project I demonstrates that the poor performance of bPEI 1.8kDa could be due to poor uptake rather than a proven inability to facilitate endosomal escape, an encapsulating vehicle might present an opportunity to eliminate the use of high MW PEI for transfection altogether.

On the other hand, it might also be possible to find a better lysosomotropic agent than free polycation. More importantly, cationic lipids are able to condense nucleic acids themselves. In project I, Lipofectamine® RNAiMAX even compared favorably with polycation-based polyplexes in terms of induced knockdown per internalized amount of siRNA. As the latter indicate that a higher fraction of the siRNA delivered by cationic lipids reaches the cytosol than is the case for siRNA delivered by PEI or DOPE-PEI, Lipofectamine® RNAiMAX may either be internalized by another route, more efficient at facilitating endosomal escape or otherwise superior downstream of internalization. To conclude, rather than developing a delivery system based on encapsulated siRNA-PEI polyplexes, it might be more straightforward to base a delivery system on cationic lipids, which would likely reduce the complexity of the delivery system.

# Project II – Cancer Immunotherapy

## 5 Background

### 5.1 Cancer immunotherapy - concept and current state

With gene therapy realistically being some years from reaching the clinic and traditional chemotherapeutics by nature showing low discrimination between malignant and healthy cells, much faith has been put into cancer immunotherapy both as a stand-alone treatment strategy and in combination with other types of treatment.

This optimism rests on the advances in general immunobiology and tumor immunology, which have made it clear that in many cases the tumors are recognized by the immune system as pathogenic growths in spite of the limited difference between the tumor cells and the host tissue. Consequently, the host immune system usually attempts to mount an immune response, which for a variety of reasons is ineffective at eliminating the tumor[112].

While the concept of manipulating the powerful and highly specific immune system for treatment of cancer has been considered extremely attractive for a long time[113], the practical implementation has been slow, partly owing to insufficient understanding of the complexity of the immune system as well as tumor biology.

The first clinically used therapies, which could claim to be immunotherapies, were the passive transfer of anticancer monoclonal antibodies and donor T cells, the latter in the context of allogeneic bone marrow transplantation. Both strategies have shown good efficiency in the treatment of a variety of malignancies[114] and the current arsenal of therapeutic anticancer

antibodies (Abs) comprises 14 distinct molecules targeting 9 different antigens, with many more in clinical trials[115]. While studies have indicated that the therapeutic Abs also stimulate adaptive immune responses in some settings, they mainly work through interference with oncogenic pathways[4]. Therefore, although both Ab therapy and allogeneic bone marrow transplantation reflect the ability of the donor cells or Abs to induce an immediate immune reaction against the cancer and are a testament to the power of the components of the immune system, these therapies are usually not considered "real" immunotherapies. The active stimulation of specific and durable antitumor immunity has proved to be a more challenging objective, the notable exception from the numerous failures being intravesical injection of live bacillus Calmette-Guerin used in the treatment of superficial bladder cancer[116].

## 5.2 Mechanisms of cancer immunity and opportunities for intervention

To achieve an anti-cancer immune response, three key actions must be performed by the components of the immune system (Fig. 5.1):

1. Antigen-presenting cells (APCs), i.e. dendritic cells (DCs), must sample tumor derived antigens under activating conditions
2. Activated DCs must generate cancer specific T cells
3. Cancer-specific T cells must enter the tumor tissues and perform their functions in cooperation with activated macrophages

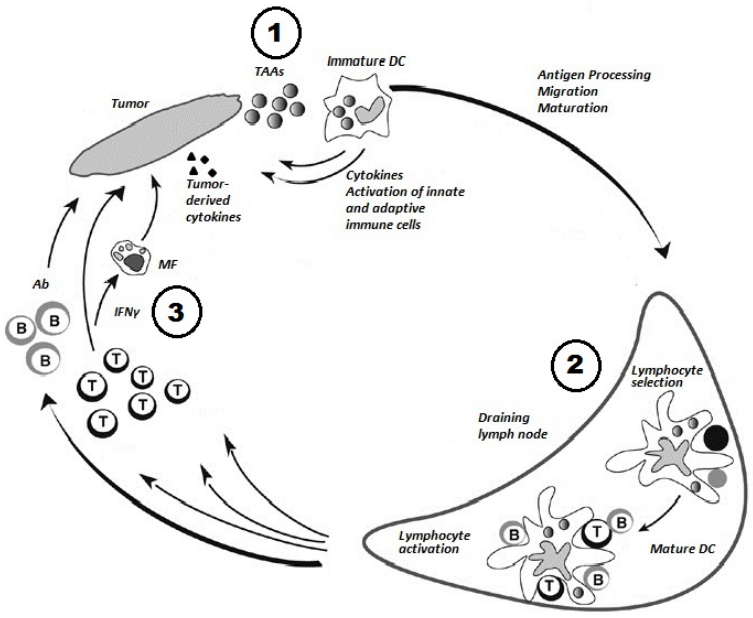


**Figure 5.1.** Overview of the fundamental steps involved in generation of antitumor immunity. **1**: TAAs are sample by DCs. In the presence of sufficient co-stimulatory signals DCs mature and migrate to draining lymph nodes. **2**: Antigen is (cross)-presented by matured DCs, which are able to stimulate naive adaptive effector cells. **3**: Activated, TAA-specific adaptive effector cells migrate to the tumor tissues and eliminate the malignant cells. Adapted from[117].

Each of these three steps represents monumental challenges for the immune system. Tumor-associated antigens (TAAs) do exist and may for instance reflect one or more of the many mutated proteins that are typical of the cancer or the products of non-mutated genes that are preferentially expressed by cancers. However, they may not be sufficiently abundant or immunogenic[114]. If TAAs are ingested in sufficient quantity by the DCs, the crucial second signal – such as stimulation of the DCs through Toll-like receptors (TLRs) or CD40 – may be absent. This will result in insufficient activation/maturation of the DCs and tolerance rather than migration to the lymph node and presentation of the ingested antigen. If the DCs migrate to the lymph node and present the ingested antigen and the maturating stimulus was insufficiently potent and failed to induce the crucial co-stimulatory surface molecules on the DCs, interaction with the T cells will result in anergy, T cell deletion or the production of regulatory T cells. Finally, if cancer-specific T cells are generated, they must enter the cancerous tissues to perform killing of the malignant cells, which is where the tumor-induced immunosuppressive microenvironment returns as a major obstacle. For instance, tumors may down-regulate their expression of MHC I molecules and promote accumulation of regulatory T cells in the tumor tissue, thus inhibiting the function of T-cells. Tumors produce a variety of surface molecules, which engage receptors on the T cells (receptors which are normally intended to keep the immune response from running rampant), and induce T cell anergy or exhaustion. Tumors can release immunosuppressive mediators such as indoleamine 2,3-dioxygenase and can secrete or induce the secretion of the immunosuppressive cytokine IL-10. Finally, tumors can recruit myeloid-derived suppressor cells, a cell-type distinct from tumor-associated macrophages (TAMs) and DCs, which secrete a specialized set of immunosuppressive mediators[118].

While all of the above represent major challenges to the immune system, step 1 to 3 are also possible targets for therapeutic intervention.

Step 1.

TAAs may be delivered exogenously as part of a therapeutic vaccine, which must comprise co-delivery of a sufficiently strong maturation signal for the tumor-infiltrating DCs to be activated. Such an activation signal could consist of TLR agonists or CD40 Abs. The understanding of DC activation has advanced greatly in the last decade and many initial attempts were compromised by the absence of an effective DC-activating adjuvant[119]. A recent promising improvement involves the use of 20-mer peptides, which are longer than the 10-12-mers that fit in the MHC I molecules; these peptides are thought to be more efficient at generating effector T cells,

possibly because some level of processing is benificial[120]. Full-length proteins are also being explored as targets for cancer vaccinations, as they potentially contain a broader profile of epitopes[121].

Another strategy for therapeutic vaccination is the cell-based approach, for instance DC-based vaccines. Here, DCs are isolated from a cancer patient, loaded with antigens *ex vivo*, activated and re-infused into the patient[122]. Provenge®, which is an example of this strategy and is based on the *ex-vivo* manipulation of peripheral blood mononuclear cells (PBMCs), was the first cancer therapy known to actively manipulate the immune system to receive FDA approval (in 2010). However, the strategy is somewhat inhibited by the complexities and costs associated with cell isolation, *ex vivo* manipulation and re-infusion.

Step 2.

In the lymphoid organs, TAA-loaded, activated DCs must generate protective T cell responses[123]. The precise type of T cell response needed for successful antitumor immunity is not currently known in full detail, but potent induction of $CD8^+$ T cells is assumed to be crucial, although responses based on Abs and NK cells may also contribute to tumor immunity. Accordingly, the lymph node is a potential site for therapeutic intervention e.g. by providing help to guide the T cell activation in the direction of $CD8^+$ T cells, by inhibiting regulatory T cell expansion caused by insufficiently matured DCs or by boosting the activation level of the Ag presenting DCs[124].

Step 3.

Irrespective of the lymphocyte response generated in the lymph node, all effector cells must overcome the point immune suppression potently induced by the tumor in the tumor microenvironment. Recent years have seen several attempts aimed at overcoming this hurdle. Two recombinant cytokines have been approved by FDA for cancer treatment, namely recombinant IL-2 (Proleukin™) and IFNα (RoferonA™, IntronA™), each with the potential to stimulate adaptive antitumor responses. In addition, recent years have seen the emergence and FDA approval of the checkpoint blockers, specifically the recent approval of Ipilimumab (March 2011, a CTLA-4 specific Ab), Pembrolizumab (Sep. 2014, a PD-1 specific Ab), and Nivolumab (Dec. 2014, a PD-1 specific Ab). While these drugs are also just monoclonal Abs, they target immune mechanisms, which have been confirmed to involve the modulation of endogenous T cell responses[125]. Both CTLA-4 and PD-1 are known to be key negative regulators of T cell activity and are expressed on the plasma membrane of T cells in order to control the immune response and

prevent excessive activity. However, several cancers appear to be able to hijack these two check-point systems for their own protection, and abrogation of this hijacking has proven a promising strategy.

## 5.3 Dendritic cells and macrophages in cancer immune therapy

As described above, much focus has been placed on tumor-specific $CD8^+$ T cells, their generation and tumor-mediated suppression. However, myeloid cells such as myeloid DCs (mDCs) and macrophages, as wells as plasmacytoid DCs (pDCs) are also highly involved in the antitumor immune response (or its absence) and are crucial in shaping the tumor microenvironment in a pro- or anti-tumorigenic direction.

### 5.3.1 Dendritic cells in cancer

Without the efficient antigen-presentation by activated DCs to naive T cells in the lymph nodes, no endogenously generated T cells will emerge. In addition, when properly stimulated, mDCs and pDCs are important sources of crucial cytokines which potently stimulates anti-cancer immune responses.

pDCs originate in the bone marrow from both myeloid and lymphoid progenitors[126]. The details of their development are incompletely understood, but they are generally regarded as less efficient APCs than myeloid DCs, although the specific conditions appear to have a large impact[127]. However, upon registration of viral infection, pDCs are rapidly induced to secrete large amounts of IFNα which has stimulating effects on monocytes, NK cells, T cells, B cells and mDCs[127,128]. The most important consequences of IFNα secretion are increased expression of costimulatory and MHC molecules on monocytes and mDCs, secretion of chemokines that attract other immune cells to the site of injury and increased antigen cross-presentation. While all of these actions are attractive for efficient cancer immunotherapy, cross-presentation is crucial. Cross-presentation is the display by APCs of endocytosed material on MHC I molecules, as opposed to the “normal” practice of presenting extracellular material on MHC II. This is an important aspect, as MHC I-mediated presentation is required for the generation of $CD8^+$ T cells with the capacity for direct cell killing in an antigen-specific manner. However, the TAAs are available as ingestible particles, and are thus directed towards MHC II-based presentation. This favors the generation of Th2 cells and skews the immune response in the direction of antibody (Ab) production, which is generally accepted to be far less efficient in combatting cancer.

Myeloid cells with the dendritic cell phenotype can arise in the tumor tissues either as a result of extravasation of immature dendritic cells from the blood or through extravasation and

maturation of monocytes to inflammatory mDCs, which are thus monocyte-derived[129]. In the tumor tissue, myeloid DCs are able to ingest tumor-associated antigens through the capture of dying tumor cells and through the "nibbling" of live tumor cells[117]. Importantly, mDCs are major sources of the cytokine IL-12p70, which is a potent inducer of interferon-γ (IFN-γ) production from T cells, NK cells and other cell types, and have also been shown to promote the generation of Th1 cells, which support polarization of the immune responses towards a major $CD8^+$ T cell component[130]. Recent evidence even suggests that mDCs themselves may be able to provide a boost of IFNγ-secretion when activated, thus contributing to the activation of macrophages as well as establishing an autocrine activation loop[131].

mDCs are regarded as the most efficient APC generally, but controversies remain regarding which type of DC that represents the best target for cancer immunotherapy[132] in light of the need for cross-presentation. Reports indicate that while mDCs *can* cross-present antigen, they do so with low efficiency[132]. On the other hand, the $CD141^+$ DC subset appears to be extremely efficient at cross-presenting antigen, but they are very rare, constituting ca. 0.03% of the PBMCs[133]. Further, recent reports suggest that pDC activation is attractive not only because secreted IFNα stimulates cross-presentation, but also because pDCs themselves are highly capable of cross-presenting antigen under certain conditions[134–136]. Finally, the inflammatory DCs that arise by differentiation from monocytes have also been associated with increased ability to cross-present antigen[132].

Unfortunately, while mDCs have been shown to infiltrate cancerous tissues in substantial numbers[137,138], many studies have documented that the infiltrating DCs become functionally impaired due to tumor-derived stimuli. For instance, tumors can prevent antigen presentation by switching the differentiation of monocytes to macrophages rather than inflammatory DCs[139]. Tumors also produce glycoproteins, which become confined to early endosomes when endocytosed by mDCs, thus interfering with the processing and presentation of the proteins to T cells[140]. Tumors can influence the maturation of mDCs. They can inhibit mDC maturation directly, for instance through secretion of IL-10, which results in antigen-specific anergy[141,142]. Tumor-derived factors can alter the maturation of mDCs and yield cells that indirectly promote tumor growth by favoring the generation of Th2 cells. Promoting the generation of Th2 cells has thus been shown to accelerate breast tumor development through the secretion of IL-4 and IL-13[143,144], which are cytokines that prevent tumor cell apoptosis and indirectly promote the

proliferation of tumor cells by stimulating tumor-associated macrophages to secrete epidermal growth factor.

### 5.3.2 Macrophages in cancer

Macrophages also play an important role in tumor progression and consequently represent a potential target for cancer immunotherapy. Circulating monocytes infiltrate the tumor tissues[145] where they may differentiate into inflammatory mDCs, myeloid-derived suppressor cells (MDSCs) or macrophages. Macrophages are the major differentiation product when monocytes infiltrate cancers[146], and tumor associated macrophages (TAMs) have been found to constitute up to 50% of the tumor mass[147]. Cytokines and surface-anchored molecules present in the tumor microenvironment influence the differentiation of the TAMs into broadly speaking two polarized phenotypes, termed M1 and M2. M1 TAMs, which are considered the classically activated macrophages, are stimulated by the presence of IFNγ and produce pro-inflammatory and immunostimulatory cytokines such as IL-12p70. However, it is generally observed that most of the TAMs are polarized towards the M2 phenotype, which is activated by Th2 cytokines (e.g. Il-4, IL-10 and IL-13)[147]. These M2 TAMs play a pro-tumorigenic role favoring cancer growth. They attempt to restore the tumor tissue integrity by promoting angiogenesis as they would for tissue remodeling following local injury[148], they suppress $CD8^+$ T cell proliferation, and they generate a tumor-favorable microenvironment by secreting biochemical mediators that promote cancer cell survival, proliferation, and eventual metastasis[149].

### 5.3.3 Myeloid-derived suppressor cells

A final cell-type, which contributes to the inadequate immune response to tumors, is the myeloid-derived suppressor cell (MDSC)[150–152]. Although described for the first time more than 20 years ago in cancer patients, their importance for tumor progression has only become clear within the last decade. They are known to be potent suppressors of various T cell functions, partly in a contact-dependent manner. In addition, it has been established, that they are a heterogeneous population of cells, consisting of myeloid progenitor cells and immature myeloid cells. Due to a specific set of surface markers, MDSCs can be distinguished from normally differentiated monocytes, macrophages or DCs as well as M2 TAMs[153]. Further, studies have shown that about one third of this population can differentiate into mature macrophages and DCs in the presence of the appropriate cytokines *in vitro* and *in vivo*[151,154]. Accordingly, efforts to re-program MDSCs are ongoing, and reports point towards vitamin A metabolites being able to promote differentiation of MDSCs into mature myeloid cells[155].

## 5.4 Macrophages and DC as targets of cancer immunotherapy

Due to the pivotal roles of monocytes, macrophages and dendritic cells in cancer, they constitute attractive targets for cancer immunotherapy, because whatever generated immune effector cells will have to work in the tissue microenvironment and be able to function under the stimulatory conditions present here. Accordingly, providing activated macrophages and DCs with anti-cancer functionality has become a major goal in cancer immunotherapy.

As described above, DC-based vaccines with *ex vivo* generation of activated antigen-presenting mDCs have been the subject of much experimentation, and the approval of Provenge™ shows that in some cases this strategy is feasible. However, due to the cost and complexity of this approach, investigators have turned their attention to the strategy of *in vivo* activation of desirable cellular subsets or elimination of unwanted ones[156].

Several strategies exist for the activation of the immune cells. Inhibition of the tumor-induced deactivation of T cells is described above, as is the administration of recombinant cytokines IL-2 and IFNα. A third approach is the stimulation of leukocyte subsets in a manner that mimics nature, namely by activating pattern recognition receptors (PRRs).

PRRs are soluble or cell-anchored molecules, which recognize conserved molecular patterns typical of invasive pathogens such as bacteria or virus, and are vital for activation of complement and coagulation cascades, opsonization, phagocytosis, apopotosis and induction of pro-inflammatory mediators. One of the most important classes of PRRs is the Toll-like receptors (TLRs)[157].

### 5.4.1 Toll-like receptors

TLRs are membrane glycoproteins with an external antigen recognition domain and a cytoplasmic signaling domain. 10 functionally distinct TLRs have been identified in humans although a ligand for TLR10 has yet to be discovered[157]. The TLRs show differential expression on leukocyte subsets as well as differential subcellular location: TLR1, 2, 4-6 and 10 are surface expressed, whereas TLR3 and 7 - 9 are expressed in intracellular compartments, notably in the endosomes[158–160]. The TLR ligands fall into three broad categories: lipids and lipopeptides (TLR2/TLR1; TLR2/TLR6; TLR4), proteins (TLR5) and nucleic acids (TLR3, 7, 8, 9)[158], and the responses to TLR signaling can include cell differentiation, proliferation or apoptosis, as well as induction of many secreted mediators, prominently IFNs, TNFα, IL-1, IL-6, IL-10, IL-12, as well as a variety of chemokines. In cancer immunotherapy, the interest has focused on the intracellular

TLRs, particularly TLR7-9, as they are believed to be responsible for the detection of viral infection, thus stimulating immune responses favoring direct killing of infected cells.

### 5.4.2 Toll-like receptor agonists

Owing to the interest in exploiting TLR-mediated activation both to improve the efficiency of modern subunit-based vaccines and in cancer immunotherapy, a large amount of TLR7-9 agonists has been synthesized and are being evaluated both in experimental settings and in clinical trials[161,162]. However, as of 2014 only two drugs with known TLR agonistic mode of action are used in the clinic for cancer treatment, namely the previously mentioned bacillus Calmette-Guérin (an attenuated strain of Mycobacterium bovis originally developed as a vaccine against tuberculosis and a potent stimulator of TLR2 and 4) and the TLR7 agonist Imiquimod (Fig. 5.2C). While only used topically, Imiquimod has become the "gold standard" against which all newly synthesized TLR7 agonists are compared.

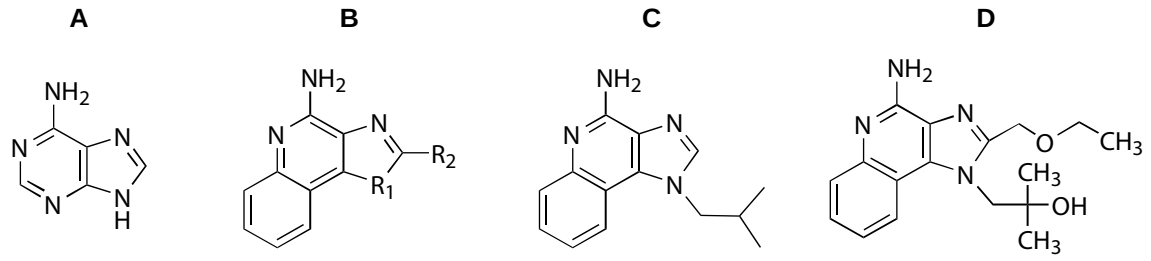


**Figure 5.2**. Examples of imidazoquinoline-based TLR7 agonists[163]. A. The purine nucleobase Adenine. B. Generic imidazoquinoline. C. Imiquimod. D. Resiquimod (R848).

Imiquimod is an imidazoquinoline (Fig. 5.2B), a class of compounds where several members have shown strong TLR 7/8-stimulating potency. As the pharmaceutical properties of Imiquimod and the more potent Resiquimod (Fig. 5.2D) prevents systemic administration, newer imidazoquinolines have been developed[161,164], some of which are currently being tested in phase II clinical trials[165].

Another promising class of TLR7 agonists is the guanine analogs[166,167] (Fig. 5.3), some of which have shown improved efficiency as TLR7 agonists compared to Imiquimod. As one of the major barriers to immunotherapy based on systemically administered TLR agonists is the risk of inducing potentially toxic cytokine syndrome[168,169], one group of researchers conjugated such a guanine-like TLR7 agonist to mouse serum albumin by the rationale that stable conjugation to a macromolecule, such as a protein, would restrict systemic absorption[170]. They observed a 10-100 fold increased potency compared to the free drug[171] and were able to achieve efficient delivery

to the respiratory system without induction of systemic cytokine syndrome in two mouse models of pulmonary infectious disease[171].

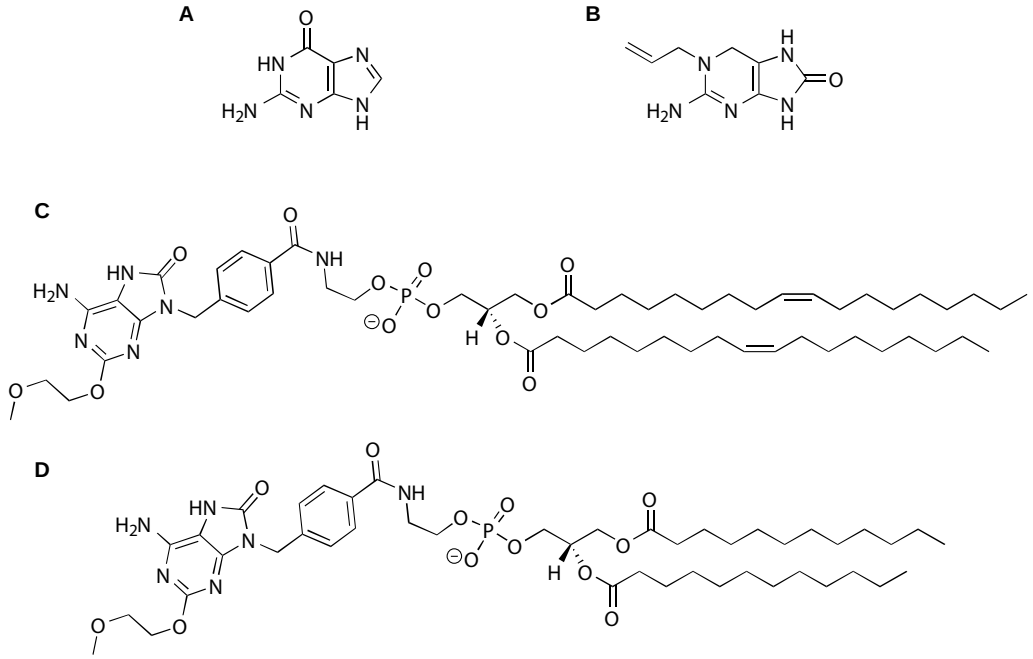


**Figure 5.3**. Examples of guanine-analogues with TLR7 agonist activity[163,172,173]. A. The purine nucleobase Guanine. B. Loxoribine. C. UC-1V150. D. TMX-202.

Further, as TLR7 is expressed in the endosomes and conjugation of various chemical entities to phospholipids has been shown to facilitate endocytosis[170], the same group investigated the impact of conjugating the TLR7 agonist to phospholipids[172,173], and structures of their lipid conjugates are shown in Figure 5.3C and 5.3D. They observed increased potency of the lipid-conjugate in human PBMCs compared to the unmodified TLR7 agonist and also saw prolonged increases in the levels of pro-inflammatory cytokines in serum when the lipid-conjugate was administered to mice in a systemic fashion[172]. No observations were made as to whether the cytokine syndrome could also be prevented by the lipid-conjugation under the conditions of systemic delivery.

### 5.4.3 Targeted delivery

While the conjugation of the receptor-interacting entity to a macromolecule is one way to achieve some level of targeting to phagocytic cells, a much more focused and versatile way to achieve targeted delivery is through the use of Ab- or protein-conjugated liposomes. While direct conjugation of the drug to a targeting ligand employs the same fundamental mechanism, targeted liposomes are theoretically superior since a relatively low number of targeting ligands are needed to deliver a large number of drug molecules, thus ensuring efficient and potent

receptor-agonist interaction. If the drugs are encapsulated, the liposomes are also able to protect the drugs from degradation in the bloodstream[174].

Liposomes themselves are versatile carriers of drugs and contrast agents, and are extensively used in drug delivery research, often to ameliorate the side effects of traditional cancer therapeutics. As of 2013, nine liposome-based drugs have received FDA approval and many are showing promising results in clinical trials[175]. Their attraction lies in their composition; as they consist of an aqueous core entrapped by one or more bilayers composed of natural or synthetic lipids, they are completely biocompatible and biodegradable, and they possess low intrinsic toxicity[176].

Liposomes were first described by Bangham[177] in 1964, while the idea to use liposomes as drug delivery vehicles is normally attributed to Gregory Gregoriadis[178]. However, the implementation of this idea was for a long time hampered due to extensive interaction with the complement system and rapid clearance by the MPS system, which could not be eliminated by the use of saturated phospholipids and cholesterol alone. However, in 1991 it was discovered that decoration of the liposomes with a hydrophilic polymer such as PEG could dramatically increase the circulation time of the liposomes. The dominant underlying mechanism for this extended circulation is believed to be the flexible PEG chain occupying the space immediately adjacent to the liposome surface ("periliposomal layer"), thus excluding other macromolecules from this space[179]. Consequently, access and binding of blood plasma opsonins to the liposome surface are hindered and interaction with the MPS is minimized.

### 5.4.4 Immunoliposomes

Another highly attractive aspect of liposomes is the relative ease of surface modification, through conjugation to the lipid head groups. Consequently, liposomes have been modified with a wide variety of ligands[174] and one of the most popular modifications for targeted delivery is the conjugation of Abs or Ab fragments to the liposomes, which are then often referred to as immunoliposomes. The best described use of immunoliposomes is for treatment of cancers, e.g. HER2/neu positive breast cancer. However, for treatment of solid cancers, conjugation of Abs to the liposomes will usually not in itself lead to increased accumulation in the tumor microenvironment as this process remains dependent on the passive accumulation of liposomes. Rather, the Abs will provide an advantage after exit of immunoliposomes from the bloodstream, where they will facilitate sequestration in the tissues as well as potentially the uptake.

Procedures for preparation of immunoliposomes are well-described in the literature and can be separated into two general strategies: post-insertion and post-functionalization (Fig 5.4). In the post-insertion approach, the Abs are covalently coupled to preformed lipid-PEG micelles, which have a reactive functionality in the distal end of the PEG that allows coupling of the Ab. Subsequent incubation with preformed liposomes allows the lipid-Ab conjugates to transfer from the micelles into the outer liposomal membrane, if the process is otherwise thermodynamically favored. Post-functionalization of liposomes with Abs is carried out using the same basic ingredients, but here the liposomes are prepared comprising the lipid, which on the surface of the liposomes displays the linker. Upon incubation of these "surface reactive" liposomes with the Ab, the Ab is tethered to the liposome surface. In cases where the liposomes are loaded with drugs in the aqueous lumen, the decoupling of the conjugation from the liposome formation can be an advantage. In addition, post-insertion allows easier fine-tuning of the number of Abs on display on the liposomes surface and upscaling is also easier. However, separation of the prepared immunoliposomes from the micelles can be troublesome. On the other hand, post-functionalization allows straightforward separation of the immunoliposomes from the un-conjugated protein, although the yield of post-functionalization is often lower. The latter is probably due to inherent instability of the reactive linker combined with a somewhat extended procedure as well as the fact that reactions that work well in solution may proceed very slowly on a surface and not go to completion[174].

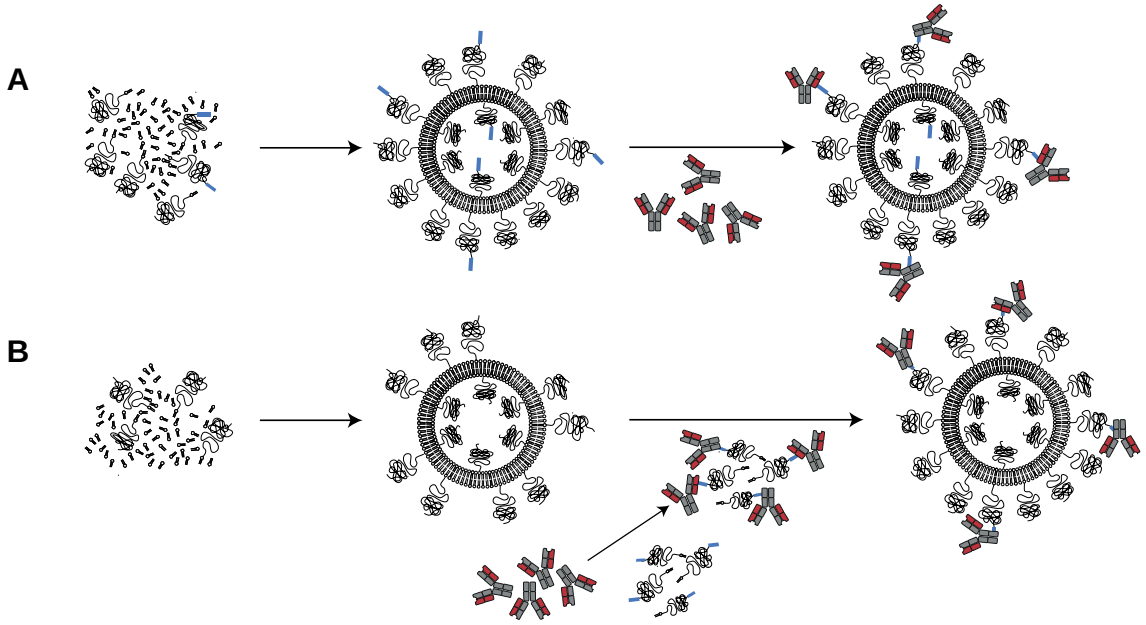


**Figure 5.4.** Cartoon representation of Ab functionalization of liposomes by post-functionalization (A) or post-insertion (B) approaches. A. PEGylated liposomes are prepared, which on the distal end of the PEG expose a reactive linker (blue segment) and are then mixed with Abs, which are suitably preconditioned for reaction with the linker. B. PEGylated liposomes are prepared, and Abs are covalently coupled to preformed lipid-PEG micelles through a reactive linker. Upon mixing of the PEGylated liposomes and Ab-conjugated micelles, Ab-conjugated lipids may transfer from the micelles to the liposomal membrane.

### 5.4.5 Targeting monocytes, macrophages or DCs

Clearly, a deciding parameter in Ab-based delivery is selection of a suitable target. The antigen must be differentially expressed on the target cells as well as have high surface expression to ensure efficient association of the immunoliposomes. Further, a specific Ab with high affinity must be available. For the purpose of delivering compounds to monocytes, macrophages or dendritic cells, C-type lectin receptors (CLRs) have been popular antigenic targets[180–182].

The CLRs is a large class of receptors, in which the members are united by their ability to recognize specific carbohydrate moieties through their carbohydrate-binding domain (CRD). In humans, the CLRs perform a variety of functions such as facilitating adhesion between cells, adhesion of cells to the extracellular matrix, or acting as PRRs. Depending on the specific function of the CLR, ligand recognition can induce a variety of cellular responses, and accordingly CLRs can be functionally divided into those that inhibit or those that induce cellular activation. Some CLRs are known to function as antigen-uptake receptors with CLR-mediated antigen uptake leading to efficient antigen presentation and immune stimulation[183,184]. As immunoliposomal drug delivery (whether the intent is elimination or stimulation of the cell) is often facilitated by internalization, selecting CLRs as targets for immunoliposomal delivery to

myeloid cells may thus be an attractive strategy. However, as activation of the C-type lectins may have a profound functional impact on the cell, careful selection is necessary[185,186].

The Dectin-2 cluster of CLRs contains Dectin-2 (CLEC6A), DCIR (CLEC4A), DCAR, BDCA-2 (CD303), which are all member of the Group II family of C-type lectins. BDCA-2 is the best known member of the group, as it is frequently used as a specific marker for plasmacytoid dendritic cells. In contrast, Dectin-2 and DCIR surface expression has been detected on multiple leukocyte subsets[187–189], while DCAR protein expression remains un-characterized[190]. BDCA-2, Dectin-2 and DCIR are examples of CLRs that have been shown to be endocytosed as a result of cross-linking, thus potentially constituting targets for delivery of drugs to the populations.

# 6 Aim of Project II

The aim of project II was to prepare immunoliposomes capable of targeting monocytes, myeloid dendritic cells and plasmacytoid dendritic cells. For this purpose, the antigen target was chosen to be the Dendritic Cell Immunoreceptor (DCIR), which is highly expressed on the surface of monocytes and mDCs as well as showing some expression on pDCs and B-cells. Further, the project aimed to test if the targeted delivery of a TLR7 agonist to monocytes, myeloid dendritic cells and plasmacytoid dendritic cells using the developed liposomal platform could activate the targeted cells. Finally, the project aimed to investigate if the targeted liposomal delivery of the TLR7 agonist would increase the potency of the agonist with respect to activation of the targeted cells. The activation of the targeted cells was evaluated by measuring the secretion of selected pro-inflammatory cytokines to the culture supernatants, some of which have been crucially linked to successful antitumor immune response.

# 7 Article 2: Activation of dendritic cells and monocytes by targeted delivery of a TLR7 agonist

This section contains the manuscript in preparation for submission to *Nanomedicine: Nanotechnology, Biology and Medicine*.

Thomas C. B. Klauber[1], Daniel Zucker[2], Roberto Maj[3], Simon S. Jensen[4], Susanne B. Pedersen[5], Janne M. Lauersen[5], Thomas L. Andresen[1]

[1]DTU Nanotech, Department of Micro-and Nanotechnology, Center for Nanomedicine and Theranostics, Technical University of Denmark, Building 423, 2800 Kgs. Lyngby, Denmark

[2]Lipoid GmbH, Frigenstraße 4, 67065 Ludwigshafen am Rhein, Germany

[3]Telormedix SA, Via della Posta 10, CH-6934 Bioggio, Switzerland

[4]MonTa Biosciences, Technical University of Denmark, Building 423, 2800 Kgs. Lyngby, Denmark

[5]DTU Systems Biology, Department of Systems Biology, Technical University of Denmark, Building 222, 2800 Kgs. Lyngby, Denmark

## 7.1 Abstract

Targeted delivery of immune modulators to specific leukocyte subsets in the bloodstream is a promising approach to increase the efficiency and reduce the side effects of immunotherapy. Monocytes and dendritic cells (DCs) are attractive targets for immune response modifiers (IRMs), as they have central roles in both innate and adaptive immune responses and play crucial roles in shaping the nature of the tumor microenvironment. In this study, we describe a liposomal platform for simultaneous targeting of monocytes and DCs in the bloodstream. We demonstrate the potential of this platform by delivering a TLR7 agonist to monocytes, myeloid DCs (mDCs) and plasmacytoid DCs (pDCs) in PBMC culture. Monocytes and mDCs are targeted with high specificity over lymphocytes, and we demonstrate potent induction of the pro-inflammatory cytokines IL-12p70, TNFα, and IFNα2a. Importantly, we also detect high levels of IFNγ, indicating subsequent activation of NK or T cells. This delivery system may be able to improve cancer treatment either as a vaccine with co-formulated antigen or by increasing the potency of IRMs with respect to activation of monocytes and DCs.

## 7.2 Introduction

Cancer immunotherapy theoretically offers high specificity and potentially long-lasting protection. If the therapy is successful, antitumor immunity leads to production of cytotoxic immune cells that can recognize and eliminate cancer cells effectively, as well as generation of immunological memory[191].

Advances in tumor immunobiology have demonstrated that the immune system almost always has the ability to recognize and attack cancerous cells, despite the cells being very similar to normal 'self'. However, in clinically identified cancer the tumor develops immunosuppressive mechanisms that manipulate the immune system and protect the tumor against immune surveillance[112].

The tumor-induced immunosuppressive actions severely impair the functionality of macrophages and DCs. Tumor tissues are often heavily infiltrated by macrophages (tumor-associated macrophages, TAMs)[147], but the majority of the TAMs adopt an inactive or immuno-suppressive phenotype, de facto promoting tumor growth and metastasis by supporting matrix remodeling, angiogenesis and suppressing antitumor activities[192,193]. Similarly, while numerous studies have concluded that myeloid DCs (mDCs) infiltrate tumors[138] and the immune system has the ability to recognize and attack cancer cells, tumors often evade detection by down-regulating antigen presentation and impairing mDC function and migration[137,139,142]. Finally, due to mediators released by the tumor cells, tumor-infiltrating plasmacytoid DCs (pDCs) are maintained in a semi-mature state with strongly impaired secretion of IFN-α[194].

Accordingly, a number of strategies aim to provide activated dendritic cells and/or macrophages to the tumor tissue, hoping to reduce tumor-mediated immunosuppression and reinstate immune surveillance of the tumor. A strategy which has enjoyed some success in clinical trials is DC vaccination – the *ex vivo* activation of autologous mDCs followed by re-administration to the patient; however, widespread translation into the clinic is inhibited by the complexity and cost of the procedure[137]. Another attractive strategy is to re-polarize the tumor microenvironment by administration of recombinant cytokines or IRMs, e.g. Toll-like receptor (TLR) agonists.

The reliable detection of pathogenic invasion is crucial to the function of the immune system. One strategy is based on the recognition of conserved molecular patterns that are exclusive to the microbial world. These are detected by pattern recognition receptors (PRRs) that alert the host immune system to the presence of infectious material[157]. The TLR family is one of the best characterized classes of PRRs in mammals[158]. 10 distinct subtypes exist in man[195,196], and ligand

recognition and TLR activation have been shown to boost adaptive immune responses significantly[157]. TLR7 is expressed in monocytes, mDCs and pDCs, and B-cells although the expression levels remain debated[157,172,197]. It is localized in the endosomal membrane, where it is activated by single-stranded RNA of viral origin[198], and has been suggested as an important target for future vaccine and cancer immunotherapy[199].

Several commercially available TLR7 agonists exist, more are in clinical development and new derivatives are continuously being reported[161,200]. The TLR7 agonist used in this study is designated TMX-202. It belongs to a relatively new class of TLR7 agonists, namely the guanine-like agonists, and has been shown to potently stimulate mammalian immune cells[171,172].

Liposomes are versatile carriers for a broad spectrum of compounds[52,201] and are ideally suited as vehicles for the lipid-based TMX-202. Liposomal formulations are currently in use for cancer treatment[201], primarily for delivery of conventional cytotoxic compounds such as doxorubicin. However, tumor-accumulation remains a challenge, partly because it hinges on the enhanced permeability and retention (EPR) effect, which varies greatly across cancer types and species, often due to insufficient vascularization of hypoxic areas of solid tumors[29,202].

Due to the variability of the EPR effect, it is an attractive and elegant strategy to target leukocyte subsets while they are present in the bloodstream, activate/precondition them, and leave the egress from the circulation and migration to the tumor to the evolutionarily perfected biological mechanisms. As PEGylated liposomes are only minimally cleared from the circulation by the mononuclear phagocyte system[29,203], one way to theoretically ensure rapid and specific association and internalization by leukocyte subsets is decoration of the liposomes with antibodies (Abs) against a subset-specific antigen. Abs against the C-type lectin “Dendritic Cell Immunoreceptor” (DCIR) is an attractive choice in order to achieve uptake of liposomes by monocytes and DCs: DCIR is differentially expressed on leukocytes with high surface levels present on both monocytes and mDCs and lower levels present on pDCs and B-cells[204]. Further, it has been shown that binding of the receptor leads to endocytosis of the receptor-ligand complex[204] thus ensuring optimal conditions for interaction between the TLR7 receptor and a TLR7 agonist.

In the present study, we report a liposomal drug delivery system for robust and specific targeting of monocytes and DCs consisting of PEGylated liposomes with surface-conjugated antibodies against DCIR. We show that the liposomes effectively target monocytes and mDCs over other leukocytes in a PBMC suspension, as well as to a lesser extent pDCs. Further, we show that the

targeted delivery of a TLR7 agonist to monocytes, mDCs and pDCs using the presented platform, results in significantly upregulated production of pro-inflammatory cytokines *in vitro* compared to the non-sense targeted control and the free agonist.

We believe that our targeted delivery platform, which enables simultaneous targeting of monocytes and DCs, may support future development of cancer immunotherapy by targeting peripheral monocytes and DCs with liposomes loaded with immune stimulating adjuvants.

## 7.3 Materials and Methods

### 7.3.1 Materials

1,2-dipalmitoyl-sn-glycero-3-phosphocholine (DPPC), 1,2-distearoyl-*sn*-glycero-3-phosphoethanolamine-N-[methoxy(polyethylene-glycol)-2000] (DSPE-$PEG_{2000}$), 1,2-distearoyl-sn-glycero-3-phosphoethanolamine-N-[maleimide(polyethylene glycol)-2000] (DSPE-mal), 1,2-dipalmitoyl-*sn*-glycero-3-phosphoethanolamine-N-(lissamine rhodamine B sulfonyl) (DPPE-RhB) and cholesterol (Chol) were purchased from Avanti Polar Lipids (Alabaster, AL, USA) and used without further purification. 2-(4-{[6-Amino-2-(2-methoxyethoxy)-8-oxo-7H-purin-9(8H)-yl]methyl}benzamido)ethyl 2,3- Bis(dodecanoyloxy)propyl phosphate (TMX202) was kindly supplied by Telormedix, Bioggio, CH). 2-iminothiloane (Traut's reagent), 5,5 '-dithio-bis(2-nitrobenzoic acid) (DTNB) and 4-(2-hydroxyethyl)-1-piperazineethanesulfonic acid (HEPES) were purchased from Sigma-Aldrich (St. Louis, MO, USA) as was Ficoll-Paque Premium, PBS, RPMI, penicillin (pen), streptomycin (strep), Trypan blue and Human AB serum (heat-inactivated). Herceptin™ was kindly supplied by Anders Elias Hansen (Department of Biomedical Sciences, University of Copenhagen). Flat-bottom polystyrene 96-well plates (clear and black), round-bottom polystyrene 96-well plates and 96 well maxisorb™ plates for ELISA were purchased from Thermo Scientific (Waltham, MA, USA). Disposable UV micocuvettes, 15 mm center height, were purchased from Brand (Wertheim, Germany). Human buffy coats were acquired from the blood bank at the National Hospital of Denmark (Rigshospitalet) collected from anonymous healthy donors. Blood samples were handled in accordance with guidelines put forward in the 'Transfusion Medicine Standards' by the Danish Society for Clinical Immunology (www.dski.dk). All standard chemicals were purchased from Sigma-Aldrich (St. Louis, MO, USA) and they were analytical grade.

*Antibodies*

Murine anti-human DCIR monoclonal Ab (IgG1) and matching control monoclonal Ab (IgG1 specific for a non-human epitope) was purchased from R&D Systems (Minneapolis, MN, USA). Fluorochrome-conjugated Abs for flow cytometry were as follows: CD16-FITC, CD123-APC, CD141-BV510 (BD Biosciences, San Jose, CA, USA); CD14-PE-Cy7, CD3-eFluor450, CD19-eFluor 450, CD1c-PerCP-eFluor710 (Ebiosciences, San Diego, CA, USA), CD303-APC (Miltenyi Biotec, Bergisch Gladbach, Germany), and CD56-Pacific Blue (Biolegend, San Diego, CA, USA).

### 7.3.2 Methods

*Preparation of maleimide-functionalized liposomes*

Maleimide functionalized liposomes (m-liposomes) composed of DPPC:chol:TMX-202:DSPE-$PEG_{2000}$:DSPE-mal:DPPE-Rhd with mole ratio of 59.70:30:5:4.6:0.5:0.2 were prepared by the lyophilization method[205]. Briefly, the lipids were dissolved in tert-butanol:isopropanol:ethanol:DMSO at a ratio of 166:1:8:2 to a final lipid concentration of 9 mM, mixed thoroughly, frozen in liquid nitrogen and lyophilized to a dry powder over-night. The powder was hydrated with 10 mM Hepes, 150 mM NaCl, pH 7.4 (HBS) to a lipid concentration of 15-20 mM. This solution was incubated at 55 °C for 1 h with stirring and extruded through polycarbonate membranes (400, 200, and 100 nm pore size) using an Avanti® mini-extruder in a heating block (Avanti Polar Lipids, Alabaster, AL, USA) at 55 °C.

*Antibody thiolation*

Herceptin™ (for process optimization), anti-DCIR Ab, and control Ab were dissolved in 0.2 M Borax, pH 8.5 (Borate buffer) to a concentration of 2.5 mg/mL. 2-iminothiloane (Traut's reagent[206]) was dissolved in the same buffer to a concentration of 0.4 mg/ml. Ab and 2-iminothiloane were mixed together and incubated at RT in the dark for 1 h, after which the solution was ultrafiltrated twice using Borate buffer and Amicon spin filters (30 kDa cut-off, Merck Millipore, Billerica, MA, USA).

*Determination of thiolation using Ellman's reagent*

Thiolation was determined using Ellman's reagent[207,208]. Briefly, 2 nmol of thiolated protein was added to a disposable cuvette, Borate buffer was added to the cuvette to a total volume of 0.4 mL, and absorbance at λ = 412 nm was recorded (sample and blank) on a Unicam Helios α spectrophotometer (Thermo Scientific, Waltham, MA, USA). 30 µL of Ellman's reagent[207] (2 mM DTNB in Borate buffer) was added to sample and blank, mixed, incubated at RT for 15 min, and

absorbance at λ = 412 nm was recorded. The number of thiols per Ab was calculated using the following formula (ε = 0.0141[208]): (0.4 x (ΔA / 0.0141) / 2.

*Determination of lipid concentration*

Phospholipid concentrations were measured by inductively coupled plasma mass spectrometry (ICP-MS). Liposomes were diluted to a final phosphate concentration of 30-95 PPB in a solution of 2% HCl and 10 PPB Gallium, and the phosphate concentration was measured using ICP-MS (iCap Q, Thermo Scientific, Waltham, MA, USA). For relative estimates of lipid concentration for size exclusion chromatography (SEC), the fluorescence intensity of Rhodamine B was measured using excitation and emission wavelengths of 570 and 610 nm on a Victor 3 plate reader (Perkin Elmer, Waltham, MA, USA).

*Determination of Ab concentration*

Ab concentration was determined using Coomassie Plus Assay with BGG as reference protein (Thermo Scientific, Waltham, MA, USA) with the A595 measurements performed on a Sunrise plate reader (Tecan, Männedorf, Schweiz). If the unknown samples contained RhB-labeled liposomes, the contribution from RhB was subtracted through measurement on a suitably prepared background series of non-Ab-conjugated RhB labeled liposomes.

*Conjugation of thiolated Ab to m-liposomes*

Thiolated Ab and m-liposomes were mixed in a glass vial at a DSPE-mal:Ab mole ratio of 10. The air phase was replaced with $N_2$, the bottle capped, and the vial placed on a shaker table for over-night reaction at RT in the dark. As the conjugation efficiency was strongly influenced by maleimide degradation as a function of time[209], liposome hydration and extrusion followed by Ab thiolation and start of conjugation were performed within 6-8 h. Further, as the conjugation efficiency was highly dependent on the pH of the conjugation mixture, the pH of the conjugation mixture was always adjusted to 8.5.

*Purification of immunoliposomes*

The Ab-conjugated liposomes were purified by size exclusion chromatography using Sepharose CL-4B resin (GE Healthcare, Piscataway, NJ, USA), HBS solvent and a flowrate of 1 mL/min. SEC equipment was from Bio-Rad (Hercules, CA, USA). Fraction analysis was performed by determination of RhB fluorescence (≈100 µL fraction per well in a dark 96-well plate measured on a Victor 3 plate reader and relative Ab concentration in the fractions was determined using Coomassie Plus Assay.

*Calculation of number of Abs per immunoliposome*

For a given solution of immunoliposome: Ab concentration and lipid concentration ($C_{lipid}$) was determined. Ab concentration was converted to number of Ab using Avogadro's number ($N_A$). Liposome concentration (liposomes per mL, $N_L$) was determined using the following formula: $\mathbf{N_L = C_{lipid} \times N_A / (N \times 1000)}$. $N_A = 6.0 \times 10^{23}$, $C_{lipid}$ is the concentration as determined by ICPMS, and N = the number of lipids per liposome which is calculated according to the following formula: $\mathbf{N = 17.69/B \times [(d/2)^2 + (d/2 - 5)^2)]}$. d = outer diameter of the liposomes and B is a correction factor for cholesterol, which in a lipid membrane has approximately half the volume of a phospholipid. At 30 mole% cholesterol, B = 0.85.

*Size, polydispersity index (PDI) and ξ-potential*

Size (hydrodynamic diameter) and PDI were measured by dynamic light scattering (DLS) using a ZetaPALS (Brookhaven Instruments Corporation, Holtsville, NY, USA). ξ-potentials were determined using laser-Doppler electrophoresis on the ZetaPALS. Liposomes were diluted to a final concentration of ≈1 mM lipid in HBS (size) or 10 mM Hepes, 300 mM glucose, pH 7.4 (HBG) and measured after equilibration at room temperature (RT) for 15 min.

*Determination of TMX-202 concentration*

TMX-202 concentration was determined using HPLC and correlating to a standard curve comprising the following TMX-202 concentrations (µg/mL): 60, 30, 15, 7.5, 3.75, 1.875, 0.0. A Gilson HPLC system (Middleton, WI, USA) fitted with the following column: Xbridge TM C18, 5 µm, 4.6 x 150 mm (Waters, Milford, MA, USA) was used. All samples were dissolved in water:tetrahydrofuran (THF) 1:1. Solvent A: Millipure water with 0.1 % Trifluoroacetic acid (TFA). Solvent B: THF with 0.1% TFA. The liposomes were diluted 5x in water:THF 1:1 before the injection. HPLC parameters: Starting solvent ratio = 20% B; Ending solvent ratio = 68% B; Gradient time = 19 min; Total run time: 25 min; Injected sample volume = 100 µL; UV detection at λ = 293 nm; Column temperature = 30°C.

*Separation of peripheral blood mononuclear cells (PBMCs) from buffy coats*

Human PBMCs were isolated from buffy coats of healthy blood donors after informed consent using standard Ficoll-Paque density gradient centrifugation. Briefly, the buffy coat was diluted 5x with RPMI with 5% pen/strep. 25 mL diluted buffy coat was carefully placed on top of 12.5 mL density gradient medium in 50 mL falcon tubes, and the tubes were centrifuged at 500xg for 30 min at RT without brake. The PBMC fraction was separated and washed 3x with RPMI with 5%

pen/strep (centrifugation at 280xg). Finally, all the PBMCs from one donor was resuspended in ≈20 mL RPMI with 5% pen/strep, stained for vitality using trypan blue and counted.

*In vitro association of anti-DCIR-, control- and m-immunoliposomes with PBMCs*

7 mio PBMCs in 2 mL RPMI with 5% human AB serum and 5% pen/strep (PBMC medium) were incubated for 1 h with rotation at 37°C in the presence of free agonist (1 and 10 µM), m-liposomes (1 and 10 µM), control immunoliposomes (1 and 10 µM) and anti-DCIR immunoliposomes (1 and 10 µM) in 2 mL eppendorf tubes. Following incubation the cells were washed with RPMI with 5% pen/strep (centrifugation at 300xg, RT) and analyzed for RhB positivity using flow cytometry. The normalizing parameter was chosen to be the agonist concentration. Accordingly, 1 and 10 µM TMX-202 concentration corresponds to 22.22 and 222.2 µM lipid concentration for the anti-DCIR immunoliposomes (in the rest of the article referred to as DCIR liposomes), 21.66 and 216.6 µM lipid for the control immunoliposomes (in the article referred to as control liposomes) and 19.64 and 196.4 µM lipid for m-liposomes.

*Flow cytometry analysis of liposome association to PBMC subsets*

Stimulated PBMCs were stained with a premixed cocktail of fluorochrome-conjugated Abs. Briefly, the PBMCs were washed 2x with PBS with 1% heat inactivated FBS, 0,10% (w/v) $NaN_3$ (FACS buffer) and incubated for 15 min at 4°C in the dark with Fc blocker (FACS buffer with 2 % Human Serum). To the cells was then added the premixed cocktail of fluorochrome-conjugated Abs, with which they were incubated for 30 min at 4°C in the dark. Then the cells were washed 2x in FACS buffer and flow cytometry data was acquired using a BD FACS CANTO II (BD Bioscience, San Jose, CA, USA) and BD FACS Diva software. Data analysis was done using FlowJo software vs 10 (TreeStar, San Carlos, CA, USA).

The gating strategy (Supplementary Fig. 7.1) divided the PBMCs into 4 subsets: monocytes, mDCs, pDCs, and T, B and NK cells. PBMCs were gated on FSC-SSC. T, B and NK cells were identified as $CD3^+$, $CD19^+$ or $CD56^+$ ($lin^+$) PBMCs. Monocytes were identified as $lin^-CD16^-CD14^+$ PBMCs. pDCs were identified as $lin^-CD14^-CD16^-CD123^+$. mDCs were identified as $lin^-CD14^-CD123^-CD16^-CD1c^+$ PBMCs. However, comparing the $lin^-CD14^-CD16^-CD123^+$ PBMCs with $lin^-CD14^-CD16^-CD303^+$ PBMCs (Fig. 3F) revealed that the use of CD123 as a pDC marker led to inclusion of cells, which were excluded by the CD303 marker. As CD303 is exclusively expressed on pDCs and is the recommended pDCs marker[210], we therefore analyzed PBMCs from 2 separate donors but substituted CD123 with CD303 as marker for pDCs (same isotype, fluorophore and instrument

settings) and constructed a not-gate to exclude $lin^-CD14^-CD16^-CD123^+CD303^-$ cells from our original pDC population (Fig. 3G). Consequently, in our final analysis pDCs were identified as $lin^-CD14^-CD16^-CD123^+$ PBMCs, which were not excluded by the $lin^-CD14^-CD16^-CD123^+CD303^-$ not-gate. We speculate that the $lin^-CD14^-CD16^-CD123^+CD303^-$ PBMCs might be basophils, as they have been shown to express CD123[211].

The gates showing the percentage of RhB positive cells were set based on HBS treated control cells without addition of liposome.

*In vitro stimulation of PBMCs*

Based on the available literature on TMX-202 and TMX-202-like compounds administered in a non-targeted fashion[172,173], we chose a TMX-202 concentration of 1 µM for the stimulation experiments. 7 mio PBMCs in 2 mL PBMC medium were incubated for 1 h with rotation at 37°C in the presence of free agonist (1 µM TMX-202), m-liposomes (1 µM TMX-202), control liposomes (1 µM TMX-202) and DCIR liposomes (1 µM TMX-202) in 2 mL eppendorf tubes. Then, the cells were washed with RPMI with 5% pen/strep (centrifugation at 300xg, RT), resuspended in PBMC medium plated in round-bottom 96-well cell culture plates (175,000 cells per well, 175 mL medium per well, 30 wells per population). Cell free supernatants were collected after incubation for 1, 2, 3, 4, and 5 days - the supernatants were collected, spun down (400xg, 5 min), where after the supernatants were stored at -80°C until analysis for secreted cytokines.

*Analysis of culture supernatants for secreted cytokines*

Cytokine analysis was performed using Meso Scale Discovery's electrochemiluminescence-based multiplex assays following the instructions from the manufacturer. The culture supernatants were analyzed for IL-6, IL-10, IL-12p70, TNF-α and IFN-γ using V-PLEX Proinflammatory panel 1 kit and for IFNα2a using "Human IFNα Ultra-Sensitive Kit". Both kits were developed on Sector Imager 2400, all from Meso Scale Discovery (Rockville, MD, USA). Minimum detection levels were: 7.74 pg/mL (IFNγ), 0.69 pg/mL (TNFα), 1.58 pg/mL (IL-6), 0.68 pg/mL (IL-10), 1.22 pg/mL (IL-12p70), 0.7 pg/mL (IFNα2a).

*Statistics*

Flow cytometry data are presented as percentages of positive cells based on the uptake of DSPE-RhB. Association of liposomes to PBMCs and cytokine secretion data were analyzed using one-way ANOVA and two-tailed T-tests, all non-parametric.

## 7.4 Results

### 7.4.1 Preparation of immunoliposomes

Traut's reagent was used to thiolate Abs, and initial experiments focused on investigating how the average number of thiols per Ab depended on the molar ratio between Traut's reagent and Ab. A linear dependency was found for the thiolation degree as a function of the Traut's:Ab ratio (Fig. 7.1). To minimize potential cross-binding of immunoliposomes mediated by too highly thiolated antibodies, while simultaneously maximizing Ab conjugation efficiency, a Traut's:Ab molar ratio of 25 was found to be optimal yielding approximately 1.2 thiols per Ab for both anti-DCIR Ab and IgG1 control Ab.

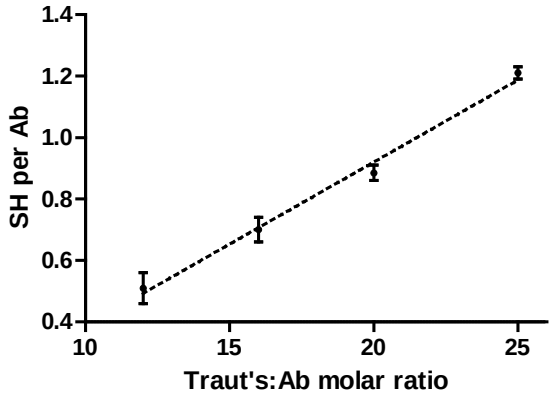


**Figure 7.1.** Linearity of thiolation. Ab (Herceptin™) was dissolved in 0.2 mM Borate pH 8.5 at 2.5 mg/mL. 2-iminothilane was dissolved to 0.4 mg/mL and immediately added to the dissolved Ab and incubated for 1 h at RT in the dark with shaking. Error bars = S.E.M. Results from 2 independent experiments.

TMX-202 was formulated into maleimide-functionalized liposomes (m-liposomes) and conjugated to thiolated Ab by reaction over-night at a molar maleimide:Ab ratio of 10. As the thiol specificity of the conjugation reaction at high pH was a concern, reaction specificity at pH 8.5 was evaluated by conjugating non-thiolated Ab to m-liposomes. No conjugation could be detected, which demonstrates that even at pH 8.5 the maleimides react specifically with the thiols on the Abs (results not shown).

After over-night conjugation, immunoliposomes were purified using size exclusion chromatography (SEC) (Fig. 7.2). DCIR liposomes, (Fig. 7.2A) and control liposomes (Fig. 7.2B) essentially eluted over 2-3 fractions with peak fractions being no. 6 and 7, respectively. Non-conjugated anti-DCIR Ab eluted in fraction 14-24, non-conjugated control-Ab in fraction 18-28, both well separated from the liposomes in the SEC method used.

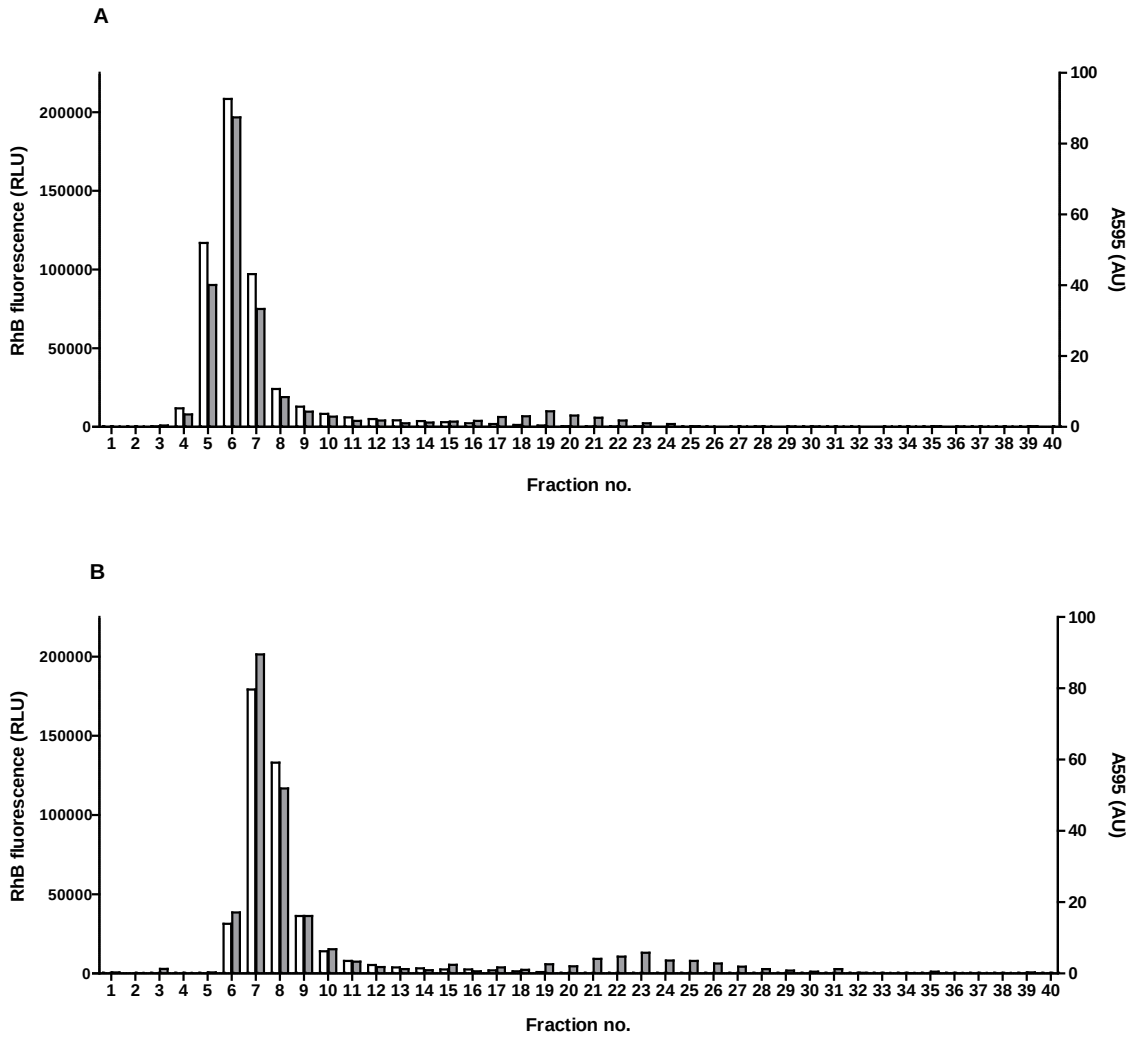


**Figure 7.2**. SEC purification of DCIR liposomes (A) and control liposomes (B). Lipid concentration was quantified by RhB fluorescence (left y-axis), protein concentration was measured using Bradford Plus (right Y-axis). Measured values are relative. Representative of 3 independent experiments each.

### 7.4.2 Characterization of liposomes – size, ξ-potential and polydispersity index (PDI)

Characterization of the liposomes with respect to size (hydrodynamic diameter) and ξ-potential (Table 7.1) showed that all liposomes carried a ξ-potential of -25 to -30 mV and further indicated a slight tendency of the DCIR liposomes towards aggregation. As neither m-liposomes nor control liposomes displayed this aggregation tendency, we attribute this to interaction mediated by the conjugated anti-DCIR Abs.

As a stability control, we assessed the aggregation tendency over time as evaluated through size measurements using DLS (Table 7.1). The measurements show that 48 h post-purification aggregation was minimal and after this time point no further aggregation could be detected.

| | Type of liposome | Particle size (nm) | PDI | ξ-potential (mV) |
|---|---|---|---|---|
| **A** | m-liposomes | 145.3 ± 3.9 | 0.12 ± 0.03 | -28.6 ± 0.8 |
| | m-liposomes | 153.4 ± 2.9 | 0.13 ± 0.01 | -27.1 ± 0.3 |
| **B** | Control liposomes | 154.9 ± 1.5 | 0.22 ± 0.01 | -26.9 ± 0.4 |
| | DCIR liposomes | 185.1 ± 3.7 | 0.28 ± 0.01 | -25.8 ± 0.7 |
| | m-liposomes | 154.2 ± 1.9 | 0.16 ± 0.01 | -26.2 ± 0.6 |
| **C** | Control liposomes | 154.8 ± 1.7 | 0.17 ± 0.04 | -26.9 ± 0.5 |
| | DCIR liposomes | 179.4 ± 1.9 | 0.19 ± 0.01 | -26.6 ± 1.0 |

**Table 7.1**. DLS measurements of size, ξ-potential and polydispersity index (PDI). Size and PDI was measured in 10 mM Hepes, 150 mM NaCl, pH 7.4. ξ-potential was measured in 300 mM glucose, pH 7.4. A. Measured after extrusion and acclimatization to RT; B. Measured after 48 h of storage at 5°C and acclimatization to RT; C. Measured after 72 h of storage at 5°C and acclimatization to RT. Values are mean ± S.E.M (n=3).

### 7.4.3 Characterization of liposome preparations

The preparations of m-liposomes, control liposomes and DCIR liposomes were characterized with respect to lipid concentration, number of Abs per liposome, concentration of TMX-202 and efficiency of conjugation (Table 7.2). In order for immunoliposomes to efficiently target leukocyte subsets, on average 40 Abs per liposome has been reported as sufficient[156], a criterion that our conjugation procedure met for both control and DCIR liposomes. Further, as the m-liposomes were formulated with 5 mole% TMX-202, a minor but acceptable loss of agonist occurred during the conjugation and purification procedure, resulting in a retrieval percentage of 90 for control liposomes and 88 for DCIR liposomes of the TMX-202 originally formulated into the m-liposomes. Finally, the preparation procedure resulted in a conjugation efficiency of 59% and 67% for control liposomes and DCIR liposomes, respectively.

| Type of liposome | Lipid Concentration (mM) | Ab per liposome | Conjugation efficiency (%) | TMX-202 conc. (μM) | Mole% of TMX-202 |
|---|---|---|---|---|---|
| m-liposomes | 15.1 ± 0.4 | NA | NA | 770 ± 19.1 | 5.1 |
| Control liposomes | 1.2 ± 0.1 | 76 | 59 | 55.4 ± 2.8 | 4.6 |
| DCIR liposomes | 1.2 ± 0.1 | 68 | 67 | 54.0 ± 3.5 | 4.5 |

**Table 7.2**. Characterization of liposome preparations. Lipid concentration was measured by ICPMS (triplicates). Ab concentration was measured by Coomassie Plus assay using BGG as standard (triplicates). TMX-202 content was measured by quantitation of absorbance at 293 nm after HPLC separation (duplicates). Ab per liposome was calculated as described in the methods section.

### 7.4.4 Liposome association to peripheral blood mononuclear cell (PBMC) subsets

To establish the targeting properties of the liposomes, a gating strategy was devised, which could identify monocytes, mDCs, pDCs and a population comprising of T, B and NK cells (Supplementary Fig. 7.1). The gating strategy produced the following PBMC subset percentages: 13.2% monocytes, 0.8% mDCs and 0.9% pDCs. We incubated PBMCs with liposomes corresponding to TMX-202 concentrations of 1 and 10 µM and analyzed the PBMC subsets for Rhodamine B (RhB) signal. We found that the DCIR liposomes preferentially associated to monocytes, mDCs and pDCs over the combined population of T, B, and NK cells (Fig. 7.3, $p < 0.005$).

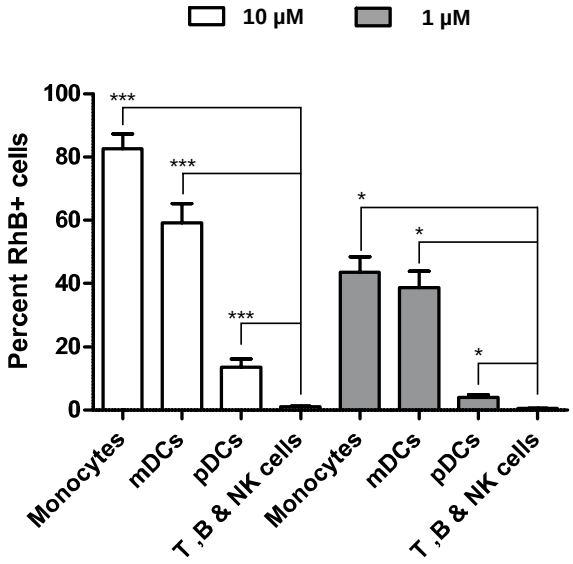


**Figure 7.3.** DCIR liposomes associate preferentially to monocytes, mDCs and pDCs. PBMCs were incubated with DCIR liposomes for 1 h with rotation at liposome concentrations corresponding to 10 µM TMX-202 (clear bars) or 1 µM TMX-202 (shaded bars), and association to PBMC subsets was analyzed by flow cytometry. *** $p < 0{,}0001$, * $p < 0{,}005$, t-test. n = 9. Error bars = S.E.M.

At 10 µM TMX-202 concentration, the targeting resulted in 84% and 59% RhB positive monocytes and mDCs, respectively, whereas the more physiologically relevant agonist concentration of 1 µM resulted in 44% and 39% RhB positive monocytes and mDCs (Fig. 7.3). While the preferential targeting of pDCs was also significant, it was substantially lower than observed for the monocytes and mDCs with the 10 µM TMX-202 concentration causing 14% of the pDCs to be RhB positive, and 1 µM agonist concentration resulting in only 4% RhB positive pDCs. The T, B, and NK cell population were only 1 and 0.5% RhB positive at 10 and 1 µM TMX-202, respectively, indicating very limited association of the DCIR liposomes to these cells. As monocytes, mDCs and pDCs all perform pinocytosis and are able to present internalized antigen[135,212,213], some unspecific uptake of the control liposomes was expected, although the

observed level was higher than expected (Fig. 7.4). Because this investigation of liposome association to PBMCs used normalization to TMX-202 concentration rather than lipid concentration and the mole% of TMX-202 is slightly higher for the m-liposomes than for the control liposomes (Table 7.2), PBMCs incubated with m-liposomes were exposed to slightly lower lipid concentrations than the PBMCs incubated with control liposomes. Still, the differences in unspecific association of control liposomes and m-liposomes by particularly the monocytes and mDCs at the 10 µM concentration (Fig. 7.4A and B) suggest that part of the association of the control liposomes could be mediated by the conjugated Ab. Together, the data in Figure 7.3 and 7.4 demonstrate that the DCIR liposomes efficiently and preferentially targeted monocytes and mDCs and also showed some association to pDCs.

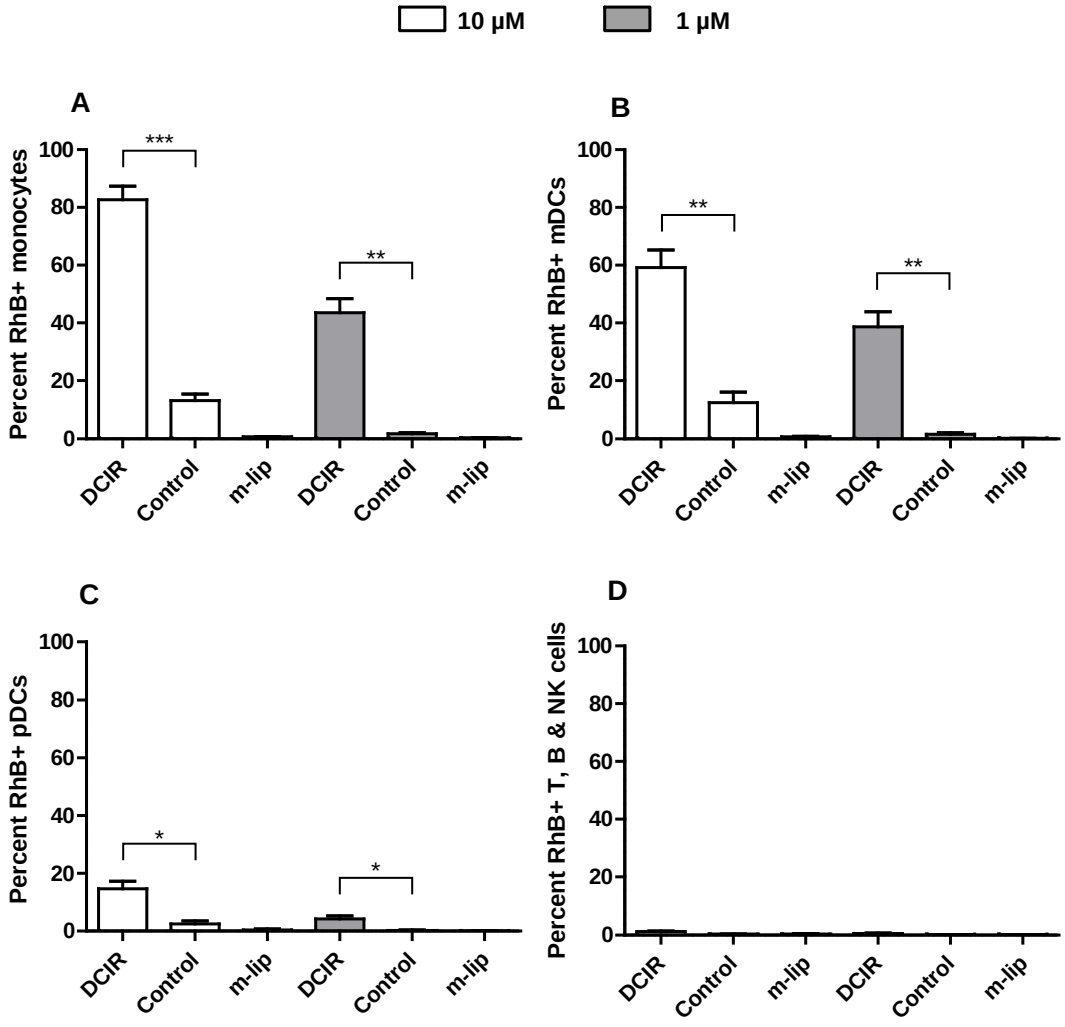


**Figure 7.4.** Association of DCIR liposomes, control liposomes and m-liposomes to PBMC subsets. A. Association to monocytes; B. Association to mDCs; C. Association to pDCs; D. Association to B, T, and NK cells. PBMCs were incubated with DCIR liposomes (DCIR), control liposomes (Control), m-liposomes (m-lip) or HBS for 1 h with rotation at liposome concentrations corresponding to 10 µM TMX-202 (clear bars) or 1 µM TMX-202 (shaded bars), and association to PBMC subsets was analyzed by flow cytometry. *** $p < 0.0001$, ** $p < 0.0005$, * $p < 0.005$, t-test. n = 9. Error bars = S.E.M.

### 7.4.5 Cytokine secretion from *in vitro* stimulated PBMCs

As the DCIR liposomes associated differentially to PBMC subsets, we wished to examine the impact of targeted delivery of the TLR7 agonist with respect to activation of the targeted cells, as evaluated through measurement of cytokine secretion to the supernatant. PBMCs were incubated with DCIR liposomes, control liposomes, free agonist or HBS at a TMX-202 concentration of 1 µM. The PBMCs were then washed and cultured for 5 days, and the culture supernatants analyzed for the secretion of selected cytokines indicative of subset activation on each day.

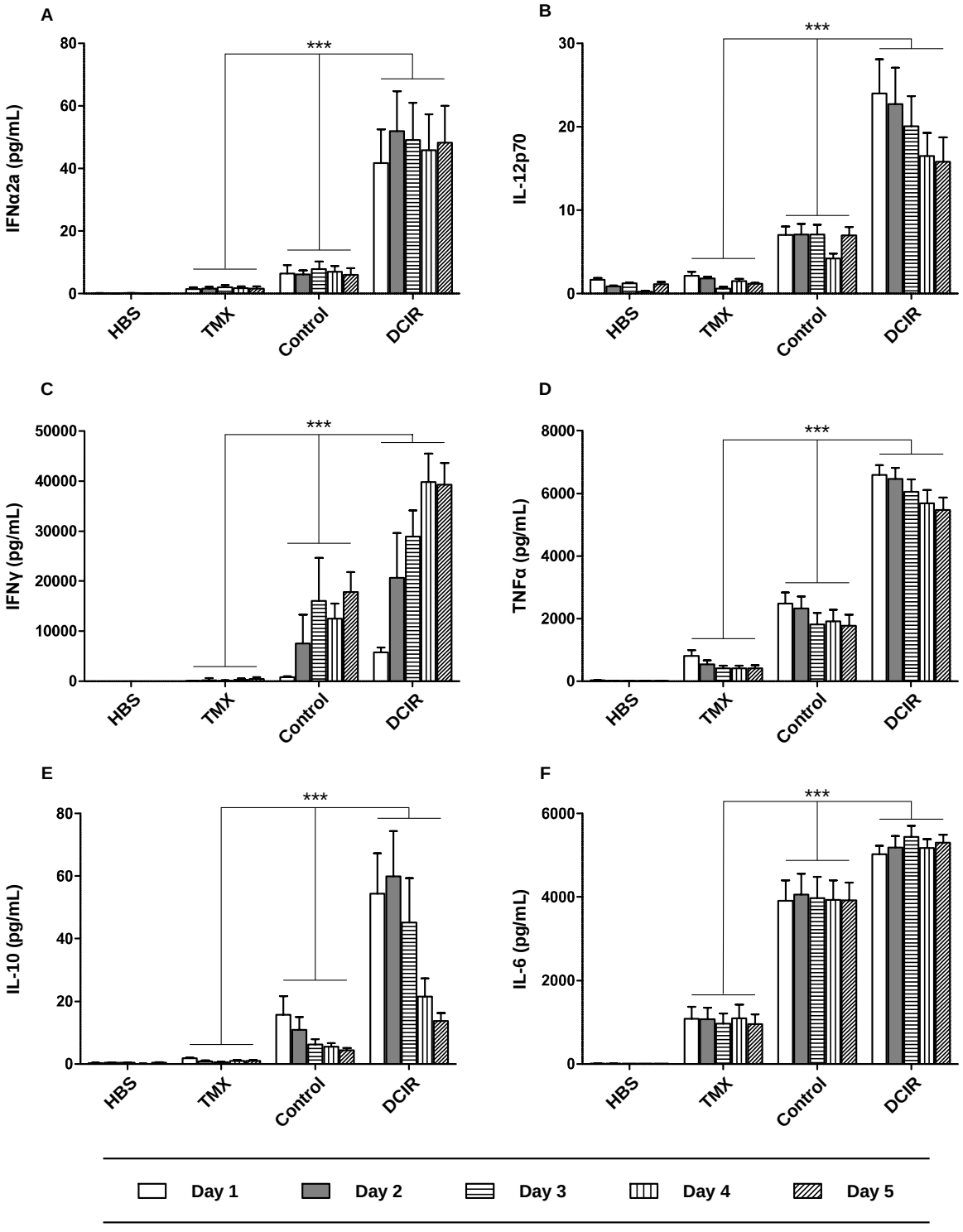


**Figure 7.5.** Cytokine secretion into the culture supernatants on day 1-5. A. IFNα, B. IL-12p70, C. IFNγ, D. TNFα, E. IL-10, F. IL-6. PBMCs were incubated with DCIR liposomes (DCIR), control liposomes (Control), free agonist (TMX) or HBS for 1h with rotation at concentrations corresponding to 1 μM TMX-202, washed and cultured for 1-5 days. Cell-free supernatants were collected and cytokine secretion was measured by ELISA. *** $p < 0.0001$, one-way ANOVA. n = 9. Error bars = S.E.M.

In vivo, pDCs are the principal source of IFNα[214], which is a cytokine associated with potent cancer-inhibition[134,215,216]. Further, pDCs have been shown to secrete IFNα when stimulated via TLR7 *in vitro*[217], and we therefore analyzed the culture supernatants for IFNα2a (Fig. 7.5A). We found that the targeted liposomal delivery of TMX-202 significantly increased the amounts of secreted IFNα2a ($p < 0.0001$) compared to the controls. The cytokine levels for PBMCs stimulated with DCIR liposomes were on average 7 fold higher than for PBMCs incubated with control liposomes and 28 fold higher than for PBMCs incubated with non-liposomal TMX-202, with the IFNα2a-leves detectable from the latter being close to the detection limit of our assay. Additionally, it is notable that the cytokine levels remained constant throughout the 5 days of culture.

IL-12p70 is another cytokine which is associated with strong antitumor effects[218] and is known to be secreted, when PBMCs are stimulated with TLR7-specific agonists[164,219]. To evaluate whether our targeting strategy improved the ability of TMX-202 to induce IL-12p70 secretion, we measured IL-12p70 in the culture supernatants (Fig. 7.5B) and were able to demonstrate a significantly increased secretion compared to both non-liposomal TMX-202 and control liposomes ($p < 0.0001$). In contrast to IFNα, a gradual reduction of IL-12p70 supernatant levels was observable from day 1 to 5, although it didn't reach statistical significance. The increased secretion of IL-12p70 indicates activation of monocytes and/or mDCs, as these subsets (among PBMCs) are known to the primary sources of this cytokine[130].

As the targeted delivery of TMX-202 resulted in increased IL-12p70 secretion and IL-12p70 is known to be a potent inducer of IFNγ production from NK and T cells[130], we wanted to know if the increased potency would impact the induction of IFNγ secretion (Fig. 7.5C). We observed that free (non-liposomal) TMX-202 was able to induce relatively low amounts of IFNγ, namely 68 pg/mL on day 1 climbing to 434 pg/mL on day 5. In contrast, incubation with DCIR liposomes induced secretion of significantly larger amounts of IFNγ into the supernatant ($p < 0.0001$), the IFNγ levels ranging from 5731 pg/mL on day 1 and climbing to 39 ng/mL on day 4 and 5. The temporal profile of the IFNγ levels in the supernatant displayed a clear and significant ($p < 0.0005$) increasing trend from day 1 to day 4, where after the level remained constant.

To further examine the monocyte activation indicated by IL-12p70 secretion, we measured the increase in IL-10 and TNFα protein in the culture supernatant, as both these cytokines are potently secreted by stimulated monocytes[220,221] (Fig. 7.5D and E). Targeted delivery of the TLR7 agonist resulted in a 3 fold increase of TNFα secretion compared to control liposomes and a 12

fold increase compared to treatment with the free agonist (Fig. 7.5D, $p < 0.0001$). Support for the potent activation of monocytes also comes from the secretion of the immunosuppressive IL-10[220] (Fig. 7.5E), where the day 1 protein levels for PBMCs stimulated with DCIR liposomes were 4 and 30 fold higher than the protein levels for PBMCs incubated with control liposomes and free agonist, respectively ($P < 0.0001$). Interestingly, where the cytokine levels of the pro-inflammatory TNFα remained essentially unchanged from day 1 to day 5, the IL-10 protein levels waned significantly over time ($P < 0.005$) and on day 4 the protein levels are reduced to approximately one third of the peak level on day 2.

Finally, we evaluated the IL-6 secretion to the culture supernatants (Fig. 7.5F). IL-6 is produced by many different cell types including monocytes and T cells, and can be interpreted as a general measure of pro-inflammatory response. The DCIR liposomes induced high levels of IL-6 secretion compared to free TMX-202 ($p < 0.0001$); however, so did the control liposomes ($p < 0.0001$). Similar to IFNα2a and TNFα, neither increase nor decline in the measured protein levels could be detected over the 5 days of culture.

Combined, the cytokine measurements demonstrate that the DCIR-mediated targeted delivery increased the efficiency of TMX-202 at inducing a pro-inflammatory response, and the data are congruent with the activation of monocytes, mDCs and pDCs. Crucially, the increased cytokine secretion comprised IFNα, IL-12p70 and IFNγ, which are associated with antitumor immune responses based on NK and $CD8^+$ T-cell mediated killing of malignant cells and tumor suppressive activity by tumor infiltrating macrophages and DCs[216,218,222,223].

## 7.5 Discussion

Several studies indicate that dendritic cells, macrophages and T cells are present in the tumor tissues in substantial numbers but become polarized towards an inactive phenotype due to the immunosuppressive tumor microenvironment[112,224]. Accordingly, a major goal of cancer immunotherapy is to provide activated leukocytes to the tumor tissues through direct activation of leukocyte subsets and/or re-polarization of the tumor microenvironment. However, attempts to activate tumor infiltrating antigen-presenting cells, macrophages and T cells through systemic administration of recombinant cytokines or IRMs such as TLR agonists have had limited success. Challenges include dose-limiting toxicity of the compounds, and the fact that systemic presence of pro-inflammatory cytokines can result in sepsis-like immune responses[168].

We have developed a delivery platform, which targets selected leukocyte subsets in the bloodstream, by conjugation of a monoclonal anti-DCIR antibody to stealth-type liposomes (saturated lipids, 30 mole% cholesterol, 5 mole% PEGylated lipid). The stealth formulation was selected to achieve good circulation properties for future *in vivo* studies and applications as well as ensuring that cell association was mediated by the Ab-antigen interaction and not unspecific uptake[179,225]. Our data, which show that the DCIR liposomes associate to a large fraction of the monocytes and mDCs as well as a small fraction of the pDCs (Fig. 7.3), are in agreement with the reported expression of DCIR, which shows high expression on monocytes and mDCs and lower expression on pDCs and B cells[204]. The very small RhB signal in the T, B and NK cell population is most likely due to the DCIR expression on B-cells, which make up 5 - 20 % of the T, B and NK cell population[226]. A more efficient targeting of the pDCs would likely be achievable through conjugation of an Ab against BDCA-2 (CD303), which is highly and exclusively expressed on pDCs (as well as internalized upon ligand binding)[186,227], but this would sacrifice the specific association to monocytes and mDCs.

The control liposomes also showed considerable association to the PBMC subsets (Fig. 7.4). Some unspecific uptake due to pinocytosis was expected in spite of the PEGylation of the liposomes[228]. However, as comparison with the uptake of non-Ab conjugated liposomes reveals significantly higher uptake of the control liposomes, we conclude that a substantial part of the unspecific internalization is mediated by the conjugated Ab. This mediation is probably due to the recognition of the murine Fc region by human Fc-receptors. While the conserved nature of antibodies across species suggests that this is a possibility, the experimental evidence is incomplete[229–232]. However, two studies have indicated that monocytes in particular are able to recognize murine IgG1-Fc[230,231], which is the Ab subtype used for this study.

If a large fraction of the unspecific interaction is caused by recognition of murine Fc, one way to eliminate this would be the use of an antibody fragment. Preferably such a fragment should be humanized and expressed recombinantly in a way that eliminates the need for the non-specific thiolation using Traut's reagent, which potentially results in thiolation in the antigen recognizing part of a fraction of the antibodies, thus rendering them non-functional. Omitting the thiolation procedure would also be advantageous as it would allow the fast progress from hydration and extrusion of the maleimide-functionalized liposomes to conjugation with the antibody, thus minimizing the time wherein the maleimide functional group potentially undergoes degradation. We and others[209] have observed that degradation of maleimide is a source of variability and

diminished yield. Accordingly, minimizing the time from hydration to conjugation, especially in buffers with pH above 6.5, is likely to improve yield and reproducibility.

To functionally activate the targeted cells, we formulated the liposomes with a potent and specific TLR7 agonist, TMX-202[171–173], which integrated into the control and DCIR liposomes to a similar extent (Table 7.2). As TLR7 is located in the endosomes and DCIR is internalized upon ligand binding[204], the use of DCIR as targeting ligand is a rational choice for facilitation of this receptor-agonist interaction.

To evaluate the activation of monocytes, mDCs and pDCs, we stimulated PBMCs and measured cytokines, which were indicative of activation of monocytes, mDCs or pDCs and/or were associated with important antitumor activity. Overall, our study demonstrates that targeting of TMX-202 to monocytes, mDCs and pDCs significantly increased the potency of TMX-202 with respect to induction of a pro-inflammatory cytokine response compared to the free drug (Fig. 7.5). As the selected cytokines are primarily produced by a limited subset of cells, we may form tentative conclusions about the producer cells, even if a correlation analysis did not reach statistical significance.

TLR7-induced secretion of IFNα has been shown to be highly pDC-dependent[164,217,219,233]. Therefore, our results, which demonstrate a substantially increased IFNα secretion with relatively limited targeting to pDCs, are evidence of the inducibility of the pDCs and their synthetic and secretory capacity, as well as the power of even low levels of targeting compared to non-targeted delivery (Fig. 7.3, 7.4 and 7.5A). Further, the presented data suggest that IFNα-therapy based on the presented platform could represent a significant improvement compared to the current therapeutic approach of administering recombinant IFNα intravenously. The relatively low absolute protein levels shown here are due to the sub-type specific assay, which only measures IFNα2a. However, the work of Birmachu and collegues[234] indicates that IFNα2a is approximately averagely expressed compared to the other 12 IFNα subtypes when stimulating pDCs or PBMCs through TLR7. Therefore, as it is unlikely that each particular TLR7-specific agonist has its own distinct expression pattern of IFNα subtypes, IFNα2a may be considered indicative of the relative expression levels of all IFNα subtypes. Apart from the ability to secrete IFNα, pDCs are also emerging as important in tumor immunology because of their putative ability to cross-present ingested antigen[134,213]. Thus, while the percentage of cells which associate with the DCIR liposomes is quite low, these activated pDCs may still make a deciding difference in the therapeutic setting.

The increased secretion of TNFα and IL-10 as a result of incubation with DCIR liposomes (Fig. 7.5D and E) indicate activation of monocytes, which are generally accepted to be a primary source of these cytokines[118]. T and NK cells are also capable of TNFα secretion, but they do not express DCIR, and a recent study demonstrated that even relatively weak T cell activation as a result of TLR7-mediated stimulus required prolonged incubation of purified $CD4^+$ T cells with the agonist. Thus the monocytes are the most likely source of TNFα.

Activation of monocytes is further supported by the detection of secreted IL-12p70 in the culture supernatants (Fig. 7.5B). However, as mDCs are considered equally capable of secreting IL-12p70[130,218,219] and both monocytes and mDCs are TLR7 positive[157,197], we are not able to determine the accurate cellular origin of the secreted IL-12p70 based on the present data.

The observation that IL-12p70 is most highly secreted on day 1 is congruent with a primary response from directly stimulated cells. In contrast, IFNγ levels increase over 4 days showing almost 4 fold higher levels on day 4 compared to day 1 (Fig. 7.5C). The buildup supports that the IFNγ secretion is a reaction from T and NK cells to IL-12p70. However, the day 1 levels are also very high, indicating either a very fast initial response from T and NK cells or that the IFNγ may – at least in part – also be produced as a primary response. While gene expression analyses have indicated that $CD4^+$ T cells express low levels of TLR7[235] and react to prolonged stimulation with Resiquimod (a TLR7/8 agonist) by secretion of IFNγ[236], T cells are DCIR negative[189] and thus unlikely to produce large amounts on IFNγ as a direct reaction to the DCIR liposomes. However, recently B cells and mDCs have also been shown to be able to produce IFNγ[131,237,238], although the protein levels and functional significance remain to be determined. It is conceivable that under these conditions either or both of these subsets contribute to the high initial IFNγ-levels. Irrespective of the cellular source, IFNγ secretion is potently induced which is highly attractive in a cancer immunotherapeutic setting, as IFNγ together with IFNα and IL-12p70 are viewed as indicative of an immune response dominated by cytotoxic T lymphocytes and instrumental in re-polarizing immune cells already present in the tumor tissues[131].

Finally, incubation of PBMCs with DCIR liposomes resulted in increased IL-6 secretion compared to incubation with free TMX-202. As the major sources of IL-6 are monocytes/macrophages and T cells, and the latter are DCIR negative, this supports monocyte activation due to treatment with the DCIR liposomes. However, incubation with control liposomes also induced substantial IL-6 secretion (Fig. 7.5F). The reason for this is presently unclear, but could be related to the detailed balance of the producing cells and their susceptibility to uptake of the liposomes

through association with the Fc part of the conjugated Abs. Elucidation of this phenomenon requires further experiments to clearly establish the cellular source of the secreted IL-6. This could be compared to the secretion of IL-10 and TNFα, which in our system are also primarily synthesized by monocytes, but are induced much less by the control liposomes.

An attractive therapeutic mechanism of the DCIR liposomes *in vivo* would be the activation of the target cells in the bloodstream followed by infiltration of the tumor tissues and cytokine secretion from the activated immune cells in the tumor tissues. A minimal requirement for this to be possible is a long-lasting induction of cytokine secretion. To investigate the temporal durability of the activation, we therefore measured the cytokine levels for 5 consecutive days (Fig. 7.5). In the light of a cell culture with a very high ratio of responder-to-producer cells, it is reasonable to assume that when cytokine levels are constant, as seen for IFNα2a and IL-6, some level of daily synthesis is likely to have taken place. In addition, the gradual increase in IFNγ secretion unequivocally demonstrates freshly secreted IFNγ for each day of culture, while no conclusions can be drawn regarding the temporal aspect of cytokine secretion based on these data for TNFα, IL-12p70 and IL-10.

On this premise, we suggest that our approach could result in differentially increased levels of IFNα, IFNγ, and IL-6 in the tissues rather than systemically, with the potential to re-polarize the tumor microenvironment and eliminate some of the challenges faced by current therapies based on systemic administration of cytokines and TLR agonists. Compared to the current practice of intravenous administration of recombinant IFNα, IFNα produced by activated pDCs after infiltration into the tumor tissues could result in a higher effective dose at the target site and lower systemic toxicity as well as comprising all subtypes and not just one recombinant form[239].

In conclusion, we have developed a platform for targeted delivery to monocytes, mDCs and pDCs. Using this platform to deliver a TLR7 agonist, we demonstrate that we are able to activate the target cells and improve the ability of the agonist to induce the secretion of key pro-inflammatory cytokines, IL-12p70, IFNγ and IFNα, all considered highly important in obtaining an efficient antitumor immune response mediated by $CD8^+$ T cells and NK cells. We hypothesize that the strategy of targeting leukocyte subsets in the circulation might be able to supply activated immune cells to the tumor tissues. Further, this strategy may be a way to achieve secretion of anti-cancer cytokines in the tumor tissues, which may be able to re-polarize the tumor microenvironment and thus facilitate tumor elimination. We envision the use of this therapeutic strategy either as adjuvant therapy after surgical removal of accessible tumors, as is

currently the case for the therapeutic use of recombinant IFNα, or in combination with other therapeutic modalities. A recent study demonstrated the benefits of combining systemic delivery of a TLR7 agonist with radiotherapy in a mouse lymphoma model[240], and our delivery platform could be a way to enhance the potency of the TLR7-mediated stimulation and/or reduce the side-effects of systemic induction of cytokine expression.

## 7.6 Supplementary Figure 7.1

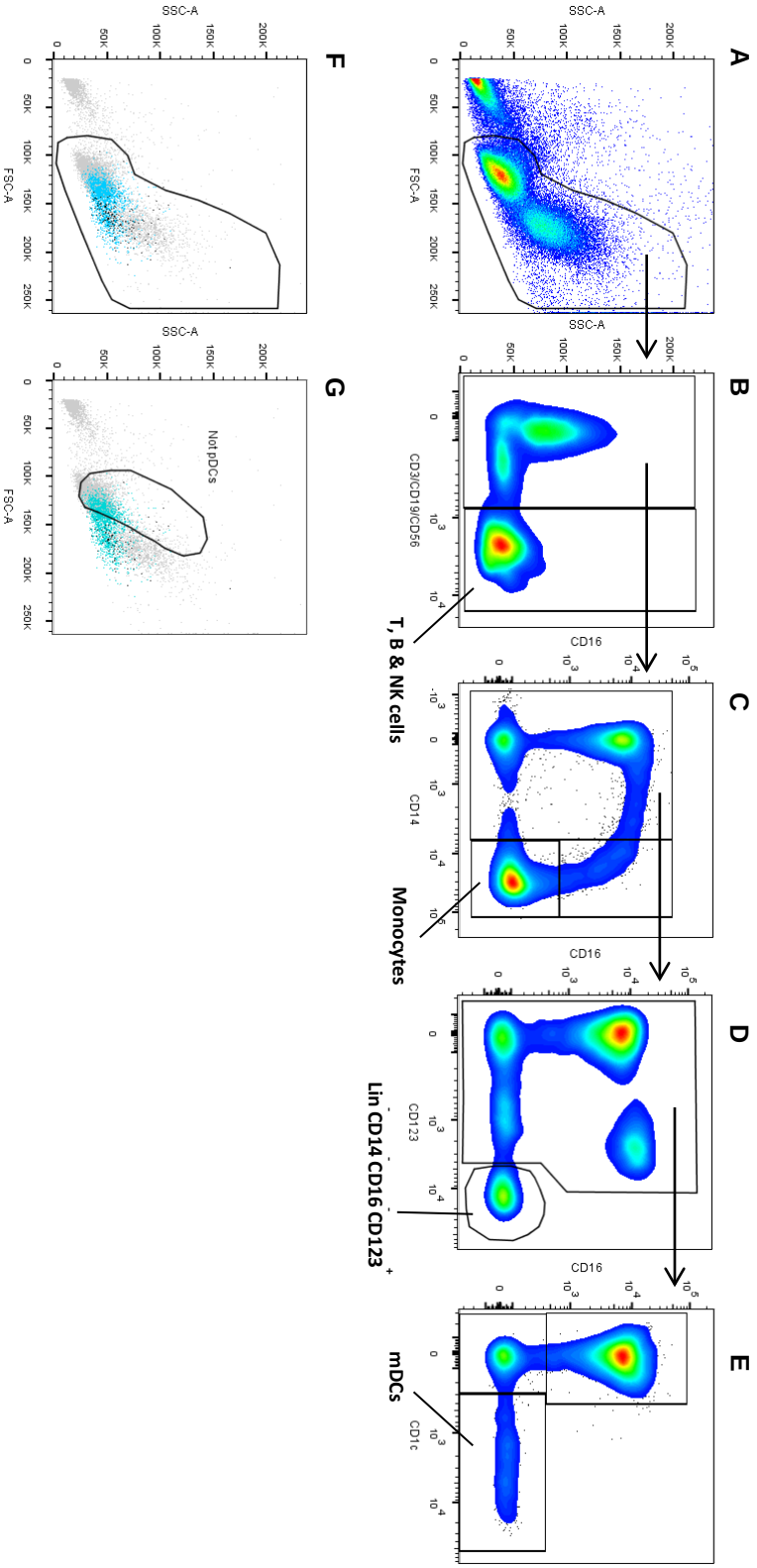


**Supplementary Figure 7.1.** Gating strategy. A. Ungated, B. PBMCs, C. Lineage$^-$, D. CD14$^-$, E. CD123$^-$, F. Backgating of lin$^-$CD14$^-$CD16$^-$CD123$^+$ PBMCs (blue) and lin$^-$CD14$^-$CD16$^-$CD303$^+$ PBMCs (black) on PBMCs (grey). G. The not-gate identifying pDCs by subtracting lin$^-$CD14$^-$CD16$^-$CD123$^+$CD303$^-$ PBMCs from the full lin$^-$CD14$^-$CD16$^-$CD123$^+$ population. PBMCs were gated on FSC-SSC. T, B and NK cells were identified as CD3$^+$, CD19$^+$ or CD56$^+$ (lin$^+$) PBMCs. Monocytes were identified as lin$^-$CD16$^-$CD14$^+$ PBMCs. mDCs were identified as lin$^-$CD14$^-$CD123$^-$CD16$^-$CD1c$^+$ PBMCs. pDCs were identified as lin$^-$CD14$^-$CD16$^-$CD123$^+$ which were not excluded by the not-gate illustrated in G. For details refer to the methods section.

# 8 Concluding remarks on Project II

The results of project II, which are presented in the article draft entitled “Activation of dendritic cells and monocytes by targeted delivery of a TLR7 agonist” demonstrate that we succeeded in designing a liposomal delivery platform capable of preferential targeting of the monocytes and DCs by post-functionalizing liposomes with Abs against DCIR. Further, the results show that formulation of a TLR7 agonist into the immunoliposomes produced a system which was highly capable of activating monocytes, mDCs and pDCs *in vitro*. Incubation of PBMCs with the DCIR liposomes resulted in secretion of pro-inflammatory cytokines, which have been associated positively with the development of cancer immunity. Finally, Project II demonstrates that the targeted delivery of the TLR7 agonist dramatically increased the potency of TMX-202 compared to the non-liposomal formulation.

While the presented results demonstrate the power of targeted delivery of TMX-202, several opportunities exist for providing a clearer and more nuanced picture of the effects. A first step would be to assess the targeting properties of the DCIR liposomes in whole blood to closer imitate systemic administration and investigate complement activation by the liposomes. To more accurately establish, which of the targeted (or non-targeted) subsets is responsible for the synthesis and secretion of each of the cytokines, such a detailed investigation should include intracellular flow cytometry on *in vitro* stimulated PBMCs to investigate the synthetic activity of the immune cell subsets. Further, this should be combined with *in vitro* stimulation of purified cells (e.g. purified monocytes) to establish, which of the synthetically active subsets actually secrete each of the cytokines and in what amounts. Finally, a more nuanced picture of the cellular activation could be obtained by monitoring of up- or down-regulation of cell-surface molecules indicative of subset activation.

While the results demonstrate that efficient targeting of the monocytes and dendritic cells are achieved, the immunoliposomal delivery platform also represents interesting opportunities for improvement. Currently, insufficient data is available regarding targeting of liposomes to cells in the bloodstream. It is for instance unclear how many Abs per liposome are required to obtain efficient targeting. As the Abs represent a source of unwanted, non-specific interaction, the number of Abs displayed on the liposomes should be minimized. Further, it might be attractive to use Ab fragments rather than whole Abs. For instance, the use of recombinantly expressed Ab-fragments could tailor the targeting Ab fragment to maleimide-mediated liposome

conjugation, thus making comparison of different Ab surface densities more accessible. Employing the post-insertion procedure would further contribute to the accessibility of such studies and might also reduce loss of Ab.

Finally, the current *in vitro* data should be supplemented with *in vivo* studies, for instance in mice. However, this will require switching Ab to one that recognizes the murine equivalent of human DCIR. Further, such *in vivo* studies should take into account that although DCIR is also expressed in murine monocytes, DCs and B cells[241], the details of the expression pattern may differ and Ab binding of murine DCIR may have additional consequences not associated with ligation of human DCIR.

# 9 Final concluding remarks and perspectives

This thesis is concerned with investigation of gene silencing and immunotherapy. Both are strategies that - in an envisioned therapeutic setting - promise high specificity through the exploitation of endogenous mechanisms intended for regulation of gene expression and immune defense, respectively.

The study of non-viral siRNA delivery focused on strengthening the understanding of polyplex interaction with the target cells as well as their intracellular processing. Increased understanding is pivotal in order to bring non-viral siRNA delivery closer to the clinic, and a fitting example of this is our incomplete understanding of the endosomal escape.

The presented results confirm that the use of PEI "off the shelf" for siRNA delivery has no future. Importantly, the study demonstrates the importance of the bound and the free fraction of polycation for siRNA delivery – in the absence of co-delivered free fraction, both conventional PEI and lipid conjugated PEI are ineffective delivery agents. Further, lipid conjugation in itself did not improve the delivery properties or the cytotoxicity profile of PEI, and consequently other, more elaborate modifications of PEI are required to provide the significant improvements necessary to make this polymer a potential part of an efficient vector for non-viral siRNA delivery.

Section 4 of this thesis briefly describes one such hypothetical modification, namely the encapsulation of the polyplex, bound and free fraction, in a delivery vehicle. However, as also described, such an approach is probably overly complicated compared to lipofection.

Our observations regarding the efficiency of lipofection are to some extent reflected in the delivery platforms, which are currently attracting the most interest commercially. So far, the only polycation-based delivery platform to show substantial promise has been the Rondel™ delivery technology developed by Mark Davis and colleagues at Caltech[80,242]. The Rondel™ platform is based on a cyclodextrin-containing polymer and showed promising initial results in phase I trials against melanoma, but further development was discontinued due to the emergence of adverse events.

However, the current trend in non-viral RNAi therapy is a move towards lipofection[243] and a number of early-stage cancer indications are being pursued, many of them using the SNALP technology developed by Pieter Cullis' group at UBC, Canada[244]. However, as only one of these

efforts has so far reached stage II clinical trials, cancer treatment based on non-viral delivery of siRNA still has some way to go before realizing the potential envisioned at the time of its discovery.

On the other hand, the research into cancer immunotherapy is starting to produce positive results. With the introduction of cytokine therapy, the use of the TLR7-based Imiquimod for treatment of melanoma, and – notably – the approval of the checkpoint blockers, the world is seeing the emergence of therapies, which are able to assist the immune system in its effort to eliminate the malignant cells.

A major hurdle to the use of systemically administered immune response modifiers such as TLR agonists has been the risk of introducing an uncontrolled systemic immune response. While the presented platform does not specifically target the tumor tissues, the increased potency it offers by directing the agonist to DCs and macrophages could provide higher effectivity, which could lower the required administrated dose, thus lowering the risk and/or severity of the induced side-effects.

As recombinant IFNα is already used in the clinic, we find it particularly interesting that even a modest targeting of the pDCs results in a dramatically increased concentration of IFNα2a in the culture supernatants compared to the non-targeted control. It would be highly interesting to investigate the level of activation and IFNα secretion achievable by efficient targeting specifically to the pDCs of the TLR7 agonist, as well as investigate the release of all the IFNα subtypes. Finally, as a measure of the potential therapeutic applicability, the effect on tumor progression in an animal model would complete the picture.

Interestingly, the presented data indicate that for some of the cytokines at least part of the secretory activity is sustained over several days. We therefore hypothesize, that our strategy of activating or preconditioning the DCs and macrophages in the blood could be an elegant way of increasing the concentration of pro-inflammatory anti-cancer cytokines in the tumor microenvironment. The resulting increased concentration of pro-inflammatory cytokines with antitumorigenic effects might be able to drive the re-polarization of the tumor microenvironment. Currently, this remains highly speculative, but the temporal profile of the cytokine secretion observed in Project II certainly warrants further examination. The concept of achieving cytokine secretion in the tumor tissues by activating cells in the blood rather than in the tumor tissue is highly attractive because it circumvents the need for passive accumulation of nanoparticles in the tumor tissues by the EPR effect. While the EPR effect is present in certain

cancer forms without a doubt, it is equally clear that in other cancer types it is absent or insufficiently pronounced to ensure adequate accumulation. The described approach could thus enable nanoparticle based treatment of such cancers while simultaneously limit the induction of cytokine syndrome associated with systemically administrated IRMs.

# References


1. WHO. Cancer Fact Sheet No. 297. (2014). at <http://www.who.int/mediacentre/factsheets/fs297/en/>

2. Chiang, A. C. & Massagué, J. Molecular basis of metastasis. *N. Engl. J. Med.* **359,** 2814–23 (2008).

3. Torchilin, V. P. Drug targeting. *Eur. J. Pharm. Sci. Off. J. Eur. Fed. Pharm. Sci.* **11 Suppl 2,** S81–91 (2000).

4. Nahta, R. & Esteva, F. J. Herceptin: Mechanisms of action and resistance. *Cancer Lett.* **232,** 123–38 (2006).

5. Friedmann, T. A brief history of gene therapy. *Nat. Genet.* **2,** 93–98 (1992).

6. Wang, T., Upponi, J. R. & Torchilin, V. P. Design of multifunctional non-viral gene vectors to overcome physiological barriers: dilemmas and strategies. *Int. J. Pharm.* **427,** 3–20 (2012).

7. Blau, H. & Springer, M. Gene therapy—a novel form of drug delivery. *N. Engl. J. Med.* **333,** 1204–1207 (1995).

8. Thomas, C. E., Ehrhardt, A. & Kay, M. A. Progress and problems with the use of viral vectors for gene therapy. *Nat. Rev. Genet.* **4,** 346–58 (2003).

9. Lamarre, B. & Ryadnov, M. G. Self-assembling viral mimetics: one long journey with short steps. *Macromol. Biosci.* **11,** 503–13 (2011).

10. Lew, D., Parker, S., Latimer, T. & Abai, A. M. Cancer Gene Therapy Using Plasmid DNA: Pharmacokinetic Study of DNA Following Injection in Mice. *Hum. Gene Ther.* **6,** 553–564 (1995).

11. Rojahn, S. Y. When Will Gene Therapy Come to the U.S.? *MIT Technol. Rev.* 2013–2015 (2013).

12. European Medicines Agency. Press Release: First European Gene Therapy Product Recommended for Approval by EMA. (2012). at <http://www.ema.europa.eu/ema/index.jsp?curl=pages/news_and_events/news/2012/07/news_detail_001574.jsp&mid=WC0b01ac058004d5c1>

13. Stephenson, M. L. & Zamecnik, P. C. Inhibition of Rous sarcoma viral RNA translation by a specific oligodeoxyribonucleotide. *Proc. Natl. Acad. Sci. U. S. A.* **75,** 285–288 (1978).

14. Zamecnik, P. C. & Stephenson, M. L. Inhibition of Rous sarcoma virus replication and cell transformation by a specific oligodeoxynucleotide. *Proc. Natl. Acad. Sci. U. S. A.* **75,** 280–284 (1978).

15. Fire, A., Xu, S., Montgomery, M. & Kostas, S. Potent and specific genetic interference by double-stranded RNA in Caenorhabditis elegans. *Nature* **391,** 806–811 (1998).

16. Elbashir, S. *et al.* Duplexes of 21-nucleotide RNAs mediate RNA interference in cultured mammalian cells. *Nature* **411,** 1–5 (2001).

17. McCaffrey, A. *et al.* Gene expression: RNA interference in adult mice. *Nature* 38–39 (2002).

18. Bartel, D. MicroRNAs: genomics, biogenesis, mechanism, and function. *Cell* **116,** 281–297 (2004).

19. Kim, D. H. & Rossi, J. J. Strategies for silencing human disease using RNA interference. *Nat. Rev. Genet.* **8,** 173–84 (2007).

20. Doench, J. G., Petersen, C. P. & Sharp, P. A. siRNAs can function as miRNAs. *Genes Dev.* **17,** 438–42 (2003).

21. Davidson, B. L. & McCray, P. B. Current prospects for RNA interference-based therapies. *Nat. Rev. Genet.* **12,** 329–40 (2011).

22. Zamore, P. D., Tuschl, T., Sharp, P. A. & Bartel, D. P. RNAi: double-stranded RNA directs the ATP-dependent cleavage of mRNA at 21 to 23 nucleotide intervals. *Cell* **101,** 25–33 (2000).

23. Aigner, A. Delivery systems for the direct application of siRNAs to induce RNA interference (RNAi) in vivo. *J. Biomed. Biotechnol.* **2006,** 71659 (2006).

24. Bartlett, D. W. & Davis, M. E. Insights into the kinetics of siRNA-mediated gene silencing from live-cell and live-animal bioluminescent imaging. *Nucleic Acids Res.* **34,** 322–33 (2006).

25. Dominska, M. & Dykxhoorn, D. M. Breaking down the barriers: siRNA delivery and endosome escape. *J. Cell Sci.* **123,** 1183–9 (2010).

26. Mintzer, M. A. & Simanek, E. E. Nonviral vectors for gene delivery. *Chem. Rev.* **109,** 259–302 (2009).

27. Miyata, K., Nishiyama, N. & Kataoka, K. Rational design of smart supramolecular assemblies for gene delivery: chemical challenges in the creation of artificial viruses. *Chem. Soc. Rev.* **41,** 2562–2574 (2012).

28. Chrastina, A., Massey, K. a & Schnitzer, J. E. Overcoming in vivo barriers to targeted nanodelivery. *Wiley Interdiscip. Rev. Nanomedicine Nanobiotechnology* **3,** 421–37 (2011).

29. Taurin, S., Nehoff, H. & Greish, K. Anticancer nanomedicine and tumor vascular permeability; Where is the missing link? *J. Control. Release* **164,** 265–75 (2012).

30. Ruponen, M. Extracellular and intracellular barriers in non-viral gene delivery. *J. Control. Release* **93,** 213–217 (2003).

31. Escoffre, J.-M., Teissié, J. & Rols, M.-P. Gene transfer: how can the biological barriers be overcome? *J. Membr. Biol.* **236,** 61–74 (2010).

32. Lu, J. J., Langer, R. & Chen, J. A Novel Mechanism Is Involved in Cationic Lipid-Mediated Functional siRNA Delivery. *Mol. Pharm.* **6,** 763–771 (2009).

33. Sahay, G., Alakhova, D. Y. & Kabanov, A. V. Endocytosis of nanomedicines. *J. Control. Release* **145,** 182–95 (2010).

34. Payne, C. K., Jones, S. A., Chen, C. & Zhuang, X. Internalization and trafficking of cell surface proteoglycans and proteoglycan-binding ligands. *Traffic* **8,** 389–401 (2007).

35. Thomsen, P., Roepstorff, K., Stahlhut, M. & van Deurs, B. Caveolae are highly immobile plasma membrane microdomains, which are not involved in constitutive endocytic trafficking. *Mol. Biol. Cell* **13,** 238–250 (2002).

36. Khalil, I., Kogure, K., Akita, H. & Harashima, H. Uptake pathways and subsequent intracellular trafficking in nonviral gene delivery. *Pharmacol. Rev.* **58,** 32–45 (2006).

37. Merdan, T., Kopeček, J. & Kissel, T. Prospects for cationic polymers in gene and oligonucleotide therapy against cancer. *Adv. Drug Deliv. Rev.* **54,** 715–758 (2002).

38. Mastrobattista, E., van der Aa, M. A. E. M., Hennink, W. E. & Crommelin, D. J. A. Artificial viruses: a nanotechnological approach to gene delivery. *Nat. Rev. Drug Discov.* **5,** 115–21 (2006).

39. Sardesai, N. Y. & Weiner, D. B. Electroporation delivery of DNA vaccines: prospects for success. *Curr. Opin. Immunol.* **23,** 421–9 (2011).

40. Liu, M. A. DNA vaccines: an historical perspective and view to the future. *Immunol. Rev.* **239,** 62–84 (2011).

41. Ginn, S. L., Alexander, I. E., Edelstein, M. L., Abedi, M. R. & Wixon, J. Gene therapy clinical trials worldwide to 2012 - an update. *J. Gene Med.* **15,** 65–77 (2013).

42. Liu, Q. & Muruve, D. A. Molecular basis of the inflammatory response to adenovirus vectors. *Gene Ther.* **10,** 935–40 (2003).

43. Sun, J. Y., Anand-Jawa, V., Chatterjee, S. & Wong, K. K. Immune responses to adeno-associated virus and its recombinant vectors. *Gene Ther.* **10,** 964–76 (2003).

44. David, S., Pitard, B., Benoît, J.-P. & Passirani, C. Non-viral nanosystems for systemic siRNA delivery. *Pharmacol. Res.* **62,** 100–14 (2010).

45. El-Aneed, A. An overview of current delivery systems in cancer gene therapy. *J. Control. Release* **94,** 1–14 (2004).

46. Katas, H. & Alpar, H. O. Development and characterisation of chitosan nanoparticles for siRNA delivery. *J. Control. Release* **115,** 216–25 (2006).

47. Wolfert, M. & Seymour, L. Chloroquine and amphipathic peptide helices show synergistic transfection in vitro. *Gene Ther.* 409–414 (1998).

48. Choi, Y. H. *et al.* Polyethylene glycol-grafted poly-L-lysine as polymeric gene carrier. *J. Control. Release* **54,** 39–48 (1998).

49. Felgner, P. L. *et al.* Lipofection: a highly efficient, lipid-mediated DNA-transfection procedure. *Proc. Natl. Acad. Sci. U. S. A.* **84,** 7413–7417 (1987).

50. Ewert, K. K. *et al.* Cationic liposome–nucleic acid complexes for gene delivery and silencing: pathways and mechanisms for plasmid DNA and siRNA. *Top. Curr. Chem.* **296,** 191–226 (2010).

51. Semple, S. & Klimuk, S. Efficient encapsulation of antisense oligonucleotides in lipid vesicles using ionizable aminolipids: formation of novel small multilamellar vesicle structures. *Biochim. Biophys. Acta* **1510,** 152–166 (2001).

52. Gjetting, T., Jølck, R. I. & Andresen, T. L. Effective nanoparticle-based gene delivery by a protease triggered charge switch. *Adv. Healthc. Mater.* **3,** 1107–18 (2014).

53. Neu, M., Fischer, D. & Kissel, T. Recent advances in rational gene transfer vector design based on poly(ethylene imine) and its derivatives. *J. Gene Med.* **7,** 992–1009 (2005).

54. Lungwitz, U., Breunig, M., Blunk, T. & Göpferich, A. Polyethylenimine-based non-viral gene delivery systems. *Eur. J. Pharm. Biopharm.* **60,** 247–66 (2005).

55. Boussif, O. *et al.* A versatile vector for gene and oligonucleotide transfer into cells in culture and in vivo: polyethylenimine. *Proc. Natl. Acad. Sci. U. S. A.* **92,** 7297–301 (1995).

56. Suh, J., Paik, H. J. & Hwang, B. K. Ionization of poly(ethylenimine) and poly(allylamine) at various pH's. *Bioorg. Chem.* **22,** 318–327 (1994).

57. Benjaminsen, R. V, Mattebjerg, M. A., Henriksen, J. R., Moghimi, S. M. & Andresen, T. L. The possible "proton sponge " effect of polyethylenimine (PEI) does not include change in lysosomal pH. *Mol. Ther.* **21,** 149–57 (2013).

58. Von Harpe, A., Petersen, H., Li, Y. & Kissel, T. Characterization of commercially available and synthesized polyethylenimines for gene delivery. *J. Control. Release* **69,** 309–322 (2000).

59. Breunig, M., Lungwitz, U., Liebl, R. & Goepferich, A. Breaking up the correlation between efficacy and toxicity for nonviral gene delivery. *Proc. Natl. Acad. Sci. U. S. A.* **104,** 14454–9 (2007).

60. Parhamifar, L., Larsen, A. K., Hunter, A. C., Andresen, T. L. & Moghimi, S. M. Polycation cytotoxicity: a delicate matter for nucleic acid therapy—focus on polyethylenimine. *Soft Matter* **6,** 4001 (2010).

61. Nelson, N. Structure and pharmacology of the proton-ATPases. *Trends Pharmacol. Sci.* **12,** 71–75 (1991).

62. Behr, J. P. The proton sponge: a trick to enter cells the viruses did not exploit. *Chim. Int. J. Chem.* **2,** 34–36 (1997).

63. Won, Y.-Y., Sharma, R. & Konieczny, S. F. Missing pieces in understanding the intracellular trafficking of polycation/DNA complexes. *J. Control. Release* **139,** 88–93 (2009).

64. Bieber, T., Meissner, W., Kostin, S., Niemann, A. & Elsasser, H.-P. Intracellular route and transcriptional competence of polyethylenimine–DNA complexes. *J. Control. Release* **82,** 441–454 (2002).

65. Whitehead, K. A., Langer, R. & Anderson, D. G. Knocking down barriers: advances in siRNA delivery. *Nat. Rev. Drug Discov.* **8,** 129–38 (2009).

66. Breunig, M. *et al.* Gene delivery with low molecular weight linear polyethylenimines. *J. Gene Med.* **7,** 1287–98 (2005).

67. Pereira, P. *et al.* Characterization of polyplexes involving small RNA. *J. Colloid Interface Sci.* **387,** 84–94 (2012).

68. Thomas, M., Ge, Q., Lu, J. J., Chen, J. & Klibanov, A. Cross-linked Small Polyethylenimines: While Still Nontoxic, Deliver DNA Efficiently to Mammalian Cells in Vitro and in Vivo. *Pharm. Res.* **22,** 373–380 (2005).

69. Teng, L., Xie, J., Teng, L. & Lee, R. J. Enhanced siRNA delivery using oleic acid derivative of polyethylenimine. *Anticancer Res.* **32,** 1267–71 (2012).

70. Nimesh, S. & Chandra, R. Polyethylenimine nanoparticles as an efficient in vitro siRNA delivery system. *Eur. J. Pharm. Biopharm.* **73,** 43–9 (2009).

71. Navarro, G., Sawant, R. R., Essex, S., Tros de Ilarduya, C. & Torchilin, V. P. Phospholipid-polyethylenimine conjugate-based micelle-like nanoparticles for siRNA delivery. *Drug Deliv. Transl. Res.* **1,** 25–33 (2011).

72. Sawant, R. R. *et al.* Polyethyleneimine-lipid conjugate-based pH-sensitive micellar carrier for gene delivery. *Biomaterials* **33,** 3942–51 (2012).

73. Wang, D. *et al.* Novel Branched Poly (Ethylenimine)-Cholesterol Water-Soluble Lipopolymers for Gene Delivery. *Biomacromoles* **3,** 1197–1207 (2002).

74. Bouxsein, N. F., McAllister, C. S., Ewert, K. K., Samuel, C. E. & Safinya, C. R. Structure and gene silencing activities of monovalent and pentavalent cationic lipid vectors complexed with siRNA. *Biochemistry* **46,** 4785–92 (2007).

75. Ewert, K. K. *et al.* A columnar phase of dendritic lipid-based cationic liposome-DNA complexes for gene delivery: hexagonally ordered cylindrical micelles embedded in a DNA honeycomb lattice. *J. Am. Chem. Soc.* **128,** 3998–4006 (2006).

76. Ahmad, A. *et al.* New multivalent cationic lipids reveal bell curve for transfection efficiency versus membrane charge density: lipid-DNA complexes for gene delivery. *J. Gene Med.* **7,** 739–48 (2005).

77. Tros de Ilarduya, C., Sun, Y. & Düzgüneş, N. Gene delivery by lipoplexes and polyplexes. *Eur. J. Pharm. Sci.* **40,** 159–70 (2010).

78. Ryther, R. C. C., Flynt, A. S., Phillips, J. A. & Patton, J. G. siRNA therapeutics: big potential from small RNAs. *Gene Ther.* **12,** 5–11 (2005).

79. Elbashir, S., Lendeckel, W. & Tuschl, T. RNA interference is mediated by 21-and 22-nucleotide RNAs. *Genes Dev.* 188–200 (2001). doi:10.1101/gad.862301.vents

80. Davis, M. E. *et al.* Evidence of RNAi in humans from systemically administered siRNA via targeted nanoparticles. *Nature* **464,** 1067–70 (2010).

81. Pack, D. W., Hoffman, A. S., Pun, S. & Stayton, P. S. Design and development of polymers for gene delivery. *Nat. Rev. Drug Discov.* **4,** 581–93 (2005).

82. Godbey, W. T., Wu, K. K. & Mikos, A. G. Poly(ethylenimine) and its role in gene delivery. *J. Control. Release* **60,** 149–60 (1999).

83. Urban-Klein, B., Werth, S., Abuharbeid, S., Czubayko, F. & Aigner, A. RNAi-mediated gene-targeting through systemic application of polyethylenimine (PEI)-complexed siRNA in vivo. *Gene Ther.* **12,** 461–6 (2005).

84. Bologna, J.-C., Dorn, G., Natt, F. & Weiler, J. Linear polyethylenimine as a tool for comparative studies of antisense and short double-stranded RNA oligonucleotides. *Nucleosides. Nucleotides Nucleic Acids* **22,** 1729–31 (2003).

85. Godbey, W. T., Wu, K. K. & Mikos, A. G. Tracking the intracellular path of poly(ethylenimine)/DNA complexes for gene delivery. *Proc. Natl. Acad. Sci. U. S. A.* **96,** 5177–81 (1999).

86. Hoekstra, D., Rejman, J., Wasungu, L., Shi, F. & Zuhorn, I. Gene delivery by cationic lipids: in and out of an endosome. *Biochem. Soc. Trans.* **35,** 68–71 (2007).

87. Gabrielson, N. P. & Pack, D. W. Efficient polyethylenimine-mediated gene delivery proceeds via a caveolar pathway in HeLa cells. *J. Control. Release* **136,** 54–61 (2009).

88. Sandvig, K., Pust, S., Skotland, T. & van Deurs, B. Clathrin-independent endocytosis: mechanisms and function. *Curr. Opin. Cell Biol.* **23,** 413–20 (2011).

89. Sandvig, K., Torgersen, M. L., Raa, H. A. & van Deurs, B. Clathrin-independent endocytosis: from nonexisting to an extreme degree of complexity. *Histochem. Cell Biol.* **129,** 267–76 (2008).

90. Kanasty, R. L., Whitehead, K. A., Vegas, A. J. & Anderson, D. G. Action and reaction: the biological response to siRNA and its delivery vehicles. *Mol. Ther.* **20,** 513–24 (2012).

91. Aliabadi, H. M. *et al.* Impact of lipid substitution on assembly and delivery of siRNA by cationic polymers. *Macromol. Biosci.* **11,** 662–72 (2011).

92. Incani, V., Lavasanifar, A. & Uludağ, H. Lipid and hydrophobic modification of cationic carriers on route to superior gene vectors. *Soft Matter* **6,** 2124 (2010).

93. Kim, W. J., Chang, C.-W., Lee, M. & Kim, S. W. Efficient siRNA delivery using water soluble lipopolymer for anti-angiogenic gene therapy. *J. Control. Release* **118,** 357–63 (2007).

94. Navarro, G., Sawant, R. & Biswas, S. P-glycoprotein silencing with siRNA delivered by DOPE-modified PEI overcomes doxorubicin resistance in breast cancer cells. *Nanomedicine* **7,** 65–78 (2012).

95. Dai, Z., Gjetting, T., Mattebjerg, M. A., Wu, C. & Andresen, T. L. Elucidating the interplay between DNA-condensing and free polycations in gene transfection through a mechanistic study of linear and branched PEI. *Biomaterials* **32,** 8626–34 (2011).

96. Yue, Y. *et al.* Revisit complexation between DNA and polyethylenimine - Effect of uncomplexed chains free in the solution mixture on gene transfection. *J. Control. Release* **155,** 67–76 (2011).

97. Yue, Y. *et al.* Revisit complexation between DNA and polyethylenimine - Effect of length of free polycationic chains on gene transfection. *J. Control. Release* **152,** 143–51 (2011).

98. Sambrook, J. & Russel, D. W. *Molecular Cloning: A Laboratory Manual vol. 1-3*. (Cold Spring Harbour Laboratory Press, Cold Spring Harbour, New York, 2001).

99. Benjaminsen, R. V *et al.* Evaluating nanoparticle sensor design for intracellular pH measurements. *ACS Nano* **5,** 5864–73 (2011).

100. Boeckle, S. *et al.* Purification of polyethylenimine polyplexes highlights the role of free polycations in gene transfer. *J. Gene Med.* **6,** 1102–11 (2004).

101. Erbacher, P. *et al.* Transfection and physical properties of various saccharide, poly(ethylene glycol), and antibody-derivatized polyethylenimines (PEI). *J. Gene Med.* **1,** 210–22 (1999).

102. Tzeng, S. Y., Yang, P. H., Grayson, W. L. & Green, J. J. Synthetic poly(ester amine) and poly(amido amine) nanoparticles for efficient DNA and siRNA delivery to human endothelial cells. *Int. J. Nanomedicine* **6,** 3309–22 (2011).

103. Zuhorn, I. S. *et al.* Nonbilayer phase of lipoplex-membrane mixture determines endosomal escape of genetic cargo and transfection efficiency. *Mol. Ther.* **11,** 801–10 (2005).

104. Radwan Almofti, M. *et al.* Cationic liposome-mediated gene delivery: Biophysical study and mechanism of internalization. *Arch. Biochem. Biophys.* **410,** 246–253 (2003).

105. Dai, Z. & Wu, C. How Does DNA Complex with Polyethylenimine with Different Chain Lengths and Topologies in Their Aqueous Solution Mixtures? *Macromolecules* **45,** 4346–4353 (2012).

106. Rejman, J., Oberle, V., Zuhorn, I. S. & Hoekstra, D. Size-dependent internalization of particles via the pathways of clathrin- and caveolae-mediated endocytosis. *Biochem. J.* **377,** 159–69 (2004).

107. Ladokhin, A. S. & White, S. H. Protein chemistry at membrane interfaces: non-additivity of electrostatic and hydrophobic interactions. *J. Mol. Biol.* **309,** 543–52 (2001).

108. Navarro, G., Essex, S. & Sawant, R. Phospholipid-modified polyethylenimine-based nanopreparations for siRNA–mediated gene silencing: Implications for transfection and the role of lipid components. *Nanomedicine* 1–9 (2013). doi:10.1016/j.nano.2013.07.016

109. Utskarpen, A. *et al.* Shiga toxin increases formation of clathrin-coated pits through Syk kinase. *PLoS One* **5,** e10944 (2010).

110. Scita, G. & Di Fiore, P. P. The endocytic matrix. *Nature* **463,** 464–73 (2010).

111. Cheng, Z. *et al.* Distinct mechanisms of clathrin-independent endocytosis have unique sphingolipid requirements. *Mol. Biol. Cell* **17,** 3197–3210 (2006).

112. Dunn, G., Old, L. & Schreiber, R. The immunobiology of cancer immunosurveillance and immunoediting. *Immunity* **21,** 137–148 (2004).

113. Cann, S. A. H., van Netten, J. P. & van Netten, C. Dr William Coley and tumour regression: a place in history or in the future. *Postgrad. Med. J.* **79,** 672–681 (2003).

114. Dougan, M. & Dranoff, G. Immune therapy for cancer. *Annu. Rev. Immunol.* **27,** 83–117 (2009).

115. Vacchelli, E. *et al.* Trial Watch: Tumor-targeting monoclonal antibodies in cancer therapy. *Oncoimmunology* **3,** 1–20 (2014).

116. Sylvester, R. J. Bacillus Calmette-Guérin treatment of non-muscle invasive bladder cancer. *Int. J. Urol.* **18,** 113–20 (2011).

117. Dhodapkar, M. V, Dhodapkar, K. M. & Palucka, A. K. Interactions of tumor cells with dendritic cells: balancing immunity and tolerance. *Cell Death Differ.* **15,** 39–50 (2008).

118. Murphy, K., Travers, P. & Walport, M. *Janeway's Immunobiology*. (Garland Science, 2008).

119. Rosenberg, S. a, Yang, J. C. & Restifo, N. P. Cancer immunotherapy: moving beyond current vaccines. *Nat. Med.* **10,** 909–15 (2004).

120. Kenter, G. G., Welters, M. J. P., Valentijn, A. R. P. M., Lowik, M. J. G. & Meer, D. M. A. B. Vaccination against HPV-16 oncoproteins for vulvar intraepithelial neoplasia. *N. Engl. J. Med.* **361,** 1838–47 (2009).

121. Vansteenkiste, J. *et al.* Adjuvant MAGE-A3 immunotherapy in resected non-small-cell lung cancer: phase II randomized study results. *J. Clin. Oncol.* **31,** 2396–403 (2013).

122. Schuler, G. Dendritic cells in cancer immunotherapy. *Eur. J. Immunol.* **40,** 2123–30 (2010).

123. Palucka, K., Banchereau, J. & Mellman, I. Designing vaccines based on biology of human dendritic cell subsets. *Immunity* **33,** 464–78 (2010).

124. Liu, H. *et al.* Structure-based programming of lymph-node targeting in molecular vaccines. *Nature* **507,** 519–22 (2014).

125. Pardoll, D. M. The blockade of immune checkpoints in cancer immunotherapy. *Nat. Rev. Cancer* **12,** 252–64 (2012).

126. Pinto, A., Rega, A., Crother, T. R. & Sorrentino, R. Plasmacytoid dendritic cells and their therapeutic activity in cancer. *Oncoimmunology* **1,** 726–734 (2012).

127. Tel, J., van der Leun, A. M., Figdor, C. G., Torensma, R. & de Vries, I. J. M. Harnessing human plasmacytoid dendritic cells as professional APCs. *Cancer Immunol. Immunother.* **61,** 1279–88 (2012).

128. Puig, M. *et al.* TLR9 and TLR7 agonists mediate distinct type I IFN responses in humans and nonhuman primates in vitro and in vivo. *J. Leukoc. Biol.* **91,** 147–58 (2012).

129. Yanofsky, V. R., Mitsui, H., Felsen, D. & Carucci, J. a. Understanding dendritic cells and their role in cutaneous carcinoma and cancer immunotherapy. *Clin. Dev. Immunol.* **2013,** 1–14 (2013).

130. Trinchieri, G., Pflanz, S. & Kastelein, R. The IL-12 Family of Heterodimeric Cytokines: New Players in the Regulation of T Cell Responses. *Immunity* **19,** 641–644 (2003).

131. Frucht, D. M. *et al.* IFN-γ production by antigen-presenting cells: mechanisms emerge. *Trends Immunol.* **22,** 556–560 (2001).

132. Kreutz, M., Tacken, P. J. & Figdor, C. G. Targeting dendritic cells - why bother? *Blood* **121,** 2836–2845 (2013).

133. Jongbloed, S. L. *et al.* Human CD141+ (BDCA-3)+ dendritic cells (DCs) represent a unique myeloid DC subset that cross-presents necrotic cell antigens. *J. Exp. Med.* **207,** 1247–60 (2010).

134. Tel, J. *et al.* Human plasmacytoid dendritic cells efficiently cross-present exogenous Ags to CD8+ T cells despite lower Ag uptake than myeloid dendritic cell subsets. *Blood* **121,** 459–67 (2013).

135. Klechevsky, E. *et al.* Cross-priming CD8+ T cells by targeting antigens to human dendritic cells through DCIR. *Blood* **116,** 1685–97 (2010).

136. Liu, C., Lou, Y., Lizée, G. & Qin, H. Plasmacytoid dendritic cells induce NK cell–dependent, tumor antigen–specific T cell cross-priming and tumor regression in mice. *J. Clin. Invest.* **118,** 1165–1175 (2008).

137. Palucka, K. & Banchereau, J. Cancer immunotherapy via dendritic cells. *Nat. Rev. Cancer* **12,** 265–77 (2012).

138. Ueno, H. *et al.* Harnessing human dendritic cell subsets for medicine. *Immunol. Rev.* **234,** 199–212 (2010).

139. Chomarat, P., Banchereau, J., Davoust, J. & Palucka, A. K. IL-6 switches the differentiation of monocytes from dendritic cells to macrophages. *Nat. Immunol.* **1,** 510–514 (2000).

140. Hiltbold, E. M., Vlad, A. M., Ciborowski, P., Watkins, S. C. & Finn, O. J. The Mechanism of Unresponsiveness to Circulating Tumor Antigen MUC1 Is a Block in Intracellular Sorting and Processing by Dendritic Cells. *J. Immunol.* **165,** 3730–3741 (2000).

141. Fiorentino, D. F. *et al.* IL-10 Acts On The Antigen-Presenting Cell to Inhibit Cytokine Production by Th1 Cells. *J. Immunol.* **146,** 3444–3451 (1991).

142. Steinbrink, K., Wölfl, M., Jonuleit, H., Knop, J. & Enk, A. H. Induction of Tolerance by IL-10-Treated Dendritic Cells. *J. Immunogy* **159,** 4772–4780 (1997).

143. Aspord, C. *et al.* Breast cancer instructs dendritic cells to prime interleukin 13-secreting CD4+ T cells that facilitate tumor development. *J. Exp. Med.* **204,** 1037–47 (2007).

144. DeNardo, D. G. *et al.* CD4(+) T cells regulate pulmonary metastasis of mammary carcinomas by enhancing protumor properties of macrophages. *Cancer Cell* **16,** 91–102 (2009).

145. Hanahan, D. & Weinberg, R. a. Hallmarks of cancer: the next generation. *Cell* **144,** 646–74 (2011).

146. Franklin, R. A. *et al.* The cellular and molecular origin of tumor-associated macrophages. *Science* **344,** 921–5 (2014).

147. Solinas, G., Germano, G., Mantovani, A. & Allavena, P. Tumor-associated macrophages (TAM) as major players of the cancer-related inflammation. *J. Leukoc. Biol.* **86,** 1065–73 (2009).

148. Murdoch, C., Muthana, M., Coffelt, S. B. & Lewis, C. E. The role of myeloid cells in the promotion of tumour angiogenesis. *Nat. Rev. Cancer* **8,** 618–31 (2008).

149. Ruffell, B., Affara, N. I. & Coussens, L. M. Differential macrophage programming in the tumor microenvironment. *Trends Immunol.* **33,** 119–26 (2012).

150. Marigo, I., Dolcetti, L., Serafini, P., Zanovello, P. & Bronte, V. Tumor-induced tolerance and immune suppression by myeloid derived suppressor cells. *Immunol. Rev.* **222,** 162–79 (2008).

151. Ostrand-Rosenberg, S. Myeloid-derived suppressor cells: more mechanisms for inhibiting antitumor immunity. *Cancer Immunol. Immunother.* **59,** 1593–600 (2010).

152. Gabrilovich, D. I. & Nagaraj, S. Myeloid-derived suppressor cells as regulators of the immune system. *Nat. Rev. Immunol.* **9,** 162–74 (2009).

153. Youn, J.-I., Nagaraj, S., Collazo, M. & Gabrilovich, D. I. Subsets of Myeloid-Derived Suppressor Cells in Tumor-Bearing Mice. *J. Immunol.* **181,** 5791–5802 (2008).

154. Li, Q., Pan, P.-Y., Gu, P., Xu, D. & Chen, S.-H. Role of immature myeloid Gr-1+ cells in the development of antitumor immunity. *Cancer Res.* **64,** 1130–1139 (2004).

155. Mirza, N. *et al.* All-trans-retinoic acid improves differentiation of myeloid cells and immune response in cancer patients. *Cancer Res.* **66,** 9299–307 (2006).

156. Etzerodt, A. *et al.* Efficient intracellular drug-targeting of macrophages using stealth liposomes directed to the hemoglobin scavenger receptor CD163. *J. Control. Release* **160,** 72–80 (2012).

157. Iwasaki, A. & Medzhitov, R. Toll-like receptor control of the adaptive immune responses. *Nat. Immunol.* **5,** 987–95 (2004).

158. Akira, S., Uematsu, S. & Takeuchi, O. Pathogen recognition and innate immunity. *Cell* **124,** 783–801 (2006).

159. Janeway, C. A. & Medzhitov, R. Innate immune recognition. *Annu. Rev. Immunol.* **20,** 197–216 (2002).

160. Kawai, T. & Akira, S. Innate immune recognition of viral infection. *Nat. Immunol.* **7,** 131–7 (2006).

161. Galluzzi, L. *et al.* Trial Watch: Experimental Toll-like receptor agonists for cancer therapy. *Oncoimmunology* **1,** 699–716 (2012).

162. Aranda, F. *et al.* Trial Watch: Toll-like receptor agonists in oncological indications. *Oncoimmunology* **3,** e29179 (2014).

163. Philbin, V. J. & Levy, O. Immunostimulatory activity of Toll-like receptor 8 agonists towards human leucocytes: basic mechanisms and translational opportunities. *Biochem. Soc. Trans.* **35,** 1485–91 (2007).

164. Inglefield, J. R. *et al.* TLR7 agonist 852A inhibition of tumor cell proliferation is dependent on plasmacytoid dendritic cells and type I IFN. *J. Interferon Cytokine Res.* **28,** 253–63 (2008).

165. Dummer, R. *et al.* An exploratory study of systemic administration of the toll-like receptor-7 agonist 852A in patients with refractory metastatic melanoma. *Clin. Cancer Res.* **14,** 856–64 (2008).

166. Lee, J. *et al.* Molecular basis for the immunostimulatory activity of guanine nucleoside analogs: activation of Toll-like receptor 7. *Proc. Natl. Acad. Sci. U. S. A.* **100,** 6646–51 (2003).

167. Lee, J. *et al.* Maintenance of colonic homeostasis by distinctive apical TLR9 signalling in intestinal epithelial cells. *Nat. Cell Biol.* **8,** 1327–36 (2006).

168. Cristofaro, P. & Opal, S. M. The Toll-like receptors and their role in septic shock. *Expert Opin. Ther. Targets* **7,** 603–612 (2003).

169. Knuefermann, P. Cardiac Inflammation and Innate Immunity in Septic Shock*. *CHEST J.* **121,** 1329 (2002).

170. Takakura, Y., Mahato, R. I., Nishikawa, M. & Hashida, M. Control of pharmacokinetic profiles of drug—macromolecule conjugates. *Adv. Drug Deliv. Rev.* **19,** 377–399 (1996).

171. Wu, C. C. N. *et al.* Immunotherapeutic activity of a conjugate of a Toll-like receptor 7 ligand. *Proc. Natl. Acad. Sci. U. S. A.* **104,** 3990–5 (2007).

172. Chan, M. *et al.* Synthesis and immunological characterization of toll-like receptor 7 agonistic conjugates. *Bioconjug. Chem.* **20,** 1194–200 (2009).

173. Hayashi, T. *et al.* Application of novel phospholipid conjugated toll like receptor 7 ligands for cancer therapy by topical and systemic administration. *AACR Annu. Meet.* 2568 (2014).

174. Jølck, R. I., Feldborg, L. N., Andersen, S., Moghimi, S. M. & Andresen, T. L. Engineering liposomes and nanoparticles for biological targeting. *Adv. Biochem. Eng. / Biotechnol.* **125,** 251–280 (2011).

175. Fan, Y. & Zhang, Q. Development of liposomal formulations: From concept to clinical investigations. *Asian J. Pharm. Sci.* **8,** 81–87 (2013).

176. Mouritsen, O. G. *Life - As a Matter of Fat*. (Springer-Verlag Berlin Heidelberg, 2005).

177. Bangham, A. D. & Horne, R. W. Negative staining of phospholipids and their structural modification by surface-active agents as observed in the electron microscope. *J. Mol. Biol.* **8,** 660–668 (1964).

178. Gregoriadis, G., Swain, C., Wills, E. & Tavill, A. Drug-carrier potential of liposomes in cancer chemotherapy. *Lancet* 1313–1316 (1974).

179. Torchilin, V. *et al.* Poly(ethylene glycol) on the liposome surface: on the mechanism of polymer-coated liposome longevity. *Biochim. Biophys. Acta* **1195,** 11–20 (1994).

180. Badiee, A. *et al.* Enhanced delivery of immunoliposomes to human dendritic cells by targeting the multilectin receptor DEC-205. *Vaccine* **25,** 4757–66 (2007).

181. Gieseler, R. K. *et al.* DC-SIGN-specific liposomal targeting and selective intracellular compound delivery to human myeloid dendritic cells: implications for HIV disease. *Scand. J. Immunol.* **59,** 415–24 (2004).

182. Broekhoven, C. L. van, Parish, C. R., Demangel, C., Warwick, J. B. & Altin, J. G. Targeting Dendritic Cells with Antigen-Containing Liposomes: A Highly Effective Procedure for Induction of Antitumor Immunity and for Tumor Immunotherapy. *Cancer Res.* **64,** 4357–4365 (2004).

183. Bozzacco, L. *et al.* DEC-205 receptor on dendritic cells mediates presentation of HIV gag protein to CD8+ T cells in a spectrum of human MHC I haplotypes. *Proc. Natl. Acad. Sci. U. S. A.* **104,** 1289–1294 (2007).

184. Tacken, P. J. *et al.* Effective induction of naive and recall T-cell responses by targeting antigen to human dendritic cells via a humanized anti–DC-SIGN antibody. *Blood* **106,** 1278–1286 (2015).

185. Dzionek, A., Inagaki, Y. & Okawa, K. Plasmacytoid dendritic cells: from specific surface markers to specific cellular functions. *Hum. Immunol.* **1,** 1133–1148 (2002).

186. Röck, J. *et al.* CD303 (BDCA-2) signals in plasmacytoid dendritic cells via a BCR-like signalosome involving Syk, Slp65 and PLCgamma2. *Eur. J. Immunol.* **37,** 3564–75 (2007).

187. Taylor, P. R. *et al.* Dectin-2 is predominantly myeloid restricted and exhibits unique activation-dependent expression on maturing inflammatory monocytes elicited in vivo. *Eur. J. Immunol.* **35,** 2163–74 (2005).

188. Meyer-Wentrup, F. *et al.* Targeting DCIR on human plasmacytoid dendritic cells results in antigen presentation and inhibits IFN-alpha production. *Blood* **111,** 4245–53 (2008).

189. Bates, E. E. *et al.* APCs express DCIR, a novel C-type lectin surface receptor containing an immunoreceptor tyrosine-based inhibitory motif. *J. Immunol.* **163,** 1973–83 (1999).

190. Kanazawa, N., Tashiro, K., Inaba, K. & Miyachi, Y. Dendritic cell immunoactivating receptor, a novel C-type lectin immunoreceptor, acts as an activating receptor through association with Fc receptor gamma chain. *J. Biol. Chem.* **278,** 32645–52 (2003).

191. Mellman, I., Coukos, G. & Dranoff, G. Cancer immunotherapy comes of age. *Nature* **480,** 480–9 (2011).

192. Porta, C. *et al.* in *Adv. Mol. Oncol.* 67–86 (Springer US, 2007). at <http://link.springer.com/content/pdf/10.1007/978-0-387-69116-9_5.pdf>

193. Chen, J. J. W. *et al.* Tumor-associated macrophages: the double-edged sword in cancer progression. *J. Clin. Oncol.* **23,** 953–64 (2005).

194. Seliger, B. & Massa, C. The dark side of dendritic cells: Development and exploitation of tolerogenic activity that favor tumor outgrowth and immune escape. *Front. Immunol.* **4,** 1–13 (2013).

195. Hoebe, K. *et al.* TLR signaling pathways: opportunities for activation and blockade in pursuit of therapy. *Curr. Pharm. Des.* **12,** 4123–34 (2006).

196. Vacchelli, E. *et al.* Trial Watch: Toll-like receptor agonists for cancer therapy. *Oncoimmunology* **2,** e25238 (2013).

197. Ito, T. *et al.* Interferon-alpha and Interleukin-12 Are Induced Differentially by Toll-like Receptor 7 Ligands in Human Blood Dendritic Cell Subsets. *J. Exp. Med.* **195,** 1507–1512 (2002).

198. Kanzler, H., Barrat, F. J., Hessel, E. M. & Coffman, R. L. Therapeutic targeting of innate immunity with Toll-like receptor agonists and antagonists. *Nat. Med.* **13,** 552–9 (2007).

199. Hirsch, I., Caux, C., Hasan, U., Bendriss-Vermare, N. & Olive, D. Impaired Toll-like receptor 7 and 9 signaling: from chronic viral infections to cancer. *Trends Immunol.* **31,** 391–7 (2010).

200. Nakamura, T. *et al.* Synthesis and evaluation of 8-oxoadenine derivatives as potent Toll-like receptor 7 agonists with high water solubility. *Bioorg. Med. Chem. Lett.* **23,** 669–72 (2013).

201. Lian, T. & Ho, R. J. Trends and developments in liposome drug delivery systems. *J. Pharm. Sci.* **90,** 667–80 (2001).

202. Bae, Y. H. & Park, K. Targeted drug delivery to tumors: myths, reality and possibility. *J. Control. Release* **153,** 198–205 (2011).

203. Papahadjopoulos, D. *et al.* Sterically stabilized liposomes: improvements in pharmacokinetics and antitumor therapeutic efficacy. *Proc. Natl. Acad. Sci.* **88,** 11460–11464 (1991).

204. Meyer-Wentrup, F. *et al.* DCIR is endocytosed into human dendritic cells and inhibits TLR8-mediated cytokine production. *J. Leukoc. Biol.* **85,** 518–25 (2009).

205. Li, C. & Deng, Y. A novel method for the preparation of liposomes: freeze drying of monophase solutions. *J. Pharm. Sci.* **93,** 1403–14 (2004).

206. Traut, R. R. *et al.* Methyl 4-mercaptobutyrimidate as a cleavable crosslinking reagent and its application to the Escherichia coli 30S ribosome. *Biochemistry* **12,** 3266–3273 (1973).

207. Ellman, G. L. Tissue sulfhydryl groups. *Arch. Biochem. Biophys.* **82,** 70–77 (1959).

208. Eyer, P. *et al.* Molar absorption coefficients for the reduced Ellman reagent: reassessment. *Anal. Biochem.* **312,** 224–7 (2003).

209. Nässander, U. K. *et al.* Design of immunoliposomes directed against human ovarian carcinoma. *Biochim. Biophys. Acta* **1235,** 126–39 (1995).

210. Ziegler-Heitbrock, L. *et al.* Nomenclature of monocytes and dendritic cells in blood. *Blood* **116,** e74–80 (2010).

211. Hausmann, O. V. *et al.* Robust expression of CCR3 as a single basophil selection marker in flow cytometry. *Allergy Eur. J. Allergy Clin. Immunol.* **66,** 85–91 (2011).

212. Randolph, G., Jakubzick, C. & Qu, C. Antigen presentation by monocytes and monocyte-derived cells. *Curr. Opin. Immunol.* **20,** 52–60 (2008).

213. Nierkens, S. *et al.* Immune adjuvant efficacy of CpG oligonucleotide in cancer treatment is founded specifically upon TLR9 function in plasmacytoid dendritic cells. *Cancer Res.* **71,** 6428–37 (2011).

214. Liu, Y.-J. IPC: professional type 1 interferon-producing cells and plasmacytoid dendritic cell precursors. *Annu. Rev. Immunol.* **23,** 275–306 (2005).

215. Fuertes, M. B. *et al.* Host type I IFN signals are required for antitumor CD8+ T cell responses through CD8α+ dendritic cells. *J. Exp. Med.* **208,** 2005–16 (2011).

216. Diamond, M. S. *et al.* Type I interferon is selectively required by dendritic cells for immune rejection of tumors. *J. Exp. Med.* **208,** 1989–2003 (2011).

217. Gibson, S. J. *et al.* Plasmacytoid dendritic cells produce cytokines and mature in response to the TLR7 agonists, imiquimod and resiquimod. *Cell. Immunol.* **218,** 74–86 (2002).

218. Trinchieri, G. Interleukin-12 and the regulation of innate resistance and adaptive immunity. *Nat. Rev. Immunol.* **3,** 133–46 (2003).

219. Gorden, K. B. *et al.* Synthetic TLR agonists reveal functional differences between human TLR7 and TLR8. *J. Immunol.* **174,** 1259–68 (2005).

220. Auffray, C., Sieweke, M. H. & Geissmann, F. Blood monocytes: development, heterogeneity, and relationship with dendritic cells. *Annu. Rev. Immunol.* **27,** 669–92 (2009).

221. Shi, C. & Pamer, E. G. Monocyte recruitment during infection and inflammation. *Nat. Rev. Immunol.* **11,** 762–74 (2011).

222. Sheen, M. R., Lizotte, P. H., Toraya-Brown, S. & Fiering, S. Stimulating antitumor immunity with nanoparticles. *Wiley Interdiscip. Rev. Nanomed. Nanobiotechnol.* **6,** 496–505 (2014).

223. Banchereau, J. & Palucka, A. K. Dendritic cells as therapeutic vaccines against cancer. *Nat. Rev. Immunol.* **5,** 296–306 (2005).

224. Siveen, K. S. & Kuttan, G. Role of macrophages in tumour progression. *Immunol. Lett.* **123,** 97–102 (2009).

225. Immordino, M. L., Dosio, F. & Cattel, L. Stealth liposomes: review of the basic science, rationale, and clinical applications, existing and potential. *Int. J. Nanomedicine* **1,** 297–315 (2006).

226. Miyahira, A. Types of immune cells present in human PBMC. *Sang. Biosci.* (2012). at <http://technical.sanguinebio.com/types-of-immune-cells-present-in-human-pbmc/>

227. Dzionek, A. *et al.* BDCA-2, a novel plasmacytoid dendritic cell-specific type II C-type lectin, mediates antigen capture and is a potent inhibitor of interferon alpha/beta induction. *J. Exp. Med.* **194,** 1823–34 (2001).

228. Moghimi, S. M. & Szebeni, J. Stealth liposomes and long circulating nanoparticles: critical issues in pharmacokinetics, opsonization and protein-binding properties. *Prog. Lipid Res.* **42,** 463–478 (2003).

229. Lubeck, M. *et al.* The interaction of murine IgG subclass proteins with human monocyte Fc receptors. *J. Immunol.* **135,** 1299–1304 (1985).

230. Winkel, J. *et al.* Characterization of Two Fc Receptors for Mouse Immunoglobulins on Human Monocytes and Cell Lines. *Scand. J. Immunol.* **26,** 663–672 (1987).

231. Winkel, J. van de, Duijnhoven, H. van, Ommen, R. van, Capel, P. & Tax, W. Selective modulation of two human monocyte Fc receptors for IgG by immobilized immune complexes. *J. Immunogy* **140,** 3515–3521 (1988).

232. Ober, R. J., Radu, C. G., Ghetie, V. & Ward, E. S. Differences in promiscuity for antibody – FcRn interactions across species : implications for therapeutic antibodies. **13,** 1551–1559 (2001).

233. Dudek, A. Z. *et al.* First in human phase I trial of 852A, a novel systemic toll-like receptor 7 agonist, to activate innate immune responses in patients with advanced cancer. *Clin. Cancer Res.* **13,** 7119–25 (2007).

234. Birmachu, W. *et al.* Transcriptional networks in plasmacytoid dendritic cells stimulated with synthetic TLR 7 agonists. *BMC Immunol.* **8,** 26 (2007).

235. Zarember, K. a. & Godowski, P. J. Tissue Expression of Human Toll-Like Receptors and Differential Regulation of Toll-Like Receptor mRNAs in Leukocytes in Response to Microbes, Their Products, and Cytokines. *J. Immunol.* **168,** 554–561 (2002).

236. Caron, G. *et al.* Direct Stimulation of Human T Cells via TLR5 and TLR7/8: Flagellin and R-848 Up-Regulate Proliferation and IFN- Production by Memory CD4+ T Cells. *J. Immunol.* **175,** 1551–1557 (2005).

237. Barr, T. a, Brown, S., Ryan, G., Zhao, J. & Gray, D. TLR-mediated stimulation of APC: Distinct cytokine responses of B cells and dendritic cells. *Eur. J. Immunol.* **37,** 3040–53 (2007).

238. Schroder, K., Hertzog, P. J., Ravasi, T. & Hume, D. A. Interferon-γ: an overview of signals, mechanisms and functions. *J. Leukoc. Biol.* **75,** 163–189 (2004).

239. Yano, H. *et al.* Growth inhibitory effects of interferon-alpha subtypes vary according to human liver cancer cell lines. *J. Gastroenterol. Hepatol.* **21,** 1720–5 (2006).

240. Dovedi, S. J. *et al.* Systemic delivery of a TLR7 agonist in combination with radiation primes durable antitumor immune responses in mouse models of lymphoma. *Blood* **121,** 251–9 (2013).

241. Kanazawa, N. *et al.* DCIR Acts as an Inhibitory Receptor Depending on its Immunoreceptor Tyrosine-Based Inhibitory Motif. *J. Invest. Dermatol.* **118,** 261–266 (2002).

242. Davis, M. E. *et al.* Self-assembling nucleic acid delivery vehicles via linear, water-soluble, cyclodextrin-containing polymers. *Curr. Med. Chem.* **11,** 179–97 (2004).

243. Wu, S. Y., Lopez-Berestein, G., Calin, G. a & Sood, A. K. RNAi therapies: drugging the undruggable. *Sci. Transl. Med.* **6,** 240ps7 (2014).

244. Semple, S. C. *et al.* Rational design of cationic lipids for siRNA delivery. *Nat. Biotechnol.* **28,** 172–6 (2010).

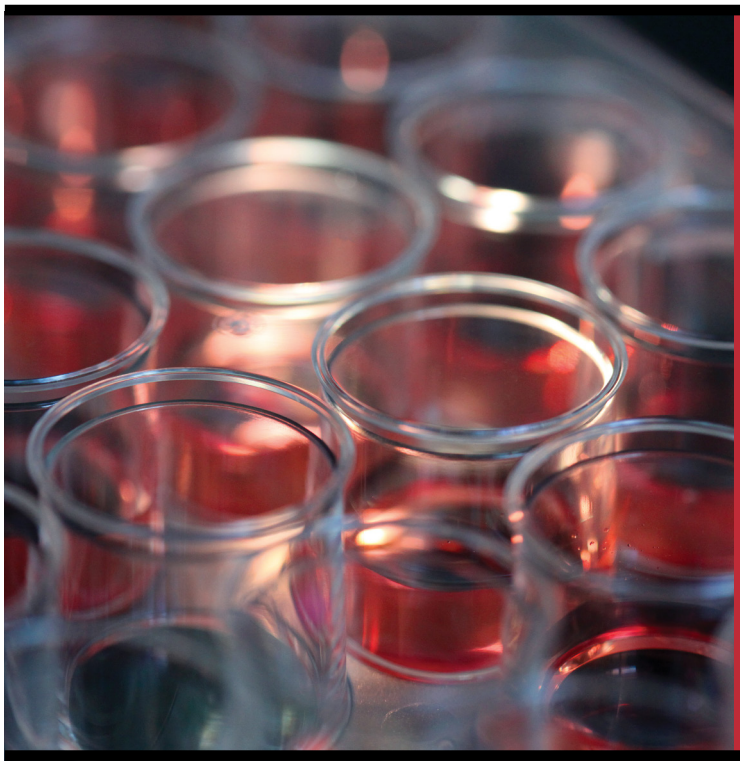



Published by:
DTU Nanotech
Department of Micro- and Nanotechnology
Technical University of Denmark
Ørsteds Plads, building 345B
DK-2800 Kgs. Lyngby

DTU Nanotech
Department of Micro- and Nanotechnology